BSC

Design Calculation or Analysis Cover Sheet

Complete only applicable items.

1. QA: QA
2. Page 1 of 58

3. System	4. Document Identifier
Monitored Geologic Repository	800-00C-MGR0-00300-000-00A

5. Title

Probabilistic Characterization of Preclosure Rockfalls in Emplacement Drifts

6. Group

Preclosure Safety Analyses

7. Document Status Designation

☐ Preliminary ☒ Committed ☐ Confirmed ☐ Cancelled/Superseded

8. Notes/Comments

This calculation supersedes Bounding Characteristics of Credible Rockfalls of Preclosure Period (800-00C-MGR0-00200-000-00A).

Robert Garrett checked the DIRS. All other checking responsibilities were assumed by Ernest Lindner.

Attachments	Total Number of Pages
Attachment A. Mathcad Calculations	38
Attachment B. Drip Shield and Waste Package Geometry in Emplacement Drift	4
Attachment C. Copy of Correspondence on Model Drift Length	4

RECORD OF REVISIONS

9. No.	10. Reason For Revision	11. Total # of Pgs.	12. Last Pg. #	13. Originator (Print/Sign/Date)	14. Checker (Print/Sign/Date)	15. EGS (Print/Sign/Date)	16. Approved/Accepted (Print/Sign/Date)
00A	Initial Issue	104	C-4	P. Macheret P.Macht 03/27/07	E. Lindner 3/27/07 R. Garrett 3/27/07	M. Frank 3/28/07	M. Wisenburg 3/29/2007

DISCLAIMER

The calculations contained in this document were developed by Bechtel SAIC Company, LLC (BSC) and are intended solely for the use of BSC in its work for the Yucca Mountain Project.

CONTENTS

Page

FIGURES

Page

TABLES

Page

ACRONYMS AND ABBREVIATIONS

APE	Annual Probability of Exceedance
BSC	Bechtel SAIC Company
DIRS	Document Input Reference System
DTN	Data Tracking Number
g	acceleration of gravity
J	joule ($kg \cdot m^2 \cdot s^{-2}$)
kg	kilogram
m	meter
mm	millimeter
m^2	square meter
metric ton	1,000 kg
Pa	pascal ($kg \cdot m^{-1} \cdot s^{-2}$)
s	second
SEAPE	Seismic Event Annual Probability of Exceedance
Tptpll	Topopah Spring Tuff Lower Lithophysal
Tptpln	Topopah Spring Tuff Lower Nonlithophysal
Tptpmn	Topopah Spring Tuff Middle Nonlithophysal
Tptpul	Topopah Spring Tuff Upper Lithophysal
yr	year

INTENTIONALLY LEFT BLANK

1. PURPOSE

Rockfalls may occur in response to the combined effects of in situ, thermal and seismic stresses in the rock mass surrounding the emplacement drifts of the repository. Conceivably, dynamic or static loadings resulting from a rockfall onto a waste package can cause the waste package to breach, possibly leading to a radioactive release.

This calculation has two purposes. The first purpose is to evaluate the characteristics of the most severe rockfalls over the preclosure period. The outputs will express these characteristics in two ways, depending on whether the loadings are dynamic or static. For dynamic loadings, the limiting characteristics will be given in terms of mass, velocity, and kinetic energy at impact. For static loadings, the pressure exerted on a waste package will be calculated. The second purpose is to evaluate the probability distribution associated with the kinetic energy of a rockfall impacting a waste package as a result of a seismic event.

The scope of this calculation is limited to credible rockfalls. Credible rockfalls are defined in relation to the probability threshold that characterizes a Category 2 event sequence, based on 10 CFR 63.2 (Reference 2.2.21). Event sequences that are expected to occur one or more times before permanent closure of the geologic repository operations area are defined as Category 1 event sequences. Other event sequences that have at least one chance in 10,000 of occurring before permanent closure are Category 2 event sequences. Accordingly, credible rockfalls are defined in this calculation as rockfalls that have at least one chance in 10,000 of occurring during the preclosure period. The rockfalls that have a lesser probability of occurrence cannot, by definition, be part of a Category 1 or Category 2 event sequence and therefore are screened out from further consideration.

In addition, the scope of this calculation is limited to the consideration of rockfalls for which no credit is taken for ground support. Taking credit for ground support could mandate its classification as important to safety, per the definition of important to safety structures, systems, and components given in 10 CFR 63.2 (Reference 2.2.21). By not taking credit for ground support, no predetermination is made as to its classification. Ground support is not credited, but is considered to the extent that it could have adverse effects with regard to the severity of rockfall impacts on waste packages.

Finally, this calculation considers only credible rockfalls that may occur in the emplacement drifts of the repository. Rockfalls in non-emplacement drifts, such as mains and turnouts, are to be addressed in a different calculation.

2. REFERENCES

2.1 PROCEDURES/DIRECTIVES

2.1.1. EG-PRO-3DP-G04B-00037, Rev. 7. *Calculations and Analyses.* Las Vegas, Nevada: Bechtel SAIC Company. ACC: DOC.20070122.0010.

2.1.2. LS-PRO-0201, Rev. 2. *Preclosure Safety Analyses Process*. Las Vegas, Nevada: Bechtel SAIC Company. ACC: DOC.20060927.0017.

2.1.3. IT-PRO-0011, Rev. 3. *Software Management.* Las Vegas, Nevada: Bechtel SAIC Company. ACC: DOC.20061221.0003.

2.1.4. BSC (Bechtel SAIC Company) 2006. *Quality Management Directive.* QA-DIR-10, Rev. 0. Las Vegas, Nevada: Bechtel SAIC Company. ACC: DOC.20060906.0001. [DIRS 177655]

2.2 DESIGN INPUTS

2.2.1. BSC 2004. *Drift Degradation Analysis.* ANL-EBS-MD-000027 REV 03. Las Vegas, Nevada: Bechtel SAIC Company. ACC: DOC.20040915.0010; DOC.20050419.0001; DOC.20051130.0002; DOC.20060731.0005. [DIRS 166107]

2.2.2. BSC 2004. *Ground Control for Emplacement Drifts for LA.* 800-K0C-SSE0-00100-000-00A. Las Vegas, Nevada: Bechtel SAIC Company. ACC: ENG.20040712.0019; ENG.20050816.0015. [DIRS 170292]

2.2.3. Atwood, C.L.; LaChance, J.L.; Martz, H.F.; Anderson, D.J.; Englehardt, M.; Whitehead, D.; and Wheeler, T. 2003. *Handbook of Parameter Estimation for Probabilistic Risk Assessment.* NUREG/CR-6823. Washington, D.C.: U.S. Nuclear Regulatory Commission. ACC: MOL.20060126.0121. [DIRS 177316]

2.2.4. BSC 2007. *2-MCO/2-DHLW Waste Package Configuration.* 000-MW0-DS00-00301-000 REV 00B. Las Vegas, Nevada: Bechtel SAIC Company. ACC: ENG.20070205.0011. [DIRS 175303]

2.2.5. BSC 2003. *Underground Layout Configuration.* 800-P0C-MGR0-00100-000-00E. Las Vegas, Nevada: Bechtel SAIC Company. ACC: ENG.20031002.0007; ENG.20050817.0005. [DIRS 165572]

2.2.6. Weast, R.C., ed. 1978. *CRC Handbook of Chemistry and Physics.* 59th Edition. West Palm Beach, Florida: CRC Press. TIC: 246814. [DIRS 128733]

2.2.7. MO0408MWDDDMIO.002. Drift Degradation Model Inputs and Outputs. Submittal date: 08/31/2004. [DIRS 171483]

2.2.8. BSC 2004. *Repository Subsurface Emplacement Drifts Steel Invert Structure Plan & Elevation.* 800-SS0-SSE0-00101-000-00B. Las Vegas, Nevada: Bechtel SAIC Company. ACC: ENG.20040520.0004. [DIRS 169503]

2.2.9. D'Agostino, R.B. and Stephens, M.A., eds. 1986. *Goodness-Of-Fit Techniques.* Statistics, Textbooks and Monographs Volume 68. New York, New York: Marcel Dekker. TIC: 253256. [DIRS 160320]

2.2.10. Coles, S. 2001. *An Introduction to Statistical Modeling of Extreme Values.* Springer Series in Statistics. London, England: Springer-Verlag. TIC: 258276. [DIRS 178199]

2.2.11. Box, G.E.P. and Tiao, G.C. 1992. *Bayesian Inference in Statistical Analysis.* New York, New York: John Wiley and Sons. TIC: 258558. [DIRS 178285]

2.2.12. BSC 2006. *Underground Layout Configuration for LA.* 800-KMC-SS00-00200-000-00A. Las Vegas, Nevada: Bechtel SAIC Company. ACC: ENG.20061115.0001. [DIRS 178323]

2.2.13. Helton, J.C. and Davis, F.J. 2002. *Latin Hypercube Sampling and the Propagation of Uncertainty in Analyses of Complex Systems.* SAND2001-0417. Albuquerque, New Mexico: Sandia National Laboratories. TIC: 254367. [DIRS 163475]

2.2.14. BSC 2002. *Critical Distance Between Impact Locations for Multiple Rock Fall on Waste Package.* 000-00C-EBS0-00200-000-00A. Las Vegas, Nevada: Bechtel SAIC Company. ACC: MOL.20020916.0313. [DIRS 161537]

2.2.15. BSC 2006. *Basis of Design for the TAD Canister-Based Repository Design Concept.* 000-3DR-MGR0-00300-000-000. Las Vegas, Nevada: Bechtel SAIC Company. ACC: ENG.20061023.0002. [DIRS 177636]

2.2.16. BSC 2007. *IED Geotechnical and Thermal Parameters III [Sheet 1 of 1].* 800-IED-MGR0-00403-000-00A. Las Vegas, Nevada: Bechtel SAIC Company. ACC: ENG.20070125.0017; ENG.20070322.0012. [DIRS 178796]

2.2.17. BSC 2003. *Design and Engineering, Emplacement Pallet Configuration.* 000-M00-TEP0-00102-000-00A. Las Vegas, Nevada: Bechtel SAIC Company. ACC: ENG.20031006.0004 [DIRS 165731]

2.2.18. BSC 2004. *D&E / PA/C IED Interlocking Drip Shield and Emplacement Pallet.* 800-IED-WIS0-00401-000-00D. Las Vegas, Nevada: Bechtel SAIC Company. ACC: ENG.20040503.0018. [DIRS 169220]

2.2.19. BSC 2004. *Design and Engineering, Interlocking Drip Shield Configuration.* 000-M00-SSE0-00102-000-00B. Las Vegas, Nevada: Bechtel SAIC Company. ACC: ENG.20040305.0021. [DIRS 168067]

2.2.20. BSC 2004. *Design and Engineering, Drip Shield Peripheral Bulkhead.* 000-M00-SSE0-01201-000-00A. Las Vegas, Nevada: Bechtel SAIC Company. ACC: ENG.20040309.0008. [DIRS 168313]

2.2.21. 10 CFR 63. 2006. Energy: Disposal of High-Level Radioactive Wastes in a Geologic Repository at Yucca Mountain, Nevada. Internet Accessible. [DIRS 176544]

2.2.22. Knowles, M.K. 2007. "Contract No. DE-AC04-94AL-85000 - Drift Length per Simulation for the Nonlithophysal Rockfall Model." Letter from M. Kathryn Knowles (SNL) to Richard J. Tosetti (BSC), March 5, 2007, 03060703493, with enclosure. ACC: CCU.20070306.0002. [DIRS 179805]

2.2.23. BSC 2007. *Repository Subsurface Emplacement Drifts Steel Invert Structure Plan & Elevation.* 800-SS0-SSE0-00201-000 REV 00A. Las Vegas, Nevada: Bechtel SAIC Company. ACC: ENG.20070125.0021. [DIRS 178767]

2.3 DESIGN CONSTRAINTS

None.

2.4 DESIGN OUTPUTS

This calculation will be used as input in a future calculation evaluating the capability of waste packages to withstand a rockfall impact without breaching.

3. ASSUMPTIONS

3.1 ASSUMPTIONS REQUIRING VERIFICATION

This calculation does not use assumptions that require verification.

3.2 ASSUMPTIONS NOT REQUIRING VERIFICATION

3.2.1. Binomial Distribution for Probability of Seismic Event over Preclosure Period

Assumption: The probability of occurrence of an earthquake over the preclosure period follows a binomial distribution.

Rationale: This modeling assumption is required in Section 6.2.1 to characterize the seismic events of interest over the preclosure period and in Section 6.4.5.1 to calculate the bounding credible rockfalls of the preclosure period. The binomial distribution is commonly used to describe, in a set of n independent trials, the number of realizations of an event with a probability p (Reference 2.2.3, p. A-12). For this calculation, the trials are the years of the preclosure period ($n = 100$ based on Reference 2.2.15, Section 2.2.2.8) and the event is the occurrence, during a given year, of a seismic event of a given severity or greater, characterized by an annual probability of exceedance (APE) p. The earthquakes considered in this calculation are rare events that can occur at any time during the preclosure period, and the occurrence of an earthquake or lack thereof in a given year has no bearing on any other year, which makes this assumption appropriate for use in this calculation.

3.2.2. Waste Package Geometry in Emplacement Drift

Assumption: For rockfall calculations, the minimum height of the waste packages above the excavation base in an emplacement drift is taken equal to 3.41 m (taking into account the additional height provided by the invert and the emplacement pallet). The width (diameter) of the waste packages is taken equal to 1.83 m.

Rationale: This assumption is used in Section 6.3.4 to calculate the pressure that would be exerted on a buried waste package in a collapsed emplacement drift, and in Assumption 3.2.5 to calculate the adjustment of rockfall velocity for impacts on waste packages. This assumption aims at simplifying the modeling of waste packages in emplacement drifts, by considering a unique set of waste package dimensions, instead of considering each type of waste package. The waste package with the smallest diameter, namely the 2-MCO/2-DHLW waste package, which has a nominal diameter of 1.83 m (value rounded to the nearest centimeter) (Reference 2.2.4) is used for calculating the width and height of the waste package in an emplacement drift, because this leads to conservative results (see Section 6.3.4 and Assumption 3.2.5). Section B.2 of Appendix B details the calculations leading to the height of 3.41 m.

3.2.3. Waste Package Behaving as if Fixed to the Invert of the Drift

Assumption: Emplaced waste packages behave as if fixed to the invert of the drift during a seismic event.

Rationale: This is a simplifying assumption used in Section 6.4.3.1 and Assumption 3.2.5 to make waste packages behave in the same manner as drip shields in Reference 2.2.1 (Section 6.3.1.1), which are considered to be fixed to the invert of the drift. In reality, waste packages in emplacement drifts would lie on a pallet and might temporarily lose contact with their support (and therefore the ground below) during a severe seismic shaking. The assumption is acceptable because a waste package behaving as if affixed to the invert would be subjected to all the movements and accelerations of the ground during the earthquake. This may randomly amplify or dampen the severity of the impact of a falling rock, depending on the vertical component of the ground velocity (and therefore the waste package velocity) which can be upwards or downwards at the time of impact. In contrast, a waste package having temporarily lost contact with its support would be subjected solely to the acceleration of gravity, which would tend to align the velocity of the waste package with that of a free falling rock, thereby mitigating the severity of the impact. Specifically, as soon as the waste package would lose contact with its support, its upward velocity would decrease from its initial value to eventually reach zero: any impact with a falling rock over this period of time would be less severe than if the impact occurred at the time right before loss of contact, when the initial upward velocity is at its maximum. After reaching its maximum upward position, the waste package would reverse direction and move downward until contact with its support was reestablished: any impact with a falling rock over this period of time would be somewhat dampened because both waste package and rock would be moving in the same direction. The impact would be less severe than if the waste package was affixed to the ground. Therefore, overall, this assumption is conservative.

3.2.4. Rockfalls Requiring Impact Velocity Adjustment

Assumption: The rockfalls that require an adjustment of their impact velocity are those that impact the top portion of the drip shield that is located at an angle more than 28 degrees from the drip shield centerline.

Rationale: The adjustment of impact velocity is necessary in Section 6.4.3.1 where this assumption is used, to account for the fact that rockfalls occurring over the preclosure period would impact a waste package, not a drip shield as modeled in Reference 2.2.1 (Section 6.3.1.1), and therefore would gain vertical velocity during the extra distance fallen due to the acceleration of gravity. The portion of the drip shield that is located at an angle more than 28 degrees above the drip shield centerline consists of its top part, down to its shoulders, as evaluated in Section B.1 of Attachment B, and displayed on Figure B-1 of that attachment, where the 28 degree angle is designated by α. Only the rockfalls which would impact the top portion of the drip shield require a velocity adjustment, because this is where the vertical distance between the drip shield and the waste package is the largest and would produce a significant change in velocity. All the

other rockfalls would strike the drip shield on its side and therefore would likely hit the waste package at a similar height, and thus do not require a velocity adjustment.

3.2.5. Rockfall Impact Velocity Adjustment

Assumption: The impact velocity is adjusted for the rockfalls that require it by adding - 0.74 m/s to the vertical component of the velocity (the adjustment term is negative to indicate that the added velocity has a downward direction in the Cartesian system of coordinates).

Rationale: As indicated in Assumption 3.2.4, the rockfalls that are modeled as hitting the upper portion of a drip shield in Reference 2.2.1 (Section 6.3.1.1) need to have their velocity adjusted to account for the fact that they would impact a waste package during the preclosure period (Section 6.4.3). The adjusted velocity of – 0.74 m/s is estimated based on the difference in height between a drip shield and the emplaced waste package below.

Since the rockfall velocities at impact on the drip shield are relative velocities (Reference 2.2.1, Section 6.3.1.1), their vertical component v_{ds} includes three contributors: the initial vertical velocity component at the time of dislodgement from the emplacement drift v_i, the velocity gained during acceleration from free fall v_a, and the vertical velocity component of the drip shield at the time of impact v_c. Based on Reference 2.2.6 (p. F-104), v_a is equal to $-\sqrt{2 \cdot g \cdot h_a}$ where h_a is the distance traveled by the rock in free fall from the emplacement drift to the impact location on the drip shield and g is the acceleration of gravity. The minus sign in front of the square root reflects the downward orientation of the free fall velocity in the Cartesian system of coordinates.

The vertical component of the rockfall velocity at impact on a waste package v_{wp} has three contributors. The initial vertical velocity component at the time of dislodgement is the same as previously, i.e., v_i. The velocity gained during acceleration from free fall is $v_b = -\sqrt{2 \cdot g \cdot h_b}$ where h_b is the distance traveled by the rock in free fall from the emplacement drift to the impact location on the waste package. The vertical velocity component of the waste package at the time of impact can be taken the same as that of the drip shield, i.e., equal to v_c, based on Assumption 3.2.3, which considers that the drip shield and waste package behave similarly.

Consequently, in the Cartesian system of coordinates, v_{wp} can be expressed as: $v_{wp} = v_{ds} - \sqrt{2 \cdot g \cdot h_b} + \sqrt{2 \cdot g \cdot h_a}$. This expression shows that v_{wp} is a decreasing function of h_b and an increasing function of h_a. Given that v_{ds} and v_{wp} will mostly take negative values (indicating that the relative rockfall velocity goes downwards in the Cartesian system of coordinates), estimates of v_{wp} will be more conservative with the use of upper values for h_b, and lower values for h_a.

An upper value of h_b is calculated in Section B.2 of Attachment B by using the waste package that has the smallest diameter (since this increases the drop height of a falling rock block). It is found that h_b can be estimated at 2.469 m. An estimate of h_a is

calculated in Section B.1 of Attachment B, based on the drip shield configuration in an intact emplacement drift used in Reference 2.2.1, which yields h_a equal to 1.974 m. As the ceiling of emplacement drifts unravels due to rockfalls during a seismic event, the 1.974 m becomes a lower value for h_a, which, as indicated previously, leads to conservative results.

Based on a value of g equal to 9.81 m/s^2 (Reference 2.2.6, p. F-335) and the estimated values of h_e and h_a, the adjustment velocity term, which is expressed as $-\sqrt{2 \cdot g \cdot h_b} + \sqrt{2 \cdot g \cdot h_a}$, is found equal to -0.74 m/s. This assumption is used in Section 6.4.3.1.

3.2.6. Rockfall Distributions Applicable to a Range of Seismic Events

Assumption: The rockfall rate, mass, and impact velocity distributions developed for seismic events having an APE equal to 10^{-4} are also applicable to seismic events having an APE less than 10^{-4}, but greater than 10^{-5}. The rockfall rate, mass, and impact velocity distributions developed for seismic events having an APE equal to 10^{-5} are also applicable to seismic events having an APE less than 10^{-5}, but greater than 10^{-6}.

Rationale: This modeling assumption is needed because the rockfall simulations used in this calculation were developed for a discrete set of seismic events (having APEs equal to 10^{-4}, 10^{-5}, and 10^{-6}), and the calculation of bounding credible rockfalls in Section 6.4.5.1, where this assumption is used, requires also an assessment of these distributions for earthquakes of intermediate severity. As explained in Section 6.2.2, the rockfall simulations of Reference 2.2.1 used in this calculation were developed based on unbounded ground motions, and the nature of the rockfall simulations is such that their assignment to an APE of 10^{-4}, 10^{-5}, or 10^{-6} is conservative. In reality, each simulation is more characteristic of rockfalls of lower APE. Therefore, the assumption is a reasonable approximation.

3.2.7. Total Length of Emplacement Drift Excavated in Nonlithophysal Rock Units

Assumption: The total length of emplacement drift excavated in nonlithophysal rock units is 10,000 m.

Rationale: Reference 2.2.5 (Table II-2) provides a partition of the emplacement areas by geologic zones (for which a definition is provided in Section 6.1.1). It is found that approximately 15 percent (745,486 m^2) of the emplacement area is excavated in the nonlithophysal rock units (i.e., in the Tptpln and Tptmn). Reference 2.2.12 (Table 9) indicates that the total available emplacement drift length is 65,273 m. Using the area ratio as a guide, the total length of emplacement drift excavated in nonlithophysal rock units is $0.15 \times 65{,}273 = 9{,}791$ m. This number is conservatively rounded up to 10,000 m, and used in Section 6.4.5.1 to calculate the total number of rockfalls in the nonlithophysal rock units of the emplacement drifts. This assumption is used in Section 6.4.5.1.

3.2.8. Length of Simulated Drift

Assumption: A bounding lower value of the length of simulated drift is 20 m per simulation.

Rationale: This assumption is used in Table 1 of Section 6.4.2.1 and in Attachment A to evaluate the rockfall rate, calculated as the ratio of the number of simulated rockfalls, over the length of simulated drift. The number of simulated rockfalls is given by Reference 2.2.16. A lower bound is used for the length of simulated drift, which results in a higher value for the rockfall rate. In turn, the rockfall rate is used in Section 6.4.5 to evaluate the number of rockfalls over the total length of emplacement drifts excavated in nonlithophysal rock units. The greater the rockfall rate, the greater the number of rockfalls, and the greater the likelihood is that a severe rockfall will be dislodged. Using a lower value for the length of simulated drift thus leads to conservative estimates of bounding rockfall characteristics.

As documented in Reference 2.2.22, appended to this calculation as Attachment C, the rockfall simulations of Reference 2.2.1 are based on a model space length of 25 m, but the actual length of drift simulated is smaller, at approximately 21.74 m. Assuming a lower drift length value of 20 m per simulation therefore is bounding for this calculation. Reference 2.2.22 is suitable for use in this assumption because it provides information to correct a condition tracked by Condition Report 10115.

4. METHODOLOGY

4.1 QUALITY ASSURANCE

This calculation is prepared in accordance with EG-PRO-3DP-G04B-00037 (Reference 2.1.1) and LS-PRO-0201 (Reference 2.1.2). The *Quality Management Directive* (Reference 2.1.4, Section 2.1.C.1.1.a.iii and 17.E) applies to this analysis and the final version is designated as QA: QA because it is part of the preclosure safety analysis.

4.2 USE OF SOFTWARE

Mathcad version 13.0 is used in this calculation. The use of this software is classified as Level 2 per procedure, IT-PRO-0011 (Reference 2.1.3, Attachment 12) and therefore the software does not need to be qualified. The results of the Mathcad calculations are verified by visual inspection of the computer-generated results shown in Attachment A. Mathcad is installed on a Dell Optiplex GX260 operated under Microsoft Windows 2000 Professional version 5.0.2195 Service Pack 4 Build 2195. All other calculations within the text were performed by hand.

4.3 PROBABILISTIC METHODOLOGY

The methodology employed to evaluate the characteristics of the most severe rockfalls that could occur in the emplacement drifts over the preclosure period is based on a probabilistic approach supported by a physical argumentation. Rockfall simulation data are used to develop probability distributions associated with the rockfall rate (number of rockfalls per meter of drift), the rockfall

velocity at impact on a waste package, and the rockfall mass. The rockfall rate is fitted to a lognormal distribution. The upper values of the rockfall velocity and mass are fitted to an exponential distribution, while medium values are fitted to a Weibull distribution. The use of unbounded distributions provides conservative estimates of the velocity, mass, and kinetic energy of the most severe rockfalls. Uncertainties are investigated by exploring the variability of key parameters and introducing conservatisms in the calculations as needed. Other methods used in this calculation involve an analytical approach to calculate the static loading of waste packages in lithophysal rock units, and standard statistical calculations to characterize the probability distribution associated with the kinetic energy of rockfalls at impact on waste packages.

5. LIST OF ATTACHMENTS

6. BODY OF CALCULATION

6.1 PRELIMINARY EVALUATION OF ROCKFALL HAZARD

6.1.1. Nonlithophysal and Lithophysal Rock Units

Determining the characteristics of the rockfalls that could damage a waste package over the preclosure period requires first to identify the types of rocks that are present at the repository horizon. This information is given in detail in the *Drift Degradation Analysis* (Reference 2.2.1) and summarized in Reference 2.2.16. As explained in Reference 2.2.1 (p. vii and Section 6.1.2), the repository horizon lies within the Topopah Spring Tuff, and essentially consists of two main types of rock: the nonlithophysal rock and the lithophysal rock. The nonlithophysal rocks, which comprise roughly 15 percent of the emplacement area, are hard, strong, jointed rock masses; in contrast, the lithophysal rocks, which comprise approximately 85 percent of the emplacement area, are relatively more deformable with lower compressive strength (Reference 2.2.1, p. vii), and also contain cavities in the rock (the lithophysae), connected by intense fracturing (Reference 2.2.1, Sections 6.1.2 and 6.4.1.1). The rock units can further be subdivided in a total of four zones (Reference 2.2.1, Section 6.1.2): two are nonlithophysal and are designated as Tptpln (lower nonlithophysal zone) and Tptpmn (middle nonlithophysal zone); two are lithophysal and are designated as Tptpul (upper lithophysal zone) and Tptpll (lower lithophysal zone).

Reference 2.2.1 (Section 6.1.4) indicates that the structural response of the repository to thermal and mechanical loadings is governed by the fracture geometry and properties, as well as the amount of lithophysae in the rock. The occurrence of lithophysae and fractures with a trace length greater than 1 m are found to be roughly inversely proportional (Reference 2.2.1, Section 6.1.4). This intrinsic difference between nonlithophysal and lithophysal rock units results in different failure modes. The fracture surfaces in the nonlithophysal rock units provide the primary weaknesses in the system and control the resulting block dimensions (Reference 2.2.16, Section I). In contrast, the intense small-scale fracturing in the lithophysal rock combined with the presence of lithophysae almost uniformly distributed in the rock result in a relatively weaker material, that, when stressed beyond its strength limits, is anticipated to break into relatively small block sizes controlled by the spacing of natural fractures (Reference 2.2.1, Section 6.4.1.1). Because of these two different failure modes, the nonlithophysal and lithophysal rock units are modeled differently in the *Drift Degradation Analysis* (Reference 2.2.1). This distinction is preserved in this calculation.

6.1.2. Factors Leading to Degradation of Rock Units

Reference 2.2.1 (p. viii) identifies three mechanisms by which rockfalls could occur in the emplacement drifts of the repository: seismic ground motions, thermal stress (generated by the temperature increase in the drift due to the decay heat from the emplaced waste packages), and time-dependent degradation of rock strength. Another mechanism, not mentioned in Reference 2.2.1, could conceivably dislodge rockfalls in the repository: vibrations created during the excavation of a drift could propagate to a nearby drift containing emplaced waste packages. This mechanism, however, is not considered further as construction activities will be carried out

far enough from drifts with emplaced waste packages for vibrations propagated to these drifts to have insignificant effects.

By nature, ground motions have more sudden and drastic effects on drift stability than thermal loading and time-dependent strength degradation, which require years to take place. In contrast to the present calculation, which is limited to the evaluation of rockfalls over the preclosure period, Reference 2.2.1 mainly investigates the postclosure period. During the preclosure period, the emplacement drifts will be ventilated to remove most of the decay heat from the drifts, therefore thermally-induced stresses in the rock are expected to be of little concern compared to those of postclosure, when forced ventilation ceases. Also, the preclosure period for the subsurface is 100 yrs (Reference 2.2.15, Section 2.2.2.8), which leaves relatively little time (compared to postclosure) for significant degradation of the emplacement drifts to take place. Lastly, the evaluation of rockfalls presented in Reference 2.2.1 does not consider ground support (Reference 2.2.1, pp. ix and x). Ground support, however, will be present in the repository and will be able, to a certain extent, to prevent rockfalls (Reference 2.2.2, Section 7). Based on the foregoing, seismic events are deemed the dominant cause for severe rockfalls in the emplacement drifts over the preclosure period. This is confirmed by the evaluation of the effects of thermal loading and time-dependent strength degradation performed in Reference 2.2.1, as explained below.

In nonlithophysal rock units, rockfalls induced by thermal loading are found to be minor, as demonstrated by several rockfall simulations which produce zero to only a few rockfalls, with a mean size less than 0.2 metric tons (Reference 2.2.16, Section II). In fact, when superimposed with stresses from ground motions, thermal stresses induced in the rocks by heating have the overall effect of locking rocks more tightly together, causing the rock mass to become more stable and resistant to ground shaking. Case in point, results of simulations reported in Reference 2.2.16 (Section III) find less rockfalls after a seismic shaking when stresses from heating are accounted for than when only in situ stresses are considered. It is thus more conservative to neglect the effects of heating than accounting for them in the evaluation of rockfalls in the nonlithophysal emplacement drifts. Neglecting the effects of heating is also a more pertinent approach because, over the preclosure period, most of the decay heat generated in the waste packages will be removed through forced ventilation.

The time-dependent drift degradation in the nonlithophysal rock units will essentially manifest itself by a reduction in joint strength; no significant geochemical alteration of the rocks nor time-related fracture growth within the intact rock blocks are anticipated to occur (Reference 2.2.1, Section 6.3.1.5). Therefore, the rockfall block dimensions, which are determined by the pre-existing fractures in the rock (Section 6.1.1), will not be affected by the time-dependent joint strength reduction. This is confirmed by comparing seismic ground motion simulations in which the nonlithophysal rock mass has conservatively degraded joint strength parameters, with the same simulations in which the nominal joint strength is applied: the maximum rockfall size remains unchanged (Reference 2.2.16, Section IV). The number of rockfalls remains stable, except in one rockfall simulation for which the number of rock blocks increased by 35 percent (Reference 2.2.16, Section IV). Over the preclosure period, however, it is unlikely that such a high percentage increase would be observed, because time-dependent degradation would not be able to degrade joint strength to the levels of the postclosure period.

In lithophysal rock units, thermal loading does not cause significant rockfall (Reference 2.2.16, Section V). However, contrary to what happens in nonlithophysal rock units, thermal loading does not render the rock mass more stable and resistant to ground shaking. Instead, it induces damage in the heated lithophysal rock mass around the drift, which, while not necessarily sufficient to trigger a rockfall under static conditions, would cause the damaged rock mass to be shaken down during a seismic event (Reference 2.2.16, Section VI). During the preclosure period, the rock damage would be insignificant anyway because the bulk of the decay heat from the waste packages would be removed through forced ventilation, leaving little heat to induce thermal stresses into the drifts.

Additional rockfall caused by the time-dependent strength degradation (static fatigue) in the lithophysal rock units is not expected to be significant (Reference 2.2.16, Section VII). Simulations accounting for thermal and time-dependent damage to the drifts predict only partial collapse at 20,000 yrs (Reference 2.2.16, Section VII), a considerably greater duration than the preclosure period. Coupling thermal loading and time-dependent strength degradation with ground motions associated with seismic events having an APE on the order of 10^{-4} causes additional, but not significant, rockfall as a result of shaking down already loose, broken ground (Reference 2.2.16, Section VII). More severe seismic events may have a more pronounced effect, such as partial to total drift collapse: this aspect is investigated in more detail in Section 6.3. In any case, partial to total drift collapse is intrinsically an extreme situation caused by severe ground motions and is not aggravated by thermal loading or strength degradation of joints.

Based on the foregoing discussion, it is concluded that in emplacement drifts excavated both in lithophysal and nonlithophysal rock units of the repository, significant rockfalls would be caused by seismic events. Thermal loading and time-dependent strength degradation of the rock units would have only a marginal role in the triggering of rockfalls. Therefore, the rest of this calculation centers on characterizing the most severe rockfalls initiated by earthquakes.

6.2 SEISMIC EVENTS OF INTEREST FOR ROCKFALL EVALUATION

6.2.1. Determination of Probabilities of Exceedance of Interest

As indicated in Section 1, this calculation focuses on credible rockfalls, that is rockfalls that have at least one chance in 10,000 of occurring during the preclosure period. Rockfalls that have a probability of occurrence less than that of a Category 2 event sequence can be eliminated from further consideration. Because the credible rockfalls are initiated by an earthquake (based on Section 6.1.2), the seismic events of interest for this calculation are those that have at least one chance in 10,000 of occurring over the preclosure period.

To characterize the probability of occurrence of seismic events over the preclosure period, a binomial distribution is used (Assumption 3.2.1). The corresponding probability distribution function evaluates, in a set of n trials, the number k of realizations of a given event that has a probability p, according to Equation 1 (Reference 2.2.3, p. A-12):

$$\Pr(k) = \frac{n!}{k!\,(n-k)!} \cdot p^{k} \cdot (1-p)^{n-k} \qquad \text{(Eq. 1)}$$

Here, the trials represent the years of the preclosure period ($n = 100$ per Reference 2.2.15, Section 2.2.2.8), and the event considered is the occurrence, in a given year, of a seismic event of a given severity or greater, the severity being associated with an APE p. Based on Equation 1, the probability of having at least one earthquake over the preclosure period is $1 - \Pr(0)$. Therefore, the most severe seismic events of interest for this calculation, i.e., those that have at least one chance in 10,000 of occurring over the preclosure period, follow the equation $1 - \Pr(0) = 10^{-4}$, which yields $1 - (1 - p)^n = 10^{-4}$. With a Taylor series development to the first order, this is approximated by $n \times p = 10^{-4}$, and therefore $p = 10^{-6}$ for the 100-yr preclosure period. Thus, the seismic events that meet the criterion of having an APE equal to or greater than 10^{-6} are the seismic events of interest for this calculation.

Among the seismic events investigated in Reference 2.2.1, those having an APE equal to 5×10^{-4}, 10^{-4}, 10^{-5}, and 10^{-6} meet the criterion developed previously. The return period for these earthquakes ranges between $1/(5 \times 10^{-4}) = 2{,}000$ yrs and $1/10^{-6} = 1{,}000{,}000$ yrs. The effects of these seismic events are considered for both the nonlithophysal and lithophysal rock units (Reference 2.2.1, Sections 6.3.1.2.1 and 6.4.2.2). The characterization of the resulting rockfalls is performed in Sections 6.3 and 6.4.

6.2.2. Conservatism of Ground Motion Hazard

Reference 2.2.1 (Section 6.3.1.6.4.2) uses ground motions that are based on expert elicitation and modeled with unbounded lognormal distributions. A consequence of this approach is that as the calculations are extended to lower and lower probabilities of exceedance, the ground motions increase without bound, eventually reaching levels that are not considered realizable (Reference 2.2.1, Section 6.3.1.6.4.2). Geological evidence shows that in the approximately 12.8 million years since the Topopah Spring Tuff that formed Yucca Mountain was deposited and cooled, no earthquake has occurred that would have subjected the rock mass to shear strain levels sufficient to result in fractures between lithophysal cavities (the existing fractures are a result of cooling) (Reference 2.2.1, Section 6.3.1.2.1, p. 6-63). Based on this geologic evidence, the unbounded peak ground velocities used in Reference 2.2.1 are highly conservative for severe earthquakes, notably those with an APE equal to 10^{-5} and 10^{-6}, and in turn produce correspondingly conservative estimates of rockfalls and drift damage for these earthquakes (Reference 2.2.16, Section VIII). Nonetheless, since estimates of rockfalls and drift damage associated with more realistic (i.e., bounded) peak ground velocities are not currently available for use, this calculation employs the estimates of Reference 2.2.1 without alteration, despite their large conservatism.

6.3 ROCKFALL CHARACTERIZATION IN LITHOPHYSAL ROCK UNITS

6.3.1. Initial Characterization

As described in Section 6.1.1, lithophysal rock units are characterized by intense small-scale fracturing and the presence of cavities (lithophysae) in the rock. The failure mode for this type of rock when stressed beyond its strength limit is expected to consist of relatively small rock block sizes, 0.1 m to 0.3 m in dimension (Reference 2.2.1, Section 6.4.1.1). Given that the approximate density of lithophysal rock is 2 metric tons/m^3 (including lithophysae)

(Reference 2.2.1, Section 6.4.2.2.2.1), a hypothetical spherical block with a diameter equal to 0.3 m (and therefore a volume of 1.41×10^{-2} m^3) would have a mass of approximately 28 kg. This rock block mass, given here for illustration purposes only, stands in contrast with the rockfalls produced by seismic events in nonlithophysal rock units, which have the potential to be considerably more massive (several hundred kilograms up to tens of metric tons, as indicated in Section 6.4.4.1).

A consequence of this inherent difference in block sizes is that rockfalls in the lithophysal rock units will induce a dynamic impact loading on waste packages significantly less important than that from the nonlithophysal rock units. In other words, the nonlithophysal dynamic impact provides a more conservative, bounding loading than the lithophysal dynamic impact (Reference 2.2.16, Section IX). Therefore, dynamic impact loading of the waste packages by falling lithophysal rock is not discussed further and only static loading resulting from the dead weight of accumulated lithophysal rocks on the waste packages is investigated in the remaining of Section 6.3.

The rockfall evaluations of Reference 2.2.1 do not account for the presence of ground support (Reference 2.2.1, p. ix). This conforms to the approach taken in this calculation, which does not take credit for ground support (Section 1). For completeness, the potential adverse effects of the presence of ground support on rockfall severity are discussed in Section 6.3.5.

6.3.2. Rockfalls Induced by Seismic Events with an Annual Probability of Exceedance Equal to 5×10^{-4} and 10^{-4}

The results of analyses reported in Reference 2.2.16 (Section X) indicate that seismic events with an APE equal to 5×10^{-4} and 10^{-4} (which respectively have return periods equal to $1/(5 \times 10^{-4}) = 2{,}000$ yrs and $1/10^{-4} = 10{,}000$ yrs) produce no to little rockfall in the emplacement drifts excavated in lithophysal rock. Thus, no significant static loading of the waste packages is to be expected from such earthquakes in these drifts.

6.3.3. Rockfalls Induced by Seismic Events with an Annual Probability of Exceedance Less than or Equal to 10^{-5}

The ground motions induced by seismic events with an APE less than or equal to 10^{-5} (which have a return period equal to $1/10^{-5} = 100{,}000$ yrs or greater) are very conservatively estimated, based on Section 6.2.2. Such ground motions are found to cause a partial to complete collapse of emplacement drifts excavated in the lithophysal rock units (Reference 2.2.16, Section XI). A seismic event with an APE less than or equal to 10^{-6} leads to the complete collapse of these drifts (Reference 2.2.16, Section XII).

Based on these results, and given that the earthquakes of interest in this calculation have a lower cutoff APE equal to 10^{-6} (Section 6.2.1), the scenario in which a severe seismic event would cause one or several emplaced waste packages to be buried under fallen rubble from a collapsed emplacement drift is credible, and cannot be screened out based on its probability of occurrence. Further investigation of this scenario is carried out by calculating an upper value of the pressure (static loading) that would be exerted on a waste package buried in a collapsed drift.

6.3.4. Analytical Evaluation of Static Loading on Waste Package

Reference 2.2.1 (Section 6.4.2.5.3) evaluates the static loading resulting from a collapsed drift; however this loading is calculated for a drip shield. During the preclosure period, a severe seismic event may occur before the installation of drip shields over the emplaced waste packages. Therefore, this calculation takes the approach that no drip shields are present in the drifts and that potential rockfalls will directly impact the already emplaced waste packages.

Reference 2.2.1 (Section 6.4.2.5.3) presents analytical solutions to calculate the vertical pressure that would be exerted on a piece of equipment buried under a collapsed drift. One of these solutions, summarized in Reference 2.2.16 (Section XIII), and designated as the piping mode of roof collapse, is used to model the extreme drift failure mode in which the rock directly above the excavated drift is considered to collapse in the drift below; no rock on the sides of the excavated drift participates in the collapse, and therefore this mechanism provides a conservative value of the dead weight exerted on the buried piece of equipment (Reference 2.2.16, Section XIII). Although the piping mode of roof collapse is a highly unlikely mode of drift collapse in the emplacement drifts (Reference 2.2.16, Section XIII), its analytical evaluation is appropriate for use in this calculation because it provides a simple and conservative method to evaluate the dead weight exerted by the rubble from a collapsed drift, and can be applied to a buried waste package rather than a buried drip shield. A quantitative evaluation of the conservatism of this analytical approach is given in Section 6.3.5.

The height H of the caved rock is controlled by the bulking factor B that measures the relative increase in volume (bulking) of the rock mass, which results from the fact that the fallen rock blocks do not fit together as they did before the caving. At a certain stage of caving, due to bulking, the volume of the caved rock completely fills the volume of the original excavation and the volume occupied by the collapsed rock before onset of collapse. When the cave is completely filled, the broken rock provides backpressure, which prevents further collapse of the rock. A value between 0.2 and 0.4 is considered to be a conservative estimate of the bulking factor (Reference 2.2.16, Section XIII). Further discussion of this range of values is provided in Section 6.3.5.

In the piping mode of roof collapse, H is calculated according to the formula (Reference 2.2.16, Section XIII):

$$\frac{H}{2 \cdot R} = \frac{1}{2} \cdot \left[\frac{\pi}{2 \cdot B} - \frac{b \cdot h}{2 \cdot B \cdot R^2} - \left(1 - \frac{\pi}{4} \right) \right] \qquad \text{(Eq. 2)}$$

where

R = radius of the emplacement drift (m)
B = bulking factor (dimensionless)
b = width of buried object (m)
h = height of buried object (m)

The value of R is 2.75 m, based on an emplacement drift diameter of 5.5 m (Reference 2.2.12, Table 8). Equation 2 shows that H is a decreasing function of b and h, which indicates that lower

estimates of b and h will yield conservative values of H. Based on Assumption 3.2.2, b is assigned a value of 1.83 m and h a value of 3.41 m. Equation 2 also shows that H is a decreasing function of B. Therefore, the value of B, which ranges between 0.2 and 0.4, is conservatively taken equal to 0.2. With these values, H is found equal to 15.3 m.

The vertical pressure P (in Pa) of the rubble on the buried waste package is given in Reference 2.2.16 (Section XIII) as:

$$P = \left(H + R - d_c\right) \cdot \frac{\rho \cdot g}{1 + B} \qquad \text{(Eq. 3)}$$

where

H = height of the caved rock (m)
R = radius of the emplacement drift (m)
d_c = height of the waste package above the drift centerline (m)
ρ = density of the rock (kg/m^3)
g = acceleration of gravity (m/s^2)
B = bulking factor (dimensionless)

The height d_c of the waste package above the drift centerline is equal to h - R = 3.41 - 2.75 = 0.66 m (the value of h is based on Assumption 3.2.2). The density ρ of the rock is taken as 2,411 kg/m^3, which is the mean density of the nonlithophysal rock units (Reference 2.2.16, Section XIV). Specifically, this mean density pertains to the Tptpln rock unit and represents the highest mean density value of the different rock units at the repository level (Reference 2.2.1, Section 4.1.3). The acceleration of gravity is equal to 9.81 m/s^2 (Reference 2.2.6, p. F-335). The bulking factor value of 0.2 is used, which is conservative given that P in Equation 3 is a decreasing function of B. Using Equation 3, and H = 15.3 m, the resulting vertical pressure P is equal to 3.4×10^5 Pa.

Thus, based on the previous calculation, the static dead weight loading on a waste package resulting from a collapsed emplacement drift is conservatively evaluated at 3.4×10^5 Pa.

6.3.5. Discussion of Conservatism of Analytical Evaluation

The conservatism of the analytical solution presented in Section 6.3.4 is further confirmed by a comparison to results of Reference 2.2.1 (Section 6.4.2.5.3), which, in addition to the analytical calculation of the static loading caused by the rubble of a collapsed drift, provides a more realistic modeling solved numerically. Although Reference 2.2.1 investigates the loading of a drip shield, not a waste package, relative variations between the drip shield loadings calculated analytically and numerically constitute a reasonable substitute to estimate the margin of conservatism of the analytical solution used for the waste package.

The numerical modeling considered in Reference 2.2.1 (Section 6.4.2.5.3) is more realistic than the analytical solution insofar as it takes into consideration the stress arching provided by the rubble, i.e., the redistribution of stresses by friction of the caved rock to the surrounding stable rock mass. In addition, Reference 2.2.1 (Section 6.4.2.5.3) uses a numerical discontinuum

approach, i.e., a modeling of the discrete rock blocks involved in the collapse of the drift, to predict a realistic shape of the caved region, in lieu of assuming it like in the piping mode of roof collapse.

The numerical discontinuum approach finds a vertical pressure on the drip shield less than 2×10^5 Pa, for values of the bulking factor close to 0.2, while the analytical solution for the piping mode of roof collapse finds a pressure on the drip shield approximately equal to 3.3×10^5 Pa for a bulking factor or 0.2 (Reference 2.2.16, Section XIII). Thus, the analytical solution yields a pressure estimate that is at least 65 percent greater than the more realistic discontinuum model.

The bulking factor in the numerical discontinuum approach is a result of the modeling, rather than an input like in the analytical solution; also, the bulking factor is found to be controlled by the size and shape of the falling rocks (Reference 2.2.1, Section 6.4.2.5.3, p. 6-225). Thus, depending on the inputs used for the simulations and because of the stochastic nature of rockfalls, different bulking factor values are predicted, as further detailed in the following paragraph.

The majority of the bulking factors calculated in the different simulations of Reference 2.2.1 are within the range of 0.2 to 0.4 mentioned in Section 6.3.4, with most of the values gravitating near 0.2 (Reference 2.2.1, Figure 6-179). Some conservative simulations produce bulk factor values slightly lower than 0.2, namely 0.17 and 0.19 (Reference 2.2.1, Figure 6-179). In these cases, however, the calculated pressure is still significantly lower (by the 65 percent margin mentioned previously) than the pressure found with the analytical solution for a bulk factor of 0.2. Finally, Reference 2.2.1 (Figure 6-179) has simulations for which the bulking factor is found to be in the 0.10 to 0.14 range. These reduced bulking factors, however, are not applicable to the present calculation because they describe rubble settlements that would occur during a seismic event with an APE equal to at most 10^{-5}, occurring after a previous seismic event having caused the drift collapse (Reference 2.2.1, Table P-10). The occurrence of two such seismic events is not credible over a preclosure period of 100 yrs, because the resulting probability would be less than 1 chance in 10,000. Indeed, the binomial distribution in Section 6.2.1 shows that the probability of having at least two earthquakes with an APE of at most 10^{-5} is approximately 5×10^{-7} over the preclosure period. In summary, the bulking factor of 0.2 used in Section 6.3.4 is in reasonable agreement with the results of the numerical discontinuum simulations performed in Reference 2.2.1.

Based on the foregoing discussion, it is concluded that the analytical solution used for calculating the static loading on a waste package buried in a collapsed drift provides a significant margin of conservatism compared to more realistic calculation methods, on the order of 65 percent. Another conservatism introduced in the analytical solution (Section 6.3.4), but whose margin is not quantified, includes the use of a rock density that pertains to a nonlithophysal rock zone (Tptpln) which represents the highest density value of the different rock units at the repository level.

The fact that the emplacement drifts have ground support is not anticipated to induce any adverse effect on a waste package in a collapsed emplacement drift. This is because the ground support would be buried in the rubble and would occupy a small fraction of the total volume of the caved

rock. The ground support considered for the emplacement drifts consists of 3 mm thick perforated stainless steel sheets, as well as rock bolts, which are 3 m long stainless steel tubes that are hollow and spaced at 1.25 m (Reference 2.2.2, Sections 7 and Table 3-6). This ground support would represent a marginal fraction of the rock mass in a collapsed drift.

6.4 ROCKFALL CHARACTERIZATION IN NONLITHOPHYSAL ROCK UNITS

6.4.1. Initial Characterization

Reference 2.2.1 (Section 6.3.1.2.1) analyzes the rockfalls in nonlithophysal rock units for seismic events having the following APE: 5×10^{-4}, 10^{-4}, 10^{-5}, 10^{-6}, and 10^{-7}. The seismic event with an APE equal to 5×10^{-4} is not given further consideration in this calculation because of the small amount of rockfall it would produce (Reference 2.2.16, Section XV). The seismic event with an APE equal to 10^{-7} is also not discussed further, based on Section 6.2.1. In the characterization of the credible rockfalls of the nonlithophysal rock units, this calculation therefore limits its investigation to the seismic events having an APE equal to 10^{-4}, 10^{-5}, and 10^{-6}.

In contrast to lithophysal rock, nonlithophysal rock is characterized by strong, intact blocks of welded tuff that are separated by fracture planes; the fracture surfaces provide the primary weaknesses in the system and control the failure mode and resulting rock block dimensions (Reference 2.2.16, Section I). To model the response of the nonlithophysal rock units to seismic shaking, Reference 2.2.1 employs a three-dimensional discontinuum program which is capable of simulating the behavior of a rock block assemblage as it is subjected to seismic loads (Reference 2.2.1, Section 6.1.6.1). The program uses a synthetic fracture geometry that is calibrated against field data from the repository area and thus ensures that the fracture characteristics of nonlithophysal rock units are appropriately represented in the model (Reference 2.2.1, Section 6.1.6.4.6).

The simulations show that even for the seismic event with an APE of 10^{-4} (a relatively mild earthquake compared to those having a lesser APE), nonlithophysal rock blocks having a mass of several metric tons are predicted at distribution extremes (see Table 6). Dynamic impacts therefore provide a more conservative loading in nonlithophysal rocks than in lithophysal rocks, which tend to produce relatively small blocks. Conversely, dead weight from a collapsed drift in lithophysal rock units will provide a more conservative static loading than in nonlithophysal rock units. This is because nonlithophysal blocks are more voluminous than lithophysal blocks, and therefore have a higher bulking factor when fallen. The bulking factor, previously mentioned in Section 6.3.4, measures the relative increase in volume of fallen rock blocks (due to bulking of the rubble composed of individual blocks that do not fit together), compared to the initial volume before the caving. Bigger rocks tend to have a higher bulking factor than smaller ones: Reference 2.2.1 (Figure 6-179) shows that bulking factors of 0.3-m rocks are larger than bulking factors of 0.2-m rocks. Because the pressure exerted by fallen rocks onto a waste package is a decreasing function of the bulking factor (Equations 2 and 3 of Section 6.3.4), the static loading from nonlithophysal rockfalls is less than the static loading of lithophysal rockfalls. Static loading in lithophysal rock units is considered in Section 6.3; only dynamic loading from nonlithophysal rockfalls requires further investigation in the rest of Section 6.4.

The rockfall evaluations of Reference 2.2.1 do not include ground support (Reference 2.2.1, p. ix). This conforms to the approach taken in this calculation, which does not take credit for ground support (Section 1). For completeness, the potential adverse effects of the presence of ground support on rockfall severity are discussed in Sections 6.4.5.2 and 6.4.6 of this calculation.

The outputs of rockfall simulations performed in Reference 2.2.1 for nonlithophysal rock units are tracked by DTN: MO0408MWDDDMIO.002 (Reference 2.2.7), in the specific following files:

- *nonlith rockfall characteristics in emplacement drifts with 1e-4 gm.xls* for rockfalls triggered by seismic events with an APE equal to 10^{-4}
- *nonlith rockfall characteristics in emplacement drifts with 1e-5 gm.xls* for rockfalls triggered by seismic events with an APE equal to 10^{-5}
- *nonlith rockfall characteristics in emplacement drifts with 1e-6 gm.xls* for rockfalls triggered by seismic events with an APE equal to 10^{-6}

DTN: MO0408MWDDDMIO.002 (Reference 2.2.7) is cited in the *IED Geotechnical and Thermal Parameters III* (Reference 2.2.16) for rockfall characteristics, and, therefore, is approved and appropriate for use in this calculation.

Sections 6.4.2 to 6.4.4 discuss the rockfall simulation outputs from Reference 2.2.7, and how they are used in this calculation.

6.4.2. Rockfall Rate in Emplacement Drifts

6.4.2.1. Evaluation of Rockfall Rate Distribution

Table 1 summarizes the main characteristics of the sets of rockfall simulations pertaining to the seismic events of interest in this calculation, i.e., having an APE equal to 10^{-4}, 10^{-5}, or 10^{-6} (Section 6.4.1).

Table 1. Summary Statistics for Rockfall Simulations

Parameter	Annual Probability of Exceedance of Seismic Event		
	10^{-4}	10^{-5}	10^{-6}
Simulations Completed	32[c]	50[d]	50[e]
Total length of Simulated Drift[a]	640 m	1,000 m	1,000 m
Total number of Rockfalls	428[c]	1,767[d]	2,797[e]
Number of Rockfalls per Meter of Simulated Drift[b]	0.669	1.77	2.80

NOTE: [a]The total length of simulated drift is the product of the number of simulations by the drift length of each simulation, which is 20 m per simulation, based on Assumption 3.2.8.
[b]Numbers are shown to three significant figures.
[c]Source is Reference 2.2.16 (Section XVI).
[d]Source is Reference 2.2.16 (Section XVII).
[e]Source is Reference 2.2.16 (Section XVIII).

As the severity of the earthquake increases, the rate of rockfalls, i.e., the number of rockfalls per meter of drift, which is calculated as the number of simulated rockfalls per meter of simulated drift, increases too. Table 1, however, is too general to draw conclusions on the distribution of the rate of rockfalls. Such a distribution does not only depend on the severity of the seismic event, but also on the fracture geometry in the rock mass around the emplacement drifts. Therefore, the rockfall rate yielded by individual simulations (each representing 20 m of drift, based on Assumption 3.2.8) must also be analyzed.

Figure 1 displays the empirical cumulative distribution associated with the rockfall rate, for each of the seismic events of interest in this calculation. The empirical cumulative distribution function of a random variable x returns the ratio of the number of observations less than or equal to x over the total number of observations (Reference 2.2.9, p. 97).

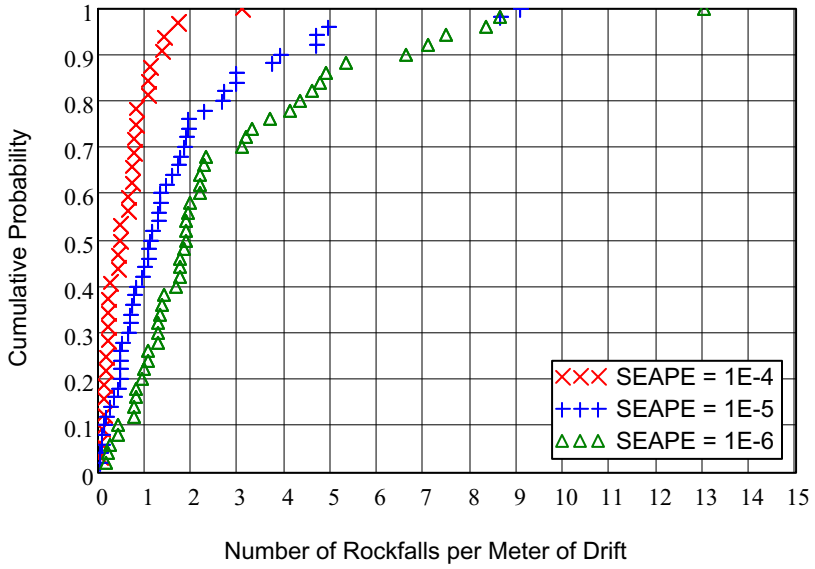

SOURCE: Attachment A, Figure A-1
SEAPE = Seismic Event Annual Probability of Exceedance

Figure 1. Empirical Cumulative Distribution for Rockfall Rate

To improve the statistical tractability of the rockfall rate distribution necessary to carry out further calculations, its empirical cumulative distribution function is fitted to a lognormal distribution.

A random variable x follows a lognormal distribution if its logarithm, $\ln(x)$, follows a normal distribution (Reference 2.2.9, p. 47). Fitting the rockfall rate data to a lognormal distribution is thus performed by fitting the logarithm of the rockfall rate data to a normal distribution. One of the simulations pertaining to the seismic event with a 10^{-5} APE yielded no rockfall (Reference 2.2.16, Section XVII), and therefore the logarithm of its rockfall rate does not exist. This particular case is conservatively addressed by considering that the simulation yielded one rockfall.

The lognormal fitting and the verification of its adequacy is carried out by following the method outlined in Reference 2.2.9 (Section 4.8), for normal distributions with mean and standard deviation that are unknown a priori. The mean and standard deviation of the fitted normal distribution are taken equal to the sample mean and sample standard deviation of the logarithm of the rockfall rate data. The adequacy of the fitting is verified by an Anderson-Darling test (that uses the Anderson-Darling statistic termed A^2) (Reference 2.2.9, Sections 4.2.2. and 4.2.3). The Anderson-Darling test is chosen because it has good power against a wide range of alternatives (Reference 2.2.9, Section 4.16.1).

The details of the goodness-of-fit calculations are shown in Attachment A. The Anderson-Darling statistic for the rockfall rate pertaining to the seismic events with an APE equal to 10^{-4}, 10^{-5}, and 10^{-6} are found respectively equal to 0.415, 0.599, and 0.393. These values are below the threshold of 0.752, which is the 5 percent significance level of the Anderson-Darling statistic (Reference 2.2.9, Table 4.7, statistic A^2). Consequently, it is concluded that the fitted lognormal distributions pass the Anderson-Darling test at the 5 percent significance level, and thus are acceptable for modeling the rockfall rate.

Figure 2 shows the rockfall rate data along with the fitted lognormal distributions.

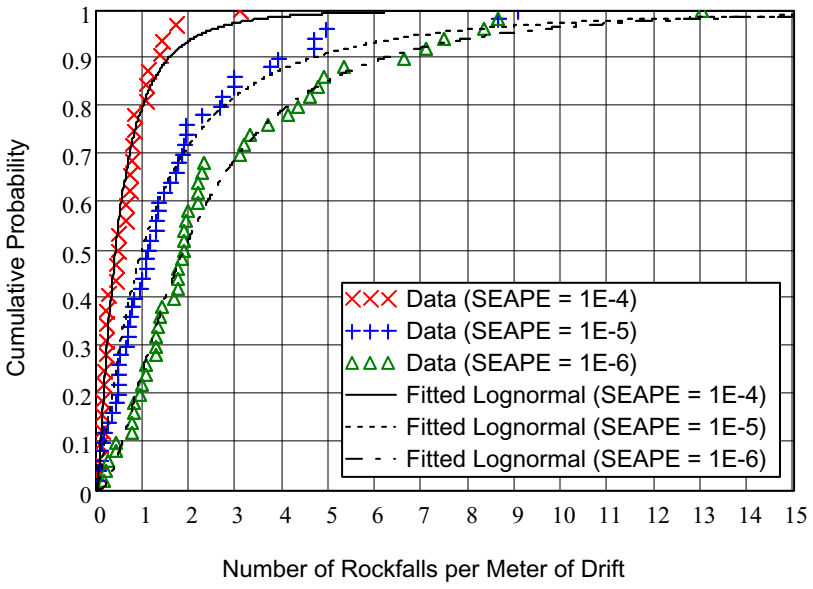

SOURCE: Attachment A, Figure A-2
SEAPE = Seismic Event Annual Probability of Exceedance

Figure 2. Rockfall Rate Data with Fitted Lognormal Distributions

6.4.2.2. Conservatism of Rockfall Rate

Reference 2.2.1 (Section 6.3.1.6.6) explains that the rockfall simulations are performed using a block deletion scheme, in which a fallen rock block is deleted after impact on the drip shield. This scheme, which is used to record all possible rockfalls that could impact the drip shield, leads to conservative estimates of the upper values of the rockfall rate distribution. Without

block deletion, the rubble would pile up, and the relative increase in volume of fallen rock blocks (due to bulking of the rock rubble composed of individual blocks that do not fit together: see Sections 6.4.1 and 6.3.4) would eventually fill the open cavity and thus prevent further rockfalls.

This is confirmed by comparing two simulations producing many rockfalls, in which the block deletion scheme is used, to the same simulations where the block deletion scheme is not used (Reference 2.2.1, Section 6.3.1.6.6). It is found that with block deletion, the number of fallen rock blocks significantly increases from the case without block deletion, averaging approximately 60 percent for two simulations (Reference 2.2.16, Section XIX). The rockfall rate for these simulations, which is directly proportional to the number of rockfalls, would likewise be increased by the same percentages.

These results indicate that the rockfall rate distribution provides significant conservatism in its upper values. Nevertheless, no quantitative adjustment of the distribution is performed, because the percentages in the previous paragraph pertain to simulations where the seismic event has an APE equal to 10^{-7}, which is below the threshold considered in this calculation (Section 6.2.1). A seismic event with an APE equal to 10^{-6} or 10^{-5} would typically dislodge less rock blocks, in which case the block deletion scheme, while still conservative, may not so significantly overestimate the number of rockfalls.

Another conservatism in the rockfall rate is in its fitting to a lognormal distribution. Such a distribution is unbounded to the right and therefore theoretically reaches infinity. In reality however, the number of rockfalls per meter of drift would have an upper value determined by the stage of degradation at which an emplacement drift reaches mechanical stability. This calculation takes the approach of not trying to estimate an upper bound for the rockfall rate; instead, it leaves the fitted rockfall rate distribution unbounded. This is conservative as a Latin hypercube sampling is performed in Section 6.4.5.2 and carried out on 1,000 samples, which implies that the lognormal distribution is sampled at least to the 99.9^{th} percentile, which corresponds to very high rockfall rate values.

Finally, the rockfall rate is also conservative because it uses a lower value for the length of simulated drift, as explained in Assumption 3.2.8.

6.4.3. Rockfall Impact Velocity

6.4.3.1. Velocity Adjustment for Impacts on Waste Packages

The simulations provide the relative velocity of the rockfalls as they hit the drip shield (Reference 2.2.1, Section 6.3.1.1). This means that the impact velocity data account both for the velocity of the rockfall and the velocity of the drip shield shaken by the ground motions at the time of impact. This is an adequate representation of impacts because it accounts for the possibility that a given drip shield could be moving upwards when it is hit by a falling rock, which would amplify the severity of the collision.

As indicated in Section 6.3.4, this calculation takes the approach that no drip shields are present in the drifts. Velocity data therefore need to be adjusted for impacts occurring on waste packages, not drip shields. To make this adjustment, the following factors are taken into account:

- The approach is taken that all rockfalls that hit a drip shield would hit the waste package below if the drip shield were not present. This is conservative given that a rockfall that would have hit the edge of a drip shield may conceivably not impact the waste package below.

- The waste package is assumed to behave as if fixed to the invert of the drift (Assumption 3.2.3). With this assumption, the velocity difference between a rock falling onto a drip shield and the same rock falling onto a waste package when no drip shield is present is due to the additional energy gained by the rock during the free fall from the virtual drip shield impact location to the waste package impact location.

- The velocity adjustment due to free fall is performed only for those rockfalls that impact the portion of the drip shield that is located at an angle more than 28 degrees above the drip shield centerline (Assumption 3.2.4). This corresponds to the top portion of the drip shield, down to its shoulders, as displayed on Figure B-1 of Attachment B, where the 28 degree angle is designated by α.

- The velocity adjustment due to free fall is assumed to add a conservative value of - 0.74 m/s to the vertical component of the velocity (Assumption 3.2.5). the adjustment is negative to indicate that the added velocity has a downward direction in the Cartesian system of coordinates.

The calculation of velocity adjustments is detailed in Attachment A. The sign of the total impact velocities is not of interest in the rest of this calculation, and therefore, from here on, the impact velocities are identified to their absolute values. Table 2 summarizes the results for the different seismic events of interest.

Table 2. Summary Statistics for Adjusted Velocities (Impacts on Waste Packages)

	Annual Probability of Exceedance of Seismic Event		
Parameter[a]	**10^{-4}**	**10^{-5}**	**10^{-6}**
Mean (m/s)	2.73	3.07	3.58
Standard Deviation (m/s)	1.53	1.60	1.82
Minimum Observed (m/s)	0.03	0.04	0.07
Maximum Observed (m/s)	7.20	10.14	12.59

NOTE: [a]Velocity statistics are shown rounded up to the closest cm/s, and as absolute values.
SOURCE: Attachment A

6.4.3.2. Assessment of Upper Tail of Impact Velocity Distribution

The calculations in Section 6.4.5 require the probabilities associated with large impact velocities, possibly greater than the maximum yielded by the simulations (Table 2), to be evaluated. This is done in this section by assessing the behavior of the upper tail of the impact velocity distribution.

Reference 2.2.9 (p. 97) defines the empirical cumulative distribution function of a random variable x as the ratio of the number of observations less than or equal to x over the total number of observations. The function therefore takes the value 1, its upper bound, for x equal to the greatest observed value, which is not practical for investigating the upper tail of a distribution, because higher values than the maximum observed data may need to be considered. The

empirical cumulative distribution function is therefore redefined as returning the ratio of the number of observations less than or equal to x over $n+1$, where n is the total number of observations. This redefinition conforms to that given in Reference 2.2.10 (p. 36), and returns very similar values to those of Reference 2.2.9 (p. 97) for large values of n, and has the advantage of not reaching its bounding probability value of 1. This redefinition is used in the rest of this calculation.

The complementary empirical cumulative distribution function (which is the complement to 1 of the empirical cumulative distribution function) is plotted on a semi-logarithmic scale. Figure 3 shows the resulting graph for the seismic events of interest in this calculation. The curves overall appear to be concave downwards, which suggests that for a given seismic event severity, the rockfall impact velocities trend towards an upper bound. This is further confirmed by a physical argument, as explained in what follows.

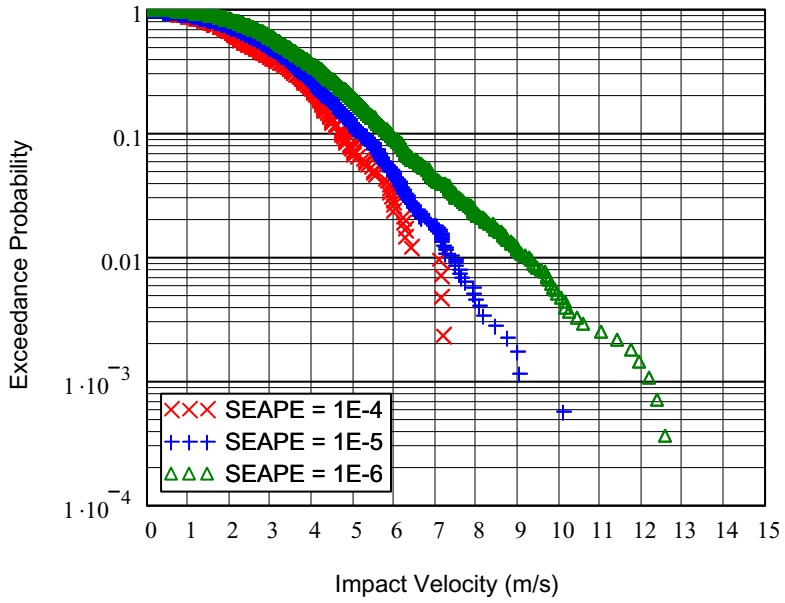

SOURCE: Attachment A, Figure A-3
SEAPE = Seismic Event Annual Probability of Exceedance

Figure 3. Complementary Empirical Cumulative Distribution for Rockfall Impact Velocity

As indicated in Section 6.4.3.1, the rockfall impact velocity is a relative velocity, and therefore has three components: the initial dislodgment velocity from the emplacement drift, the velocity gained during free fall due to acceleration of gravity, and the velocity of the waste package at the time of impact.

The first and third components are controlled by the severity of the seismic event, and therefore are within the bounds of the peak ground velocity of the earthquake that triggers the rockfalls. For example, the vertical and horizontal components of the peak ground velocities considered in Reference 2.2.1 (Table 6-5), for the seismic event with an APE equal to 10^{-4}, 10^{-5}, and 10^{-6}, are respectively less than 0.48 m/s, 1.05 m/s, and 2.45 m/s. As indicated in Section 6.2.2, the peak

ground velocities are conservative for severe earthquakes, notably those with an APE equal to 10^{-5} and 10^{-6}.

The second component of the impact velocity is inherently limited by the free-fall drop height of the rock blocks in the emplacement drifts. Although the drop height may increase as rock blocks fall from the drift ceiling and thus open it up for potentially higher-perched rock blocks, there is a limit to the ceiling opening, controlled by the intrinsic severity of the seismic event. Even for the most severe earthquakes, the relative increase in volume of fallen rock blocks (due to bulking of the rock rubble composed of individual blocks that do not fit together: see Sections 6.4.1 and 6.3.4) would eventually fill the open cavity and thus limit the rockfall drop height.

For a given seismic event, there is therefore a physical upper bound to the rockfall impact velocity on waste packages. Nonetheless, this calculation does not attempt to determine the value of this physical bound. This is because of the inherent stochastic variability of the parameters that factor in this value, which would make a quantitative estimation overly complex or conservative. Instead, this calculation takes the approach of assessing the extreme values of an unbounded rockfall impact velocity distribution, which is conservative, and basing them on statistical considerations. This is done in Section 6.4.3.3.

6.4.3.3. Characterization of Extreme Values of Impact Velocity Distribution

Reference 2.2.10 provides theoretical bases for the statistical analysis of extreme values of a distribution. It is found useful to express the high probability taken by a distribution F at x in relation to a threshold u, and focus on the excess values y defined by $y = x - u$, where x is greater than u. The probability that a value less than or equal to $u + y$ be observed, given that u is exceeded, is, modified from Reference 2.2.10 (Section 4.1, Equation 4.1):

$$P\langle x \le u + y \,|\, x > u \rangle = \frac{F(u+y) - F(u)}{1 - F(u)} \qquad \text{(Eq. 4)}$$

The conditional probability distribution expressed in Equation 4 as a function of y is the distribution of threshold exceedance H. The extreme value theory finds that for a large class of distributions and a sufficiently large value of u, H is well approximated by a generalized Pareto distribution (Reference 2.2.10, Section 4.2, Equation 4.2):

$$H(y) = 1 - \left(1 + \frac{\xi \cdot y}{\sigma}\right)^{-1/\xi} \qquad \text{(Eq. 5)}$$

where ξ and σ are constants. If ξ is negative, H has an upper bound equal to $-\sigma/\xi$; if ξ is positive, H has no upper limit; and if $\xi = 0$, H becomes an exponential distribution with parameter $1/\sigma$ (Reference 2.2.10, Section 4.2, Equation 4.4):

$$H(y) = 1 - \exp\left(-\frac{y}{\sigma}\right) \qquad \text{(Eq. 6)}$$

The previous discussion finds that the rockfall impact velocity associated with a given earthquake severity is bounded, therefore the generalized Pareto distribution approximating the distribution of threshold exceedance for sufficiently large impact velocities would have a parameter ξ less than zero. However, since this calculation follows the conservative approach of not bounding the impact velocity, ξ is assigned the smallest possible value short of a strictly negative value, i.e., zero. An exponential distribution is thus used to model the extreme values of the impact velocity distribution. Said otherwise, Equation 4 can be equated with the exponential distribution given in Equation 6, which, after re-arrangement, simplification, and using the fact that $y = x - u$, yields:

$$F(x) = F(u) + [1 - F(u)] \cdot \left[1 - \exp\left(- \frac{x-u}{\sigma} \right) \right] \quad \text{(Eq. 7)}$$

where $x > u$ and σ is a constant.

The complementary cumulative distribution, $\overline{F}(x)$, defined as $1 - F(x)$, can therefore be expressed as:

$$\overline{F}(x) = \overline{F}(u) \cdot \exp\left(- \frac{x-u}{\sigma} \right) \quad \text{(Eq. 8)}$$

where $x > u$. On the semi-logarithmic scale of Figure 3, which is equivalent to taking the logarithm in Equation 8, the complementary distribution $\overline{F}(x)$ would appear as a ray starting at a velocity u_v, having an exceedance probability equal to $\overline{F}(u_v)$, and a slope equal to $-1/\sigma$.

The parameter u_v represents the threshold beyond which the impact velocity is adequately and conservatively described by an exponential distribution. Based on Figure 3, thresholds equal to 5 m/s, 7 m/s, and 9 m/s are selected for the seismic events having an APE respectively equal to 10^{-4} , 10^{-5}, and 10^{-6}. The threshold values are chosen such that they leave enough observations for a meaningful fitting (Table 3 shows the number of observations used for the fittings), and because the complementary empirical cumulative distributions are approximately compatible with straight lines beyond these thresholds, which ensures that a fitting to an exponential distribution is appropriate. The overall concavity of the empirical curves further suggests that even if new simulations produced rockfalls with greater impact velocities than shown in Table 2, they would have an exceedance probability less than that of the fitted exponential distributions, indicating that the exponential fittings yield conservative estimates.

The quantitative fitting of the upper tail of the impact velocity distribution to an exponential distribution is performed in Section 6.4.3.5.

6.4.3.4. Characterization of Medium Values of Impact Velocity Distribution

While the exponential distribution is acceptable for evaluating the exceedance probabilities associated with impact velocities greater than u_v (Section 6.4.3.3), a different distribution is needed to adequately represent the lower part of the distribution, corresponding to impact

velocities less than or equal to u_v. A Weibull distribution is chosen. A widely utilized form of the Weibull distribution, the two-parameter form (in which the location parameter is taken equal to zero) has a cumulative distribution function given in Reference 2.2.3 (p. A-18) as:

$$W(x) = 1 - \exp\left[-\left(\frac{x}{\alpha}\right)^{\beta}\right] \quad \text{(Eq. 9)}$$

where x is the random variable ($x > 0$), α is a scale parameter ($\alpha > 0$), and β is a shape parameter ($\beta > 0$). The Weibull distribution is chosen because it is a generalization of the exponential distribution (Reference 2.2.3, p. A-18), and is therefore deemed a natural choice for prolonging the exponential distribution to lower velocity values. Considering the complementary distribution $\overline{W}(x) = 1 - W(x)$, and taking twice the logarithm in Equation 9 leads to the following expressions:

$$\overline{W}(x) = \exp\left[-\left(\frac{x}{\alpha}\right)^{\beta}\right]$$

$$\ln\left(\overline{W}(x)\right) = -\left(\frac{x}{\alpha}\right)^{\beta}$$

$$\ln\left[-\ln\left(\overline{W}(x)\right)\right] = \beta \cdot \ln\left(\frac{x}{\alpha}\right)$$

$$\ln\left[-\ln\left(\overline{W}(x)\right)\right] = \beta \cdot \ln(x) - \beta \cdot \ln(\alpha) \quad \text{(Eq. 10)}$$

A log-log graph of $-\ln\left(\overline{W}(x)\right)$ as a function of x would take the shape of a straight line having a slope equal to β. Figure 4 shows a representation of such a graph for impact velocity data ranging between 1 and 10 m/s. It is seen that the curves take the approximate shape of a straight line for velocities w_v comprised roughly between 4 m/s and the values of u_v considered earlier, i.e., 5 to 9 m/s, depending on the severity of the earthquake. A Weibull fitting over this range of data therefore appears adequate.

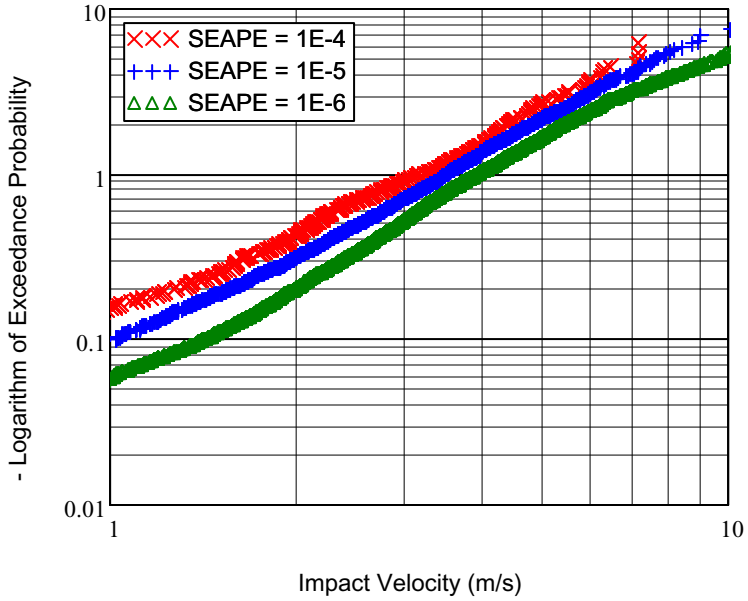

SOURCE: Attachment A, Figure A-4
SEAPE = Seismic Event Annual Probability of Exceedance

Figure 4. Negative Logarithm of Complementary Empirical Cumulative Distribution for Rockfall Impact Velocity

The quantitative fitting of medium velocities to a Weibull distribution is performed in Section 6.4.3.5.

6.4.3.5. Impact Velocity Distribution Fitted to Exponential and Weibull Distributions

To carry out the fitting of the Weibull and the exponential distribution to the impact velocity data, the following factors are taken into account:

- The data are fitted with a Weibull distribution for velocities greater than or equal to a lower threshold w_v and less than an upper threshold u_v (Section 6.4.3.4), and with an exponential distribution for velocities greater than or equal to u_v (Section 6.4.3.3).

- The exceedance probability $\overline{F}(u_v)$ associated with u_v is assigned the value determined by the Weibull fitting, namely $\overline{W}(u_v)$. This leaves σ as the only parameter to evaluate in Equation 8 for the exponential distribution. Equating $\overline{F}(u_v)$ with $\overline{W}(u_v)$ ensures a continuity between the exponential fitting and the Weibull fitting and therefore the continuity of the overall velocity distribution.

- No fitting of the velocity data having a value less than w_v is performed. Instead, these velocities are assigned the probability of the fitted Weibull distribution. This approximation is acceptable because the rockfalls having a velocity less than w_v are

not part of the severe rockfalls of interest in this calculation, as discussed in Section 6.4.5.2.5.

The values of u_v and w_v are qualitatively chosen, using Figure 3 and Figure 4 as a visual aid to determine the regions where the observations take the approximate shape of a straight line. Various values can yield acceptable Weibull and exponential fits. A selection is made that incorporates sufficient data for the fittings to be meaningful, and that at the same time allows for a qualitatively adequate overall fit of the observations of interest (i.e., those exceeding w_v). Table 3 summarizes the values selected for u_v and w_v, as well as the resulting number of observations used for each fitting.

Table 3. Input Parameters for Exponential and Weibull Fittings of Rockfall Impact Velocity Distribution

Parameter	Annual Probability of Exceedance of Seismic Event		
	10^{-4}	10^{-5}	10^{-6}
Threshold Velocity for Exponential Fitting (u_v)[a]	5 m/s	7 m/s	9 m/s
Number of Observations for Exponential Fitting[b]	30	31	33
Threshold Velocity for Weibull Fitting (w_v)[a]	4 m/s	5 m/s	5.5 m/s
Number of Observations for Weibull Fitting[b]	65	173	339

NOTES: [a]Values of this input are qualitatively selected.
[b]Source for this input is Attachment A, based on the values selected for u_v and w_v.

The parameters of the fitted Weibull and exponential distribution are determined by linear regression. As indicated in Reference 2.2.11 (pp. 113 to 115), the linear regression model relates a set of observations z_i to a set of input variables t_i (where i is an index) through a linear function and a noise term represented by random variables ε_i, referred to as errors or residuals, independently distributed as a normal distribution with a mean equal to zero and a standard deviation δ. In the context of the Weibull and exponential fittings performed in this calculation, a given observation z_i in a set of n observations is related to the input variable t_i through the relation:

$$z_i = r \cdot t_i + q + \varepsilon_i \quad \text{(Eq. 11)}$$

where r and q are constants and the residuals ε_i follow a normal distribution with mean 0 and standard deviation δ.

Specifically, for the Weibull distribution fitting, the relationship between the observed impact velocities and the input variables, i.e., the exceedance probabilities of the complementary empirical distribution function, is found by re-arrangement of Equation 10 and identification to the terms of Equation 11, which yields:

- $z_i = \ln(x_i)$ where x_i is an observed impact velocity.

- $t_i = \ln\left[-\ln\left(\overline{W}(x_i)\right)\right]$ where $\overline{W}(x_i)$ is the exceedance probability associated with x_i.
- $r = 1/\beta$ where β is the shape parameter of the fitted Weibull distribution.
- $q = \ln(\alpha)$ where α is the scale parameter of the fitted Weibull distribution.

For the exponential fitting, it is beneficial to first express the observed impact velocities as excess velocities with respect to u_v, the minimum observed velocity considered for the exponential fitting (Table 3). In the same way, the input variables, i.e., the exceedance probability of the complementary empirical distribution function, are expressed as exceedance from $\overline{F}(u_v)$. Taking the logarithm in Equation 8, re-arranging the terms and identifying to the terms of Equation 11 yields:

- $z_i = x_i - u_v$ where x_i is an observed impact velocity.
- $t_i = \ln\left(\overline{F}(x_i)\right) - \ln\left(\overline{F}(u_v)\right)$ where $\overline{F}(x_i)$ is the exceedance probability associated with x_i.
- $r = -\sigma$ where $1/\sigma$ is the parameter of the fitted exponential distribution.
- $q = 0$

As documented in Attachment A, the parameters r and q are calculated with Mathcad as least-squares estimates in the linear regressions. The calculation of the unknown parameters of the Weibull distribution, α and β, is then straightforward based on the above equalities. In the case of the exponential distribution, there is one unknown parameter, σ. Table 4 shows the calculated results.

Table 4. Parameters of Fitted Exponential and Weibull Distributions for Rockfall Impact Velocity

Parameter[a]	Annual Probability of Exceedance of Seismic Event		
	10^{-4}	10^{-5}	10^{-6}
Scale Parameter of Weibull Distribution (α)	3.41 m/s	3.48 m/s	3.53 m/s
Shape Parameter of Weibull Distribution (β)	2.59	2.06	1.64
Inverse of Parameter of Exponential Distribution (σ)	0.734 m/s	0.842 m/s	1.19 m/s

NOTE: [a]Parameters are shown to three significant figures.
SOURCE: Attachment A

Figure 5 shows the rockfall impact velocity data along with the fitted distributions.

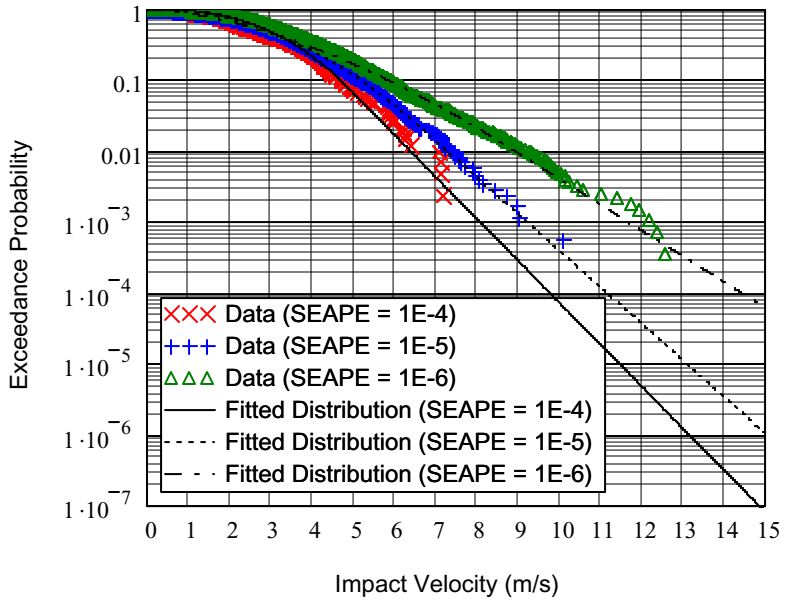

SOURCE: Attachment A, Figure A-5
SEAPE = Seismic Event Annual Probability of Exceedance

Figure 5. Rockfall Impact Velocity Data with Fitted Distributions

To quantitatively confirm that the Weibull and exponential fittings are reasonable, the normality of the residuals ε_i of the linear regressions is tested, using the approach outlined in Reference 2.2.9 (Section 4.8.5). The calculations are carried out in Attachment A. For the seismic events having an APE equal to 10^{-4}, 10^{-5}, and 10^{-6}, the Kolmogorov-Smirnov statistic D is evaluated and found respectively equal to 0.080, 0.042, and 0.053 for the Weibull fittings, and to 0.125, 0.085, and 0.214 for the exponential fittings. These values are lower than the 5 percent significance level value for the test, which is 0.895 (Reference 2.2.9, Table 4.7, Statistic D). Therefore, the test is passed at this significance level, which shows that the overall Weibull and exponential fittings are not unreasonable.

Contrary to what was done in Section 6.4.2, an Anderson-Darling test is not performed, nor would it be anticipated to be passed if used. This is because of this test's sensitivity in detecting departures in the tails of the distribution (Reference 2.2.9, Section 4.16.1). With the numerous data used in many of the fittings (going as high as 339, based on Table 3), it is expected that some data points will depart from the regression line to a sufficient extent for the Anderson-Darling test not to be passed at the 5 percent significance level. This, however, underlines the high sensitivity of the Anderson-Darling test to outliers, and does not imply that the overall fittings are inadequate. The fact that the Kolmogorov-Smirnov test is passed at the 5 percent significance level shows that the Weibull and exponential distribution fits are acceptable.

The parameters α and β of the fitted Weibull distribution and the parameter σ of the fitted exponential distribution are calculated based on the velocity data and as such are random variables with an intrinsic uncertainty. This uncertainty is examined in Section 6.4.3.6, but only for the exponential distribution, because the large number of data points used for the Weibull

distribution (Table 3) ensures that the variability of α and β is small enough to consider these parameters constant.

6.4.3.6. Parameter Variability for Exponential Fittings

Reference 2.2.11 (Section 2.7) provides bases for a Bayesian estimation of the variability of the parameters of the linear regressions used in Section 6.4.3.5. The slope of the linear regression, (r in Equation 11), which is also equal to $-\sigma$ (Section 6.4.3.5) is assigned a prior distribution. A noninformative prior is used, considering that little is known a priori about the distribution of the parameter r (Reference 2.2.11, Section 1.3.7). Reference 2.2.11 (p. 118) goes on to show that the posterior distribution for r is associated with a Student's t distribution that has $n - k$ degrees of freedom, where n is the number of data points in the linear regression (Table 3), and k is the number of unknown regression coefficients, i.e., $k = 1$ (since Equation 11 has one such coefficient, r, the other regression coefficient, q, is known and equal to 0 for the exponential fitting). The calculations are performed in Attachment A. Table 5 shows the 5th percentile, the mean, and the 95th percentile associated with σ for each of the seismic events of interest in this calculation.

Table 5. Parameter Variability of Fitted Exponential Distribution for Rockfall Impact Velocity

Value Taken by Inverse of Parameter of Exponential Distribution (σ)	Annual Probability of Exceedance of Seismic Event		
	10^{-4}	10^{-5}	10^{-6}
5th percentile[b] (m/s)	0.688	0.814	1.14
Mean[a,b] (m/s)	0.734	0.842	1.19
95th percentile[b] (m/s)	0.781	0.869	1.25

NOTE: [a] The mean is the least-squares estimate of Section 6.4.3.5 (Reference 2.2.11, p. 118).
[b] Values are shown to three significant figures.
SOURCE: Attachment A

6.4.4. Rockfall Mass

6.4.4.1. Preliminary Assessment of Rockfall Mass Distribution

Table 6 summarizes the rockfall mass statistics yielded by the simulations.

Table 6. Summary Statistics for Rockfall Mass

Parameter[a]	Annual Probability of Exceedance of Seismic Event		
	10^{-4}	10^{-5}	10^{-6}
Mean (metric tons)	0.22	0.35	0.43
Standard Deviation (metric tons)	0.33	0.93	1.30
Minimum Observed (metric tons)	0.02	0.02	0.02
Maximum Observed (metric tons)	2.72	19.07	28.22

NOTE: [a]Rockfall mass statistics are shown rounded up to the closest hundredth of metric ton.
SOURCE: Attachment A

The calculations in Section 6.4.5 require the probabilities associated with large rockfall masses, possibly greater than the maximum yielded by the simulations (Table 6), to be evaluated. This is

done in this section by assessing the behavior of the upper tail of the rockfall mass distribution, whose complementary empirical cumulative distribution is illustrated on Figure 6.

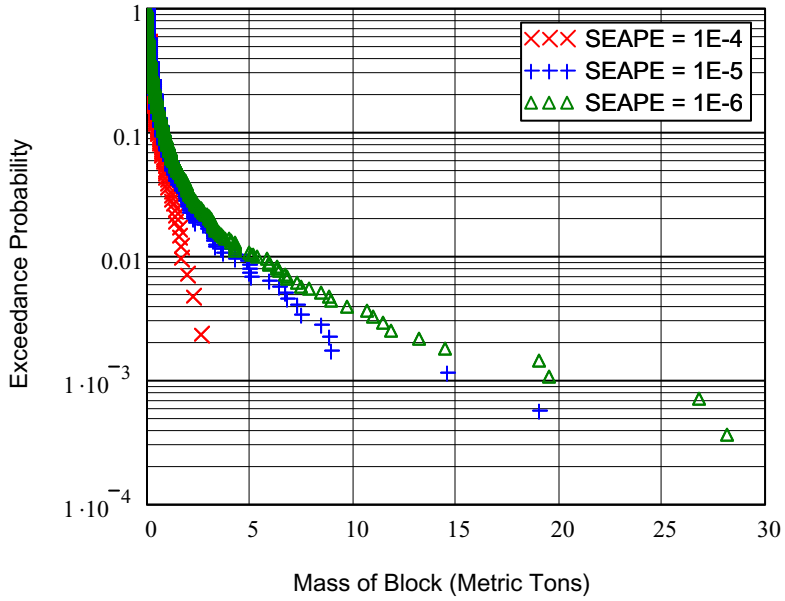

SOURCE: Attachment A, Figure A-6
SEAPE = Seismic Event Annual Probability of Exceedance

Figure 6. Complementary Empirical Cumulative Distribution for Rockfall Mass

As indicated in Section 6.4.1, the existing fracture surfaces in the nonlithophysal rock units provide the primary weaknesses in the rock mass and control the resulting rock block dimensions (Reference 2.2.16, Section I). Also, the rockfall statistics of Table 6 indicate that the maximum observed rockfall mass is dependent on the severity of the seismic event. These two pieces of information show that while the size of a given rock block dimensions is controlled by the fractures within the rock mass, the likelihood that this rock block will be dislodged during a seismic event and thus become a rockfall is dependent on the severity of the ground motions. Specifically, Figure 6 and Table 6 indicate that large rockfall masses (more than a few metric tons) are relatively rare. This means that large blocks are typically wedged in place in the rock mass and are not free to move. It is only when large ground motions from severe seismic events shake down an increasing number of blocks that a large block can be exposed, dislodged, and ultimately fall into the emplacement drift.

In addition to being rare, large rockfalls have their mass overestimated by the rockfall simulations. Rock blocks are modeled through a synthetic fracture geometry calibrated against field data from the repository area (Reference 2.2.16, Section XX). This synthetic geometry is limited to fractures with a trace length greater than or equal to 1 m (Reference 2.2.16, Section XX). Although field data found that shorter fractures account for more than 80 percent of the fractures in some areas, they are not incorporated into the three-dimensional discontinuum program used for the rockfall simulations because of the excessive computational resources required (Reference 2.2.1, Section 6.3.3). Instead, the effect of small-scale fractures is investigated using an alternate software with an efficient rock block generation algorithm, used

to compare a simulation in which small-scale fractures are included, to another one in which they are excluded (Reference 2.2.1, Section 6.3.3). It is found that, while the distributions of rock size are mostly identical (Reference 2.2.1, Figure 6-107), the maximum rock block volume (and therefore mass) is approximately 56 percent smaller in the simulation including small-scale fractures (Reference 2.2.16, Section XXI). The upper rockfall masses shown in Table 6 and Figure 6 therefore appear to be conservative, as the small-scale fractures inherently limit the size of larger rock blocks.

To assess the extreme values of the rockfall mass distribution, the same approach as that employed for the rockfall impact velocity is taken (Section 6.4.3.3). The extreme values of the rockfall mass are fitted to an exponential distribution. A qualitative evaluation of Figure 6 shows that this is appropriate, given that the complementary empirical cumulative rockfall mass distribution of each seismic event of interest takes the approximate shape of a straight line for large mass values. This approach is conservative because the exponential distribution has no upper bound, whereas in reality there is a physical bound to the rockfall mass (if only because there is a limit to the size of the rock blocks that can fit into the emplacement drift when falling). It is however recognized that this physical bound could be significantly greater than the maximum rockfall mass yielded by the data: contrary to Figure 3 for rockfall impact velocities, Figure 6 does not appear to be concave downwards. Therefore, the exponential fitting for each seismic event of interest is carried out based on the 15 greatest rockfall masses yielded by the simulations, in order to ensure that the trend suggested by the extreme observations is respected. The discussion in the previous paragraph further ensures that the resulting exponential fitting will be conservative, since it will be based on conservative upper rockfall mass values.

To evaluate the behavior of the medium rockfall masses, the same approach as in Section 6.4.3.4 is followed, by fitting the data to a Weibull distribution. The appropriateness of this fitting is qualitatively confirmed by a log-log graph of the logarithm of the complementary empirical cumulative distributions of the rockfall mass, illustrated on Figure 7, which is compatible with a straight line for a large range of rockfall masses.

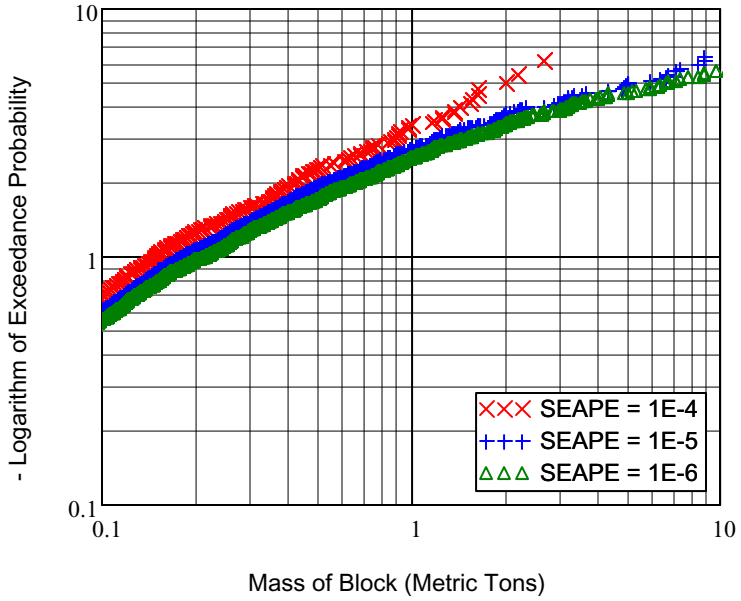

SOURCE: Attachment A, Figure A-7
SEAPE = Seismic Event Annual Probability of Exceedance

Figure 7. Negative Logarithm of Complementary Empirical Cumulative Distribution for Rockfall Mass

6.4.4.2. Fitting of Rockfall Mass Distribution to Exponential and Weibull Distributions

As in Section 6.4.3.5 for rockfall velocities, the fittings of the Weibull and exponential distribution to the rockfall masses is carried out based on the following factors:

- The data are fitted with a Weibull distribution for masses greater than or equal to a lower threshold w_m and less than an upper threshold u_m, and with an exponential distribution for masses greater than or equal to u_m (Section 6.4.4.1).

- The exceedance probability $\overline{F}(u_m)$ associated with u_m is assigned the value determined by the Weibull fitting, namely $\overline{W}(u_m)$. This leaves σ as the only parameter to evaluate in Equation 8 for the exponential distribution. Equating $\overline{F}(u_m)$ with $\overline{W}(u_m)$ ensures a continuity between the exponential fitting and the Weibull fitting and therefore the continuity of the overall mass distribution.

- No fitting of the mass data having a value less than w_m is performed. Instead, these masses are assigned the probability of the fitted Weibull distribution. This approximation is acceptable because the rockfalls having a mass less than w_m are not part of the severe rockfalls of interest in this calculation, as shown in Section 6.4.5.2.5.

As indicated in Section 6.4.4.1, the 15 greatest rockfall mass values are used for the fitting to the exponential distribution, which results in the values of u_m shown in Table 7. The values of w_m are qualitatively chosen, using Figure 7 as a visual aid to determine the regions where the observations take the approximate shape of a straight line. Various values of w_m can yield acceptable Weibull fits. A selection is made that incorporates sufficient data for the fittings to be meaningful, and that at the same time allows for a qualitatively adequate overall fit of the observations of interest (i.e., those exceeding w_m). Table 7 summarizes the values selected, as well as the resulting number of observations used for each fitting.

Table 7. Input Parameters for Exponential and Weibull Fittings of Mass Distribution

Parameter	Annual Probability of Exceedance of Seismic Event		
	10^{-4}	10^{-5}	10^{-6}
Threshold Mass for Exponential Fitting (u_m)[a]	1.02 metric tons	4.96 metric tons	7.92 metric tons
Number of Observations for Exponential Fitting[b]	15	15	15
Threshold Mass for Weibull Fitting (w_m)[b]	0.2 metric ton	1.5 metric tons	2 metric tons
Number of Observations for Weibull Fitting[c]	107	51	83

NOTES: [a]Source for this input is Attachment A, based on the number of observations used for the exponential fitting. Mass is shown rounded up to the closest hundredth of metric ton.
[b]Values of this input are qualitatively chosen.
[c]Source for this input is Attachment A, based on the values selected for w_m.

The parameters of the fitted Weibull distribution (Equation 9) and fitted exponential distribution (Equation 7) are determined by linear regressions and estimated using the least-squares method, in the same way as in Section 6.4.3.5. The calculations are detailed in Attachment A. Table 8 shows the results.

Table 8. Parameters of Fitted Exponential and Weibull Distributions for Rockfall Mass

Parameter[a]	Annual Probability of Exceedance of Seismic Event		
	10^{-4}	10^{-5}	10^{-6}
Scale Parameter of Weibull Distribution (α)	0.143 metric ton	0.051 metric ton	0.042 metric ton
Shape Parameter of Weibull Distribution (β)	0.613	0.351	0.318
Inverse of Parameter of Exponential Distribution (σ)	0.572 metric ton	4.78 metric tons	8.15 metric tons

NOTE: [a]Parameters are shown rounded to three significant figures or to the closest kg.
SOURCE: Attachment A

Figure 8 shows the rockfall mass data along with the fitted distributions.

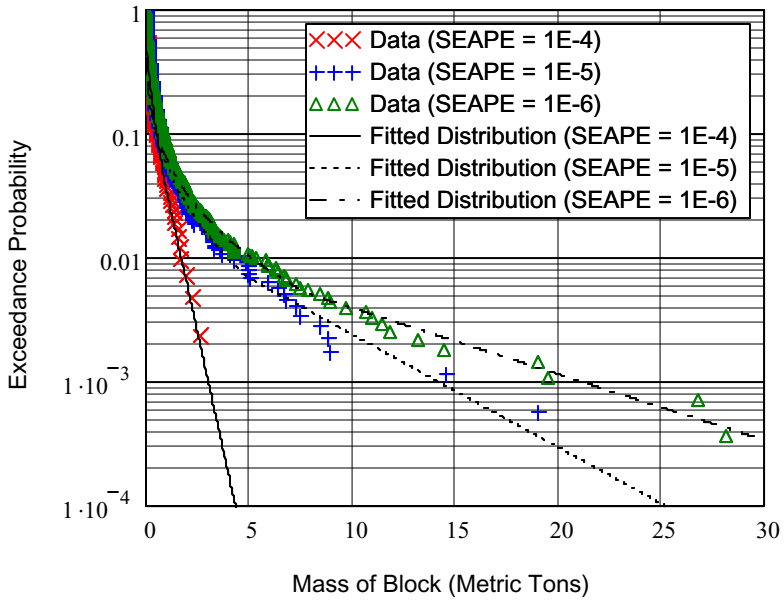

SOURCE: Attachment A, Figure A-8
SEAPE = Seismic Event Annual Probability of Exceedance

Figure 8. Rockfall Mass Data with Fitted Distributions

As in Section 6.4.3.5, a normality test is performed on the residuals of the linear regressions to quantitatively confirm the adequacy of the Weibull and exponential fittings. The calculations are carried out in Attachment A, using the Kolmogorov-Smirnov statistic. For the seismic events having an APE equal to 10^{-4}, 10^{-5}, and 10^{-6}, the Kolmogorov-Smirnov statistic is found respectively equal to 0.076, 0.080, and 0.060 for the Weibull fittings, and to 0.232, 0.124, and 0.119 for the exponential fittings. These values are lower than the 5 percent significance level critical value for the test, which is 0.895 (Reference 2.2.9, Table 4.7, Statistic *D*). Therefore, the test is passed at this significance level, which indicates that the overall Weibull and exponential fittings are not unreasonable.

6.4.4.3. Parameter Variability for Exponential Fittings

As in Section 6.4.3.6, the variability of σ, the inverse of the parameter of the exponential fitting for the rockfall mass, is investigated through a Bayesian approach. In comparison, the variability of the parameters of the Weibull distribution is limited, due to the relatively large number of data points used for the fitting (Table 7) and therefore is not further investigated. The calculations are detailed in Attachment A.

Table 9 shows the 5th percentile, the mean, and the 95th percentile associated with σ for each of the seismic events of interest in this calculation.

Table 9. Parameter Variability of Fitted Exponential Distribution for Rockfall Mass

Value Taken by Inverse of Parameter of Exponential Distribution (σ)	Annual Probability of Exceedance of Seismic Event		
	10^{-4}	10^{-5}	10^{-6}
5th percentile[b]	0.546 metric ton	4.23 metric tons	7.61 metric tons
Mean[a,b]	0.572 metric ton	4.78 metric tons	8.15 metric tons
95th percentile[b]	0.599 metric ton	5.33 metric tons	8.70 metric tons

NOTE: [a] The mean is the least-squares estimate of Section 6.4.4.2 (Reference 2.2.11, p. 118).
[b] Values are shown to three significant figures.
SOURCE: Attachment A

6.4.5. Bounding Credible Rockfalls for Impacts on Waste Packages

6.4.5.1. Method of Evaluation

As indicated in Section 1, this calculation focuses on credible rockfalls, i.e., rockfalls that have at least one chance in 10,000 of occurring over the preclosure period. Specifically, the calculation aims at evaluating the characteristics of the most severe rockfalls that could damage a waste package. The level of damage is related to the energy that is transmitted to the waste package in the form of plastic deformation, which is bounded by the rockfall kinetic energy K at impact. The rockfall kinetic energy is thus the physical quantity of interest in this calculation. The kinetic energy (in joules) is equal to $K = \frac{1}{2} \cdot m \cdot v^2$ where m is the rockfall mass (in kg) and v is the rockfall velocity at impact.

A binomial distribution is used for calculating the probability of occurrence of a seismic event over the preclosure period (Assumption 3.2.1). Specifically, $P_{se\text{-}p}$, the probability of occurrence of least one seismic event with an APE equal to p, is well approximated, based on Section 6.2.1, by $n \times p$, where $n = 100$ is the number of years of the preclosure period for the subsurface (Reference 2.2.15, Section 2.2.2.8). In the same way, $P_{se\text{-}q}$, the probability of occurrence of at least one seismic event with an APE equal to q (where q is smaller than p) is $n \times q$, and therefore, $P_{se\text{-}r}$, the probability of observing at least one seismic event with an APE ranging between q and p is $P_{se\text{-}r} = P_{se\text{-}p} - P_{se\text{-}q} = n \times (p - q)$. Applied to the seismic events having an APE less than or equal to 10^{-4}, but more than 10^{-5}, this yields: $P_{se\text{-}r} = 100 \times (10^{-4} - 10^{-5}) = 9 \times 10^{-3}$, and for the seismic events having an APE less than or equal to 10^{-5}, but more than 10^{-6}, this yields: $P_{se\text{-}r} = 100 \times (10^{-5} - 10^{-6}) = 9 \times 10^{-4}$.

Based on Assumption 3.2.6, the rockfall rate, mass, and impact velocity distributions developed for the seismic event with an APE equal to 10^{-4} are also applicable to the seismic events with an APE less than 10^{-4}, but greater than 10^{-5}. In the same way, the rockfall distributions developed for the seismic event with an APE equal to 10^{-5} are also applicable to the seismic events with an APE less than 10^{-5}, but greater than 10^{-6}. Earthquakes that have an APE less than 10^{-6} do not need to be considered because they have a probability of occurrence less than that of a Category 2 event sequence, based on Section 6.2.1.

If N is the number of rockfalls triggered by a seismic event in the nonlithophysal rock units of the emplacement drifts, it is conservative to consider that all N rockfalls strike waste packages in the drifts. For $P(K)$, the cumulative distribution function of the rockfall kinetic energy, $\overline{P}(K) = 1 - P(K)$ is the complementary distribution. The conditional probability, given an

earthquake, that N rockfalls have a kinetic energy at impact on a waste package less than K is given by $P(K)^N$, and therefore the probability that at least one rockfall has a kinetic energy greater than K is $1-P(K)^N$. The way this probability is written implies independence of rockfall kinetic energies. The kinetic energy of a given rock is controlled by its mass and impact velocity. The dimensions of a rock block (and therefore its mass) are determined by the fracture patterns in the rocks that surround the drift (Section 6.4.1). The impact velocity is determined by the initial velocity at the time of dislodgement, the waste package velocity at the time of impact, and the rockfall drop height (Section 6.4.3.1). Random variations in any of these parameters can lead to significant differences in the resulting rockfall mass and velocity at impact, which justifies the independence of rockfall kinetic energies.

Given a range of earthquakes that produce rockfalls with similar rockfall rate, mass, and impact velocity distributions, the bounding credible kinetic energy K_c is defined as the rockfall kinetic energy at impact on a waste package that has a probability less than 10^{-4} of being exceeded, over the preclosure period. Based on the previous developments, K_c is expressed by the following inequality, considering N rockfalls:

$$P_{se-r} \cdot \left[1-P(K_c)^N\right] < 10^{-4} \qquad \text{(Eq. 12)}$$

Because K_c is expected to be an extreme value of the rockfall kinetic energy, which implies $P(K_c)$ close to 1, it is beneficial to use the complementary cumulative kinetic energy distribution, $\overline{P}(K_c)$, which is close to 0 and will facilitate further calculations. After rearrangement, Equation 12 becomes:

$$\overline{P}(K_c) < 1-\left(1-\frac{10^{-4}}{P_{se-r}}\right)^{1/N} \qquad \text{(Eq. 13)}$$

In the right-hand side of Equation 13, the total number of rockfalls N is equal to the rockfall rate f, multiplied by the total length L of emplacement drift excavated in the nonlithophysal rock units. Based on Assumption 3.2.7, L is equal to 10,000 m. As an illustration of the probability levels reached by the right-hand side of Equation 13, the average rockfall rate yielded by the observations, reported in Table 1, is used to calculate the exceedance probabilities for each range of seismic events of interest in this calculation. The resulting exceedance probabilities (right-hand side of Equation 13) are equal to 1.68×10^{-6}, 6.67×10^{-6}, and 1.09×10^{-4} for the range of seismic events described by an APE respectively equal to 10^{-4}, 10^{-5}, and 10^{-6} (the calculations are carried out in Attachment A). For the latter seismic event, which is right at the credibility threshold (Section 6.2.1), P_{se-r} in Equation 13 is calculated as the probability of having at least one earthquake with an APE equal to 10^{-6} over a preclosure period of 105 yrs. 105 yrs are chosen instead of 100 yrs to ensure that the term inside the parentheses in Equation 13 remains positive.

In the left-hand side of Equation 13, $\overline{P}(K_c)$, the probability that a given rockfall's kinetic energy exceeds the value K_c, can be expressed as a function of the rockfall mass and impact velocity distribution functions. $\overline{P}(K_c)$ is the joint probability, over all possible values of the rockfall

velocity, of having 1) the rockfall velocity between v and $v + dv$, and 2) the rockfall mass m larger than $\frac{2 \cdot K_c}{v^2}$ (which represents the mass of a rockfall with kinetic energy K_c and velocity v). Considering that the rockfall mass and impact velocity are independent variables (which is justified since the rockfall mass is essentially controlled by the fractures in the rock mass, and the velocity is controlled by the drop height and the ground seismic velocity at the time of rock dislodgment and at the time of impact), $\overline{P}(K_c)$ can be expressed as:

$$\overline{P}(K_c) = \int_0^\infty p_v(v) \cdot \left[1 - P_m\left(\frac{2 \cdot K_c}{v^2} \right) \right] dv \qquad \text{(Eq. 14)}$$

where

$p_v(v)$ = probability density function associated with a rockfall impact velocity v, based on the Weibull and exponential fittings (Section 6.4.3.5)

$P_m(x)$ = cumulative distribution function associated with a rockfall mass x, based on the Weibull and exponential fittings (Section 6.4.4.2)

The bounding credible rockfall kinetic energy is calculated by substituting $\overline{P}(K_c)$ in Equation 13 with its expression in Equation 14 and solving for K_c.

The variability of the parameters in the resulting equation, i.e., the rockfall rate (Section 6.4.2.1), the parameter of the exponential fitting of the impact velocity distribution (Section 6.4.3.6), and the parameter of the exponential fitting of the rockfall mass (Section 6.4.4.3), are taken into account by a Latin hypercube sampling on these parameters. Latin hypercube sampling is a form of Monte Carlo sampling used to propagate uncertainties (Reference 2.2.13, p. 3). Like in Monte Carlo sampling, the variability of random parameters is approximated by a sample of values from the distributions associated with the parameters, but the samples in Latin hypercube sampling are stratified across the entire range of the distributions, which produces more stable analysis outcomes than the purely random Monte Carlo sampling (Reference 2.2.13, p. 13). The details of the calculation are given in Attachment A.

6.4.5.2. Results and Discussion

6.4.5.2.1 Initial Results

Figure 9 shows the cumulative distribution function associated with the bounding credible rockfall kinetic energy K_c produced by the sampling, for each range of seismic events of interest in this calculation. The cumulative distribution functions display the overall uncertainties around the parameters, and, by using the Weibull and exponential fittings performed in Sections 6.4.3.5 and 6.4.4.2, accounts for the extreme values that can be taken by the impact velocity and mass of rockfalls.

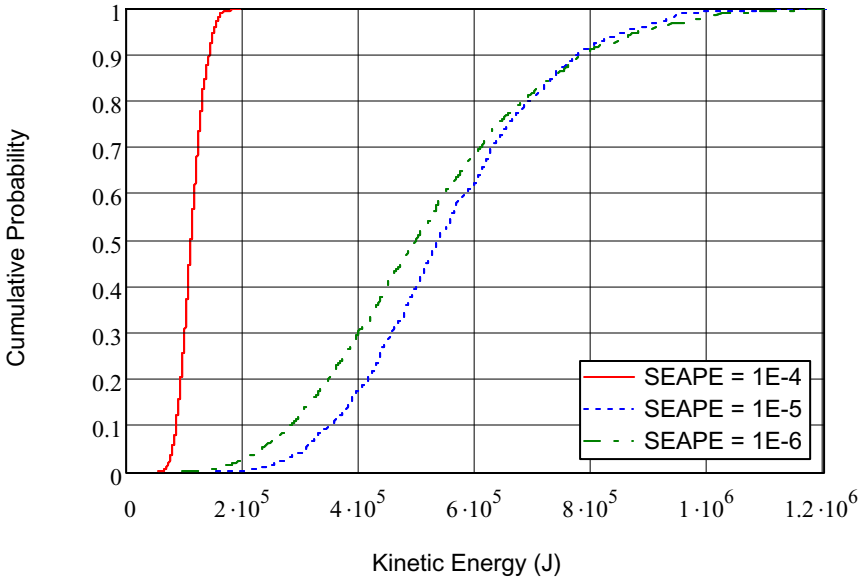

SOURCE: Attachment A, Figure A-9
SEAPE = Seismic Event Annual Probability of Exceedance

Figure 9. Cumulative Distribution Function for Bounding Credible Rockfall Kinetic Energy

The Latin hypercube sampling is carried out with 1,000 samples. The relative smoothness of the resulting distribution in Figure 9 qualitatively confirms that the number of samples is sufficient. The mean of the distribution is found to be equal to 1.1×10^5 J, 5.6×10^5 J, and 5.2×10^5 J for the range of seismic events described by an APE respectively equal to 10^{-4}, 10^{-5}, and 10^{-6}. The corresponding percentile is the 52^{nd}, 54^{th}, and 54^{th} percentile of the distributions. Attachment A shows the details of these calculations.

6.4.5.2.2 Conservatisms

The foregoing evaluation has several embedded conservatisms, which have not been quantified, and therefore are not apparent in the bounding credible rockfall kinetic energy distribution shown on Figure 9. These conservatisms are summarized below:

- The rockfall simulations are based on unbounded peak ground velocities that are very conservative for severe seismic events, notably those with an APE equal to 10^{-5} and 10^{-6}, which in turn produce correspondingly conservative estimates of rockfalls (Section 6.2.2).

- The rockfall rate is conservative because a lower value of the length of simulated drift is used (Assumption 3.2.8). In addition, the upper values of the rockfall rate yielded by the simulations are overestimated due to the block deletion scheme employed in the simulations; also, the rockfall rate is fitted to a lognormal distribution, which is unbounded, while in reality there is a physical upper bound to the rockfall rate (Section 6.4.2.2).

- The upper values of the rockfall velocities at impact on waste packages are fitted to an exponential distribution which is unbounded, while in reality there is a physical upper bound to the impact velocity; the downward concavity of the complementary empirical distribution associated with impact velocities further confirms that the observed velocities trend towards an upper bound (Section 6.4.3.2).

- The upper values of the rockfall mass yielded by the simulations are overestimated due to the fact that small-scale fractures are not incorporated in the rockfall simulation model (Section 6.4.4.1).

6.4.5.2.3 Sources of Uncertainties

The bounding credible rockfall kinetic energy distribution shown on Figure 9 accounts for the uncertainties yielded by the simulations. These uncertainties are related to the rockfall rate, the extreme values of the rockfall impact velocity distribution, and the extreme values of the rockfall mass distribution. Two other sources of uncertainties are identified, which are not reflected in the kinetic energy distribution. These are: 1) the time-dependent degradation of the emplacement drifts, and 2) the presence of ground support, whose potential adverse effects are now examined.

Section 6.1.2 indicates that the time-dependent degradation in the nonlithophysal rock units may result in a higher number of rock blocks dislodged during a seismic event. However, the same section further states that the time-dependent degradation 1) is conservatively evaluated in Reference 2.2.1, and 2) focuses on the postclosure period, which is considerably longer than the preclosure period considered in this calculation. The increase in rockfall rate that might result from time-dependent degradation over the preclosure period is deemed to be covered by the lognormal fitting performed in Section 6.4.2.1, based on the conservatisms listed in Section 6.4.5.2.2.

The calculation does not take credit for ground support (Section 1); however, ground support will be present in the emplacement drifts. The ground support considered for the emplacement drifts consists of 3 mm thick perforated stainless steel sheets, as well as rock bolts, which are 3 m long stainless steel tubes that have a wall thickness of 3 mm and are spaced at 1.25 m (Reference 2.2.2, Sections 7 and Table 3-6). Given the small thickness of steel sheets and given that rock bolts are hollow tubes, the added mass to a rock block (which typically weighs several hundred kilograms based on Table 6) would be insignificant, and therefore in that respect would not intensify the severity of a rockfall impact on a waste package.

Another adverse effect of the presence of ground support could be an increased impact severity, if the ground support affixed to the falling rock block happens to be at the location of impact. First, this impact configuration may not necessarily be common. Steel sheets are installed on the surface of the emplacement drifts and therefore would only be on one side of a dislodged rock block; rock blocks would typically rotate when falling, depending on the direction of the vector of initial velocity at the time of dislodgment, which has horizontal components from the seismic event. Therefore, at the time of impact, a rock block may have sufficiently rotated to strike the waste package on a side that has no steel sheet affixed to it. The configuration where the impact occurs between a waste package and a rock bolt is even less probable, as rock bolts are inside the

rock mass and only a small portion protrudes from the rock. Second, the shape of steel sheets is not conducive to heightening an impact; the fact that steel sheets are 3 mm thick is an indication that they would deform when stressed. The same is true of rock bolts, which are hollow tubes that would buckle on impact. Based on this qualitative evaluation, it is concluded that the ground support used in the emplacement drifts would not significantly increase the severity of rockfall impacts.

The last identified potential adverse effect of ground support on rockfalls is that it could keep adjacent rockfalls tied together that would have otherwise fallen separately. Adjacent rockfalls would be part of a multiple rockfall configuration, which is investigated in Section 6.4.5.2.4.

6.4.5.2.4 Evaluation of Bounding Multiple Rockfall Configurations

For a given waste package, two or more rockfalls with impact locations sufficiently far from each other will have independent effects on the waste package. Conversely, when rock blocks fall sufficiently close to one another, the plastic strain created by an impact could be affected by another impact. Such a configuration is designated as a multiple rockfall configuration in this calculation. As an illustration of the value of the critical distance below which two rockfall impacts have a combined effect on a given waste package, Reference 2.2.14 (p. 27) finds that a conservative estimate is 0.5 m. This corresponds to a rate of $1/0.5 = 2$ rockfalls per meter. Using the rockfall rate distribution of Section 6.4.2.1 as an approximate measure of the frequency of multiple rockfall configurations, it is found that rockfall occurrences greater than or equal to 2 rockfalls per meter of emplacement drift represent 7, 28, and 48 percent of the rockfall configurations for seismic events having an APE respectively equal to 10^{-4}, 10^{-5}, and 10^{-6} (the corresponding calculations are shown in Attachment A). Even if multiple rockfall configurations tend to be more frequent as the severity of the initiating seismic event increases, the majority of rockfall impacts appear to remain independent from each other.

As mentioned in Section 6.4.5.2.3, a potential adverse effect of ground support is that it could keep adjacent rockfalls tied together that would have otherwise fallen separately. Ground support may intensify the damage caused by a multiple rockfall configuration. For example, by keeping separate rock blocks tied together, ground support would cause a single rockfall impact in a given area of a waste package, where less massive rockfalls impacting the waste package in different locations (if only separated by a small distance) would have occurred if the ground support were not present. Accordingly, this calculation takes the conservative approach of modeling a multiple rockfall configuration as a single rockfall composed of smaller rock blocks tied together.

This section focuses on the most severe rockfalls that could occur in the emplacement drifts over the preclosure period. Such rockfalls are rare and anticipated to weigh several metric tons (specifically, Section 6.4.5.2.5 finds that a representative value for the mass of the bounding credible rockfall is 20 metric tons). This is in contrast with Table 6 of Section 6.4.4.1, which indicates that a typical rock block has a mass limited to a few hundred kilograms. Based on these two pieces of information, the most severe multiple rockfall configurations are expected to be composed of a heavy rock block (weighing several metric tons) tied together with one or several smaller rock blocks weighing a few hundred kilograms. Therefore, the total rock mass of

a severe multiple rockfall configuration would be marginally greater than the mass of the most massive rock block of the configuration.

A quantitative evaluation is performed to confirm this assessment. The evaluation starts with the calculation of the complementary cumulative distribution function associated with the total mass m_t of a rockfall configuration consisting of two rock blocks. The exceedance probability $\overline{P}(m_t)$, i.e., the probability that a random rockfall configuration has a mass greater than m_t, is the joint probability, over all possible values, of having 1) the mass of the first rock block comprised between m and $m + \mathrm{d}m$, and 2) the mass of the second rock block greater than $m_t - m$. Considering that the mass of individual rock blocks are independent, which is justified because the rock block dimensions are controlled by the fracture patterns in the rock that surrounds the drift, and because random variations in the intersection of fractures can lead to significant variations in rock block mass, $\overline{P}(m_t)$ can be expressed as the convolution of two functions, as follows:

$$\overline{P}_m(m_t) = \int_0^\infty p_m(m) \cdot \left[1 - P_m\left(m_t - m\right)\right] dm \qquad \text{(Eq. 15)}$$

where

$p_m(m)$ = probability density function associated with a rockfall mass m, based on the Weibull and exponential fittings (Section 6.4.4.2)

$P_m(m)$ = cumulative distribution function associated with a rockfall mass m, based on the Weibull and exponential fittings (Section 6.4.4.2)

Figure 10 shows the complementary cumulative distribution function associated with the total mass of a two-block configuration, along with the complementary cumulative distribution function associated with only one rock block (i.e., the same mass distribution developed in Section 6.4.4.2 and shown on Figure 8). Only the curves associated with seismic events with an APE equal to 10^{-5} and 10^{-6} are displayed because, as found in Section 6.4.5.2.1, the bounding credible rockfalls produced by the seismic event with an APE equal to 10^{-4} are much less severe and do not require further consideration.

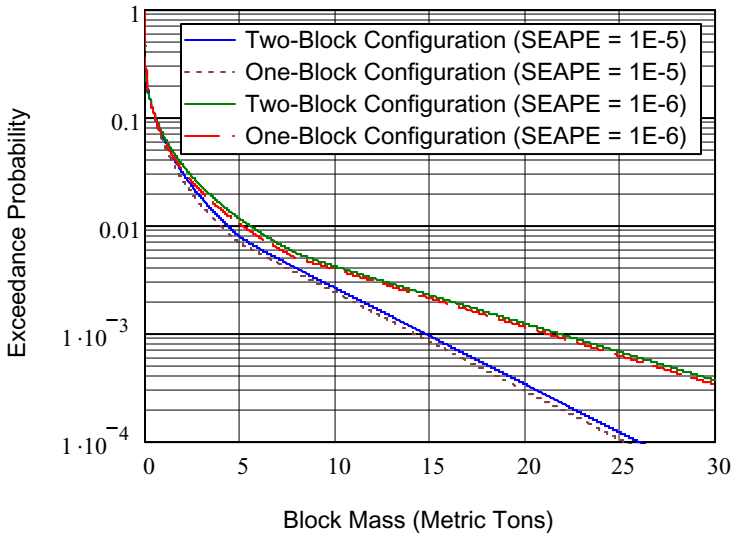

SOURCE: Attachment A, Figure A-10
SEAPE = Seismic Event Annual Probability of Exceedance

Figure 10. Complementary Cumulative Distribution Functions for Rockfall Mass of One-Block and Two-Block Rockfall Configurations

Figure 10 shows that the complementary cumulative distribution functions are almost identical for one-block and two-block rockfall configurations . For example, for the seismic event with an APE equal to 10^{-5}, the mass associated with an exceedance probability equal to 10^{-3} is equal to 14.2 metric tons for a one-block rockfall configuration, and 14.7 metric tons for a two-block rockfall configuration, a 500 kg difference (Attachment A). For the seismic event with an APE equal to 10^{-6}, the mass associated with an exceedance probability equal to 10^{-3} is equal to 21.1 metric tons for a one-block rockfall configuration, and 21.7 metric tons for a two-block rockfall configuration, a 600 kg difference (Attachment A). This confirms that a severe multiple rockfall configuration involving two rock blocks consists of one block that carries most of the weight (several metric tons), and a second lighter rock block (a few hundred kilograms), typical of the rock blocks dislodged by the earthquake.

Multiple rockfall configurations involving three rock blocks can be investigated in a similar way as previously, i.e., by convolution of the rockfall mass distribution involving two rock blocks and the rockfall mass distribution involving one rock block. The same conclusion would hold, i.e., a severe multiple rockfall configuration would consist of one rock block with the bulk of the mass, with two rock blocks of a few hundred kilograms each contributing marginally to the overall mass. Rockfall configurations involving more than three rock blocks could be evaluated in a similar way. However, such configurations become more rare as the number of rock blocks involved in the configuration increases (such configurations are associated with rockfall rates corresponding to higher and higher percentiles). Also, it is unlikely that in a severe multiple rockfall configuration, the ground support could be able to tie more than a few (two or three) rock blocks together. Most of the ground support would be attached to the most massive rock block. In the case of rock bolts, only a small portion would protrude from this massive block and be able to bring another block in the configuration. Also, steel sheets do not have a shape

conducive to efficiently tying rock blocks together, because they are affixed to the surface of the rock, leaving the other sides of the rock blocks free to separate at the time of dislodgment.

It is thus concluded that severe multiple rockfall configurations would have a total mass marginally greater than the rockfall configurations involving one rockfall. Accordingly, the total kinetic energy of a severe multiple rockfall configuration would also be marginally greater than the rockfall configuration involving one rockfall.

6.4.5.2.5 Selection of Bounding Credible Rockfall Kinetic Energy

Concurrently to the development of this calculation, numerical evaluations of the capability of a waste package to withstand an extreme rockfall were performed. These simulations used as inputs the following preliminary rockfall characteristics: rockfall mass equal to 20 metric tons and velocity at impact on a waste package equal to 10 m/s, resulting in a total kinetic energy of 1 million joules (10^6 J).

This value is significantly greater than the mean of the bounding rockfall kinetic energy distributions given in Section 6.4.5.2.1 (which are 1.1×10^5 J, 5.6×10^5 J, and 5.2×10^5 J for an APE respectively equal to 10^{-4}, 10^{-5}, and 10^{-6}). The 10^6 J value approximately corresponds to the 99^{th} and 98^{th} percentile of the distribution, for an APE respectively equal to 10^{-5} or 10^{-6} (Attachment A). This value far exceeds the range of rockfall kinetic energies yielded by earthquakes with an APE equal to 10^{-4} (the 99^{th} percentile of the bounding credible rockfall kinetic energy distribution in this case is 1.7×10^5 J).

Section 6.4.5.2.3 and Section 6.4.5.2.4 show that the two sources of uncertainty not accounted for in the development of the bounding credible rockfall kinetic energy distribution, i.e., the time-dependent degradation of drifts and the potential adverse effects of ground support, would have a marginal adverse effect on the severity of rockfall impacts onto waste packages. The 10^6 J value is sufficiently larger than the mean bounding rockfall kinetic energy values to cover these uncertainties. Thus, a value of 10^6 J is adequate for representing the bounding credible kinetic energy of rockfalls in the nonlithophysal rock units.

There are an infinite number of combinations of mass and impact velocity that are associated with a kinetic energy of 10^6 J. The most probable combination is calculated by finding the velocity that maximizes the probability density under the integral in Equation 14 of Section 6.4.5.1. Figure 11 shows this probability density as a function of the impact velocity for a kinetic energy equal to 10^6 J. Only the seismic events with an APE equal to 10^{-5} and 10^{-6} are considered, as the milder earthquake with an APE equal to 10^{-4} is not capable of producing such a highly energetic impact. For simplicity, the nominal values of the parameter of the fitted exponential distribution for the rockfall mass and impact velocity given in Table 4 and Table 8 are used (i.e., no variability of the parameters is considered).

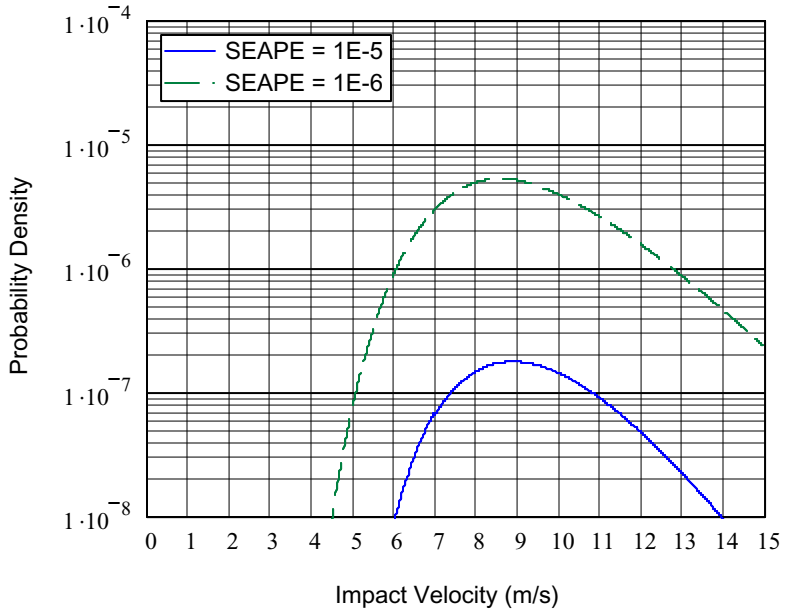

SOURCE: Attachment A, Figure A-11
SEAPE = Seismic Event Annual Probability of Exceedance

Figure 11. Probability Density as a Function of Rockfall Impact Velocity

Figure 11 shows that the probability density reaches its maximum for impact velocities ranging between 8 m/s and 9 m/s, and that the most probable rockfalls have a velocity approximately comprised between 7 m/s and 11 m/s. A rockfall with a mass of 20 metric tons and an impact velocity of 10 m/s appears thus to be an adequate representation of a 10^6 J rockfall.

The probability density function expressed as a function of the impact velocity shown on Figure 11 confirms that the approximation in Sections 6.4.3.5 consisting of assigning the values of the Weibull fitting to the cumulative distribution function probabilities associated with velocities less than w_v is adequate. Figure 11 shows that the velocities less than 5.5 m/s (the maximum velocity value for w_v, based on Table 3) have probability density levels less, by a factor of approximately 20 or greater, than the maximum probability density. Therefore, the corresponding rockfalls represent an insignificant proportion of the set of bounding credible rockfalls having a kinetic energy of 10^6 J at impact. The same conclusion is reached for rockfalls having a mass less than w_m, to which the probabilities of the Weibull fittings are assigned in Section 6.4.4.2. Rock blocks having a mass of at most 2 metric tons (the maximum value for w_m based on Table 7) would be required to have an impact velocity of at least 32 m/s to reach a kinetic energy of 10^6 J. Clearly, only an insignificant fraction of the bounding credible rockfalls have such characteristics.

Bounding multiple rockfall configurations are now discussed. Based on Section 6.4.5.2.4 and the previous discussion, the bounding multiple rockfall configuration composed of two blocks has a total kinetic energy of 10^6 J and can be represented by a block of 20 metric tons carrying the bulk of the mass, complemented by a second smaller block, typical of the rock blocks dislodged by the earthquake. Typical rock blocks have a kinetic energy at impact on waste packages in the order of a few hundred to a few thousand joules, as shown in Section 6.4.6.

Therefore, the typical rock block would contribute marginally to the total kinetic energy of the configuration, which is 10^6 J. In the case where both rock blocks would be tied together by ground support, they would have the same velocity with a total kinetic energy of 10^6 J, essentially constituting a rockfall slightly bigger than 20 metric tons and with an impact velocity slightly less than 10 m/s. The same conclusion would be reached with a multiple rockfall configuration including three or more rock blocks. It is thus concluded that the bounding multiple rockfall configurations are overall adequately represented by the single rockfall of 20 metric tons and 10 m/s.

6.4.6. Rockfall Kinetic Energy Distribution for Impacts on Waste Packages

In this section, the probability distribution of the kinetic energy of a rockfall at impact on a waste package is calculated. In contrast to Section 6.4.5, typical rockfalls are analyzed here, not bounding rockfalls. Given the large number of data yielded by the simulations, ranging from 428 to 2797 rockfalls (Table 1), it is appropriate to use the empirical cumulative distribution function to approximate the kinetic energy distribution. The kinetic energy of each individual simulated rockfall is used, in which the velocity is adjusted for impact on waste packages (Section 6.4.3.1). Calculations are performed in Attachment A.

Figure 12 shows the resulting kinetic energy distribution.

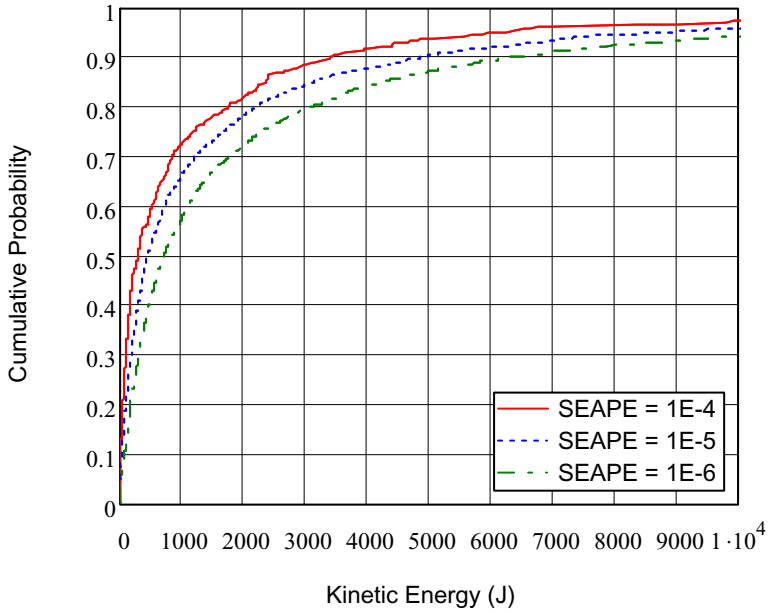

SOURCE: Attachment A, Figure A-12
SEAPE = Seismic Event Annual Probability of Exceedance

Figure 12. Cumulative Distribution Function for Rockfall Kinetic Energy

The relative smoothness of the curves in Figure 12 qualitatively confirms that the empirical cumulative distribution function is an adequate approximation of the rockfall kinetic energy distribution.

Table 10 shows the rockfall kinetic energy value associated with selected percentiles. When compared to the mean rockfall kinetic energy, which is found to be 1.3×10^3 J, 2.4×10^3 J, and 3.0×10^3 J for the seismic events with an APE respectively equal to 10^{-4}, 10^{-5}, and 10^{-6} (Attachment A), it appears that the rockfall kinetic energy distribution is highly skewed to the right. Stated otherwise, while the majority of rockfalls have a low kinetic energy at impact on waste packages (on the order of a few hundred to a few thousand joules), a few rockfalls have the potential to be highly energetic, with a kinetic energy at impact of several hundred thousand joules. This is confirmed by the calculations in Section 6.4.5.2.1, which find that the mean kinetic energy of the bounding credible rockfall is on the order of half a million joules for very severe earthquakes.

Table 10. Rockfall Kinetic Energy Associated with Selected Percentiles

Percentile	Annual Probability of Exceedance of Seismic Event		
	10^{-4}	10^{-5}	10^{-6}
10th	18 J	36 J	86 J
20th	61 J	104 J	188 J
30th	114 J	199 J	324 J
40th	176 J	309 J	483 J
50th	303 J	455 J	725 J
60th	537 J	738 J	1,116 J
70th	861 J	1,234 J	1,797 J
80th	1,758 J	2,214 J	3,107 J
90th	3,425 J	4,901 J	6,259 J
95th	6,252 J	8,873 J	11,062 J

NOTE: Kinetic energies are shown rounded to the nearest integer.
SOURCE: Attachment A

Multiple rockfall configurations are now analyzed. A typical multiple rockfall configuration would be composed of typical rock blocks, and therefore each rock block of the configuration would have a kinetic energy for which a representative value is the mean kinetic energy at impact yielded by the simulations. As the number of rock blocks involved in a multiple rockfall configuration increases, the probability of occurrence of such a configuration significantly decreases (this is because such configurations are associated with rockfall rates corresponding to higher and higher percentiles). Also, it is unlikely that in a typical multiple rockfall configuration, the ground support could be able to tie more than a few rock blocks together. Steel sheets do not have a shape conducive to efficiently tying rock blocks together, because they are affixed to the surface of the rock, leaving the other sides of the rock blocks free to separate at the time of dislodgment. Rock bolts are 3 m long stainless steel tubes (Reference 2.2.2, Section 7). Based on Table 6 of Section 6.4.4.1, a rock block has a mean mass ranging from 0.22 to 0.43 metric tons, depending on the severity of the earthquake. Considering, for illustration purposes, that rock blocks have a spherical shape, and given a mean rock density of 2,411 kg/m3 (Reference 2.2.16, Section XIV), the diameter of the 0.43 metric ton block would be 0.70 m, and therefore a rock bolt could hold approximately $3/0.70 = 5$ rock blocks (value rounded up to the nearest integer). It is concluded that a typical multiple rock fall configuration in which the rocks are tied by ground support would have a total kinetic energy at impact on a waste package on the order of 6,500 J ($5 \times 1.3 \times 10^3$) to 15,000 J ($5 \times 3.0 \times 10^3$), with an upper total mass value of $5 \times 0.43 = 2.15$ metric tons.

7. RESULTS AND CONCLUSIONS

Credible rockfalls of the preclosure period, i.e., rockfalls that have at least one chance in 10,000 of occurring over the preclosure period, were investigated for the emplacement drifts of the repository. No credit was taken for ground support; yet, the potential adverse effects of ground support on the severity of rockfall impacts on waste packages were taken into account (Section 1). Using results from Reference 2.2.1 as a major source of inputs, it was established that significant rockfalls would be initiated by seismic events (Section 6.1). Further, based on a preclosure period of 100 yrs, it was found that only the rockfalls dislodged by seismic events having an APE greater than or equal to 10^{-6} required further consideration (Section 6.2). Because they behave differently, a distinction was made between rockfalls in the lithophysal rock units (Section 6.3) and nonlithophysal rock units (Section 6.4) of the repository.

In the lithophysal rock units of the repository, it was found that severe earthquakes (with an APE less than or equal to 10^{-5}) could cause the partial to complete collapse of emplacement drifts. Static loading (dead weight) exerted by the rubble from a collapsed drift onto a buried waste package was determined to result in a pressure on the waste package conservatively evaluated at 3.4×10^5 Pa (Sections 6.3.4 and 6.3.5).

In the nonlithophysal rock units of the repository, dynamic loading by falling rocks was found to be the most severe challenge to the emplaced waste packages. A probabilistic evaluation supported by a physical argumentation was employed to calculate the kinetic energy of the bounding credible rockfalls at impact on a waste package. The uncertainty around key parameters was considered by accounting for their variability, and by introducing conservatisms as needed in the calculation. It was found that the most severe credible rockfalls would have a mean kinetic energy on the order of 1.1×10^5 J to 5.6×10^5 J, depending on the severity of the earthquake. A rockfall with a mass of 20 metric tons and a velocity at impact on a waste package of 10 m/s, representing a kinetic energy of one million joules (10^6 J), was selected as an acceptable realization of an extreme bounding rockfall. This kinetic energy was found to be near the 99^{th} percentile of the bounding credible rockfall kinetic energy distributions resulting from the most severe earthquakes of the preclosure period (Section 6.4.5).

Severe multiple rockfall configurations (i.e., rock blocks that fall sufficiently close to each other for their impacts on a waste package to have a combined effect) were also considered. It was determined that these configurations were constituted of a massive rock block carrying the bulk of the kinetic energy, accompanied by one or several rock blocks contributing marginally to the total kinetic energy of the configuration, essentially allowing severe multiple rockfall configurations to be modeled as a single severe rockfall (Section 6.4.5.2.4).

In contrast, the mean kinetic energy at impact of typical rockfalls was found to range between 1.3×10^3 J and 3.0×10^3 J, depending on the severity of the earthquake, and with an upper value of the typical rock mass equal to 0.43 metric ton. Similarly, typical multiple rockfall configurations in which individual rock blocks are tied together by ground support were represented by a single rockfall having a kinetic energy at impact on a waste package on the order of 6,500 J to 15,000 J, with a total mass of 2.15 metric tons (Section 6.4.6).

INTENTIONALLY LEFT BLANK

ATTACHMENT A - MATHCAD CALCULATIONS

This attachment contains the Mathcad calculations that support the calculation. The reader is referred to the body of the document (Section 6) for a complete justification of the calculations performed.

A.1 Inputs of Mathcad Calculations

The files used for rockfall simulations are the Excel files from Reference 2.2.7 and described in Section 6.4.1. The data used for the calculations are imported in Mathcad as follows:

Seismic event with APE equal to 10^{-4}: the data are from the file: "nonlith rockfall characteristics in emplacement drifts with 1e-4 gm.xls", in the worksheet called "impact information". The imported data range is A5:M433. Row 0 of Inputs4 contains a description of the data.

Inputs4 :=

nonlith rockfall characte

Seismic event with APE equal to 10^{-5}: the data are from the file: "nonlith rockfall characteristics in emplacement drifts with 1e-5 gm.xls", in the worksheet called "impact information". The imported data range is A5:M1772. Row 0 of Inputs5 contains a description of the data.

Inputs5 :=

nonlith rockfall characte

Seismic event with APE equal to 10^{-6}: the data are from the file: "nonlith rockfall characteristics in emplacement drifts with 1e-6 gm.xls", in the worksheet called "impact information". The imported data range is A5:M2802. Row 0 of Inputs6 contains a description of the data.

Inputs6 :=

nonlith rockfall characte

The length of a simulated emplacement drift is, based on Assumption 3.2.8, in m:

$$L_{sim} := 20$$

The total length of emplacement drifts excavated in nonlithophysal rock units is, based on Assumption 3.2.7, in m:

$$L_{tot} := 10^4$$

The Mathcad calculations are carried out with the following worksheet options, aimed at ensuring a sufficient precision of the calculations:

- convergence tolerance: 10^{-6}
- constraint tolerance: 10^{-6}

The symbols used in this attachment have the suffix 4, 5, or 6 to indicate that they respectively pertain to the seismic events with an APE equal to 10^{-4}, 10^{-5}, or 10^{-6}.

A.2 Calculations Related to Rockfall Rate distribution (see Section 6.4.2)

For each seismic event, list the simulation numbers that have yielded rockfalls:

CA4 := (14 15 16 17 18 19 20 21 22 23 24 25 27 28 29 31 32 33 34 35)

CB4 := (36 38 39 40 41 42 43 44 45 53 55 56)

Concatenated list: C4 := augment(CA4, CB4)

CA5 := (14 15 16 17 18 19 20 21 22 23 24 25 27 28 29 31 32 33 34 35)

CB5 := (36 38 39 40 41 42 43 44 45 46 48 49)

CC5 := (50 51 52 53 54 55 56 57 58 59 60 61 62 64 65 66)

CD5 := 67

Concatenated list: C5 := augment(CA5, CB5, CC5, CD5)

CA6 := (14 15 16 17 18 19 20 21 22 23 24 25 27 28 29 31 32 33 34 35)

CB6 := (36 38 39 40 41 42 43 44 45 46 48 49 50 51 52 53 54 55 56 57)

CC6 := (58 59 60 61 62 63 64 65 66 67)

Concatenated list: C6 := augment(CA6, CB6, CC6)

Number of simulations that yielded rockfalls:

$nc4 := \text{length}\left(C4^{T}\right)$ $nc4 = 32$

$nc5 := \text{length}\left(C5^{T}\right)$ $nc5 = 49$

$nc6 := \text{length}\left(C6^{T}\right)$ $nc6 = 50$

Fitting of rockfall rate to lognormal distributions:

$i := 0..nc4 - 1$ $LF4_i := \dfrac{\text{length}\left(\text{vlookup}\left(C4_{0,i}, Inputs4, 0\right)\right)}{L_{sim}}$ This vector lists the rockfall rate for each simulation.

$LF4 := \text{sort}(LF4)$ The vector is re-arranged in ascending order.

$LF4_{i,1} := \dfrac{i+1}{nc4}$ A column is added to the vector (making it a matrix) which assigns to each rockfall rate its empirical cumulative probability.

$LF4_{i,2} := \ln\left(LF4_{i,0}\right)$ A column is added to the matrix in which the logarithm of the rockfall rate is calculated.

$mc4 := \text{mean}\left(LF4^{\langle 2 \rangle}\right)$ This returns the mean of the logarithm of observed rockfall rates.

$mc4 = -0.825$

$sc4 := \text{Stdev}\left(LF4^{\langle 2 \rangle}\right)$ This returns the sample standard deviation of the logarithm of observed rockfall rates.

$sc4 = 1.006$

The same fitting is performed on the other seismic events of interest:

$i := 0..nc5 - 1$ $LF5_i := \dfrac{\text{length}\left(\text{vlookup}\left(C5_{0,i}, Inputs5, 0\right)\right)}{L_{sim}}$

$LF5 := \text{sort}(LF5)$

$LF5 := \text{stack}\left(\dfrac{1}{L_{sim}}, LF5\right)$ As indicated in Section 6.4.2, one simulation of the seismic event with an APE equal to 10^{-5} yielded no rockfall, and is conservatively assigned 1 rockfall for the lognormal fitting.

$nc5 := nc5 + 1$

$nc5 = 50$

$i := 0..nc5 - 1$ $\quad LF5_{i,1} := \frac{i+1}{nc5}$ $\quad LF5_{i,2} := \ln\left(LF5_{i,0}\right)$

$mc5 := mean\left(LF5^{\langle 2 \rangle}\right)$ $\quad mc5 = 0.013$

$sc5 := Stdev\left(LF5^{\langle 2 \rangle}\right)$ $\quad sc5 = 1.191$

$i := 0..nc6 - 1$ $\quad LF6_i := \frac{length\left(vlookup\left(C6_{0,i}, Inputs6, 0\right)\right)}{L_{sim}}$

$LF6 := sort(LF6)$

$LF6_{i,1} := \frac{i+1}{nc6}$ $\quad LF6_{i,2} := \ln\left(LF6_{i,0}\right)$

$mc6 := mean\left(LF6^{\langle 2 \rangle}\right)$ $\quad mc6 = 0.648$

$sc6 := Stdev\left(LF6^{\langle 2 \rangle}\right)$ $\quad sc6 = 0.92$

The next step is to verify that the lognormal fitting is adequate by Anderson-Darling test (see Section 6.4.2 and Reference 2.2.9 (Section 4.8)).

Evaluate the cumulative probability of the standard normal distribution associated with the logarithm of rockfall rate:

$i := 0..nc4 - 1$ $\quad LF4_{i,3} := cnorm\left(\frac{LF4_{i,2} - mc4}{sc4}\right)$

Calculate the Anderson-Darling statistic (Reference 2.2.9, p. 101, statistic A^2):

$$A4 := -nc4 - \frac{1}{nc4} \cdot \left[\sum_i \left[(2 \cdot i + 1) \cdot \ln\left(LF4_{i,3}\right) + (2 \cdot nc4 - 1 - 2 \cdot i) \cdot \ln\left(1 - LF4_{i,3}\right)\right]\right]$$

$A4 = 0.404$

Modified value of Anderson-Darling statistic (Reference 2.2.9, Table 4.7, statistic A^2):

$A4 := A4 \cdot \left(1 + \frac{0.75}{nc4} + \frac{2.25}{nc4^2}\right)$ Anderson-Darling statistic: $A4 = 0.415$

Reference 2.2.9 (Table 4.7, statistic A^2) shows that the 5 percent significance level of the Anderson-Darling test is 0.752. Therefore, the test is passed at that significance level. The same test is performed for the other seismic events of interest in this calculation:

$$i := 0..nc5 - 1 \qquad LF5_{i,3} := cnorm\left(\frac{LF5_{i,2} - mc5}{sc5}\right)$$

$$A5 := -nc5 - \frac{1}{nc5}\cdot\left[\sum_i\left[(2\cdot i + 1)\cdot\ln\left(LF5_{i,3}\right) + (2\cdot nc5 - 1 - 2\cdot i)\cdot\ln\left(1 - LF5_{i,3}\right)\right]\right]$$

$$A5 = 0.5898$$

$$A5 := A5\cdot\left(1 + \frac{0.75}{nc5} + \frac{2.25}{nc5^2}\right) \qquad \text{Anderson-Darling statistic:} \qquad A5 = 0.599$$

The Anderson-Darling test is passed at the 5 percent significance level.

$$i := 0..nc6 - 1 \qquad LF6_{i,3} := cnorm\left(\frac{LF6_{i,2} - mc6}{sc6}\right)$$

$$A6 := -nc6 - \frac{1}{nc6}\cdot\left[\sum_i\left[(2\cdot i + 1)\cdot\ln\left(LF6_{i,3}\right) + (2\cdot nc6 - 1 - 2\cdot i)\cdot\ln\left(1 - LF6_{i,3}\right)\right]\right]$$

$$A6 = 0.387$$

$$A6 := A6\cdot\left(1 + \frac{0.75}{nc6} + \frac{2.25}{nc6^2}\right) \qquad \text{Anderson-Darling statistic:} \qquad A6 = 0.393$$

The Anderson-Darling test is passed at the 5 percent significance level.

Average number of rockfall per meter of drift yielded by the observations:

$$mean\left(LF4^{\langle 0\rangle}\right) = 0.669 \qquad mean\left(LF5^{\langle 0\rangle}\right) = 1.768 \qquad mean\left(LF6^{\langle 0\rangle}\right) = 2.797$$

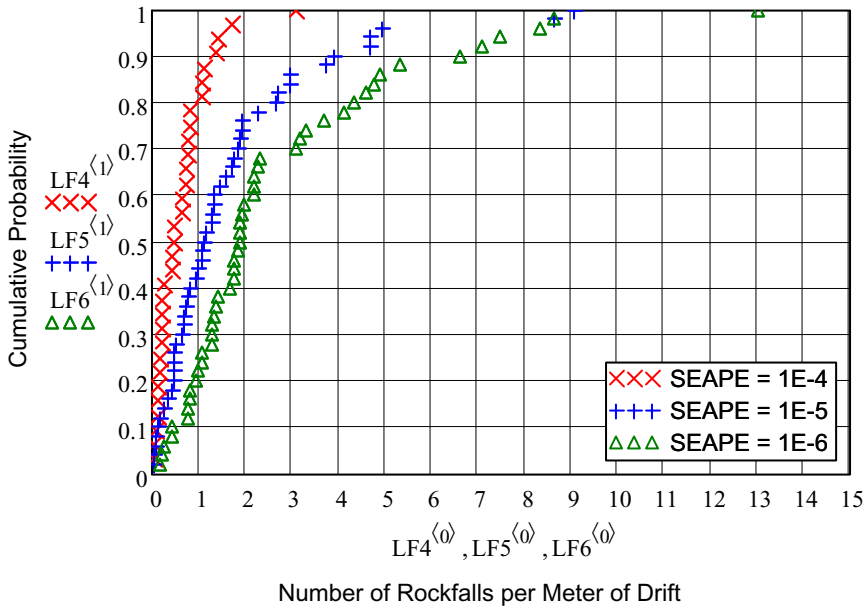

Figure A-1. Empirical Cumulative Distribution for Rockfall Rate

SEAPE = Seismic Event Annual Probability of Exceedance

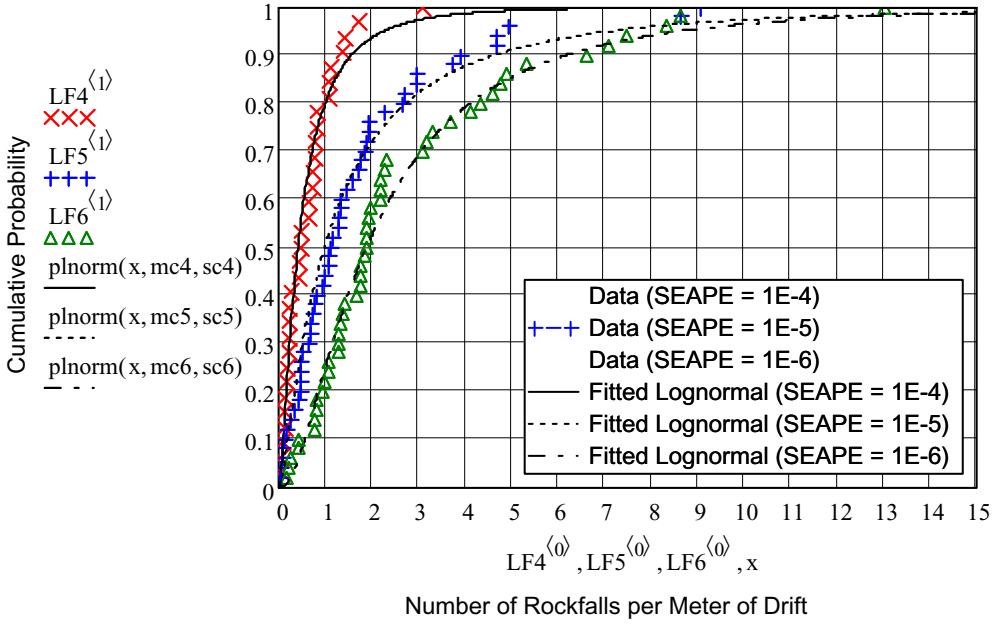

Figure A-2. Rockfall Rate Data with Fitted Lognormal Distributions

SEAPE = Seismic Event Annual Probability of Exceedance

A.3 Calculations Related to Rockfall Impact Velocity distribution (See Section 6.4.3):

Determine the total number of impact velocity data:

$n4 := \text{length}\left(\text{Inputs4}^{\langle 0 \rangle}\right) - 1$ $\quad n4 = 428$

$n5 := \text{length}\left(\text{Inputs5}^{\langle 0 \rangle}\right) - 1$ $\quad n5 = 1767$

$n6 := \text{length}\left(\text{Inputs6}^{\langle 0 \rangle}\right) - 1$ $\quad n6 = 2797$

In the matrices that gather the rockfall data (Inputs4, Inputs5, and Inputs6), the vertical component of the rockfall impact velocity on drip shields (in m/s) is in column 3, labeled "y-velocity", and the impact angle (in degrees, starting at 0 from the horizontal centerline of the drip shield, and turning counterclockwise) is in column 10, labeled "impact angle#". A new column (13) is created that contains the adjusted vertical component of the velocities for impact on waste packages, according to the specifications of Section 6.4.3.1. The adjustment affects those rocks that fall within the arc extending from 28 degrees to 180-28=152 degrees above the drip shield centerline, counting counterclockwise.

$i := 1..n4$ $\quad \text{Inputs4}_{i,13} := \text{if}\left[\left(\text{Inputs4}_{i,10} < 28\right) \vee \left(\text{Inputs4}_{i,10} > 152\right), \text{Inputs4}_{i,3}, \text{Inputs4}_{i,3} - 0.74\right]$

$i := 1..n5$ $\quad \text{Inputs5}_{i,13} := \text{if}\left[\left(\text{Inputs5}_{i,10} < 28\right) \vee \left(\text{Inputs5}_{i,10} > 152\right), \text{Inputs5}_{i,3}, \text{Inputs5}_{i,3} - 0.74\right]$

$i := 1..n6$ $\quad \text{Inputs6}_{i,13} := \text{if}\left[\left(\text{Inputs6}_{i,10} < 28\right) \vee \left(\text{Inputs6}_{i,10} > 152\right), \text{Inputs6}_{i,3}, \text{Inputs6}_{i,3} - 0.74\right]$

A vector is created that contains the absolute value of the total impact velocities on waste packages (accounting for the two horizontal components of the impact velocities, in columns 2 and 4 of matrices Inputs4, Inputs5, and Inputs6, and the adjusted vertical component of the velocity, in column 13 of these matrices. A column vector is also created to include the empirical cumulative probability for each observation, defined as explained in Section 6.4.3.2.

$i := 0..n4 - 1$ $\quad V4_i := \sqrt{\left(\text{Inputs4}_{i+1,2}\right)^2 + \left(\text{Inputs4}_{i+1,4}\right)^2 + \left(\text{Inputs4}_{i+1,13}\right)^2}$

$I4_i := \frac{i+1}{n4+1}$

$i := 0..n5 - 1$ $\quad V5_i := \sqrt{\left(\text{Inputs5}_{i+1,2}\right)^2 + \left(\text{Inputs5}_{i+1,4}\right)^2 + \left(\text{Inputs5}_{i+1,13}\right)^2}$

$I5_i := \frac{i+1}{n5+1}$

$i := 0..n6 - 1$ $\quad V6_i := \sqrt{\left(\text{Inputs6}_{i+1,2}\right)^2 + \left(\text{Inputs6}_{i+1,4}\right)^2 + \left(\text{Inputs6}_{i+1,13}\right)^2}$

$I6_i := \frac{i+1}{n6+1}$

A copy of unsorted Vectors V4, V5, and V6 is made for later use in Section A.6:

$$VV4 := V4 \quad VV5 := V5 \quad VV6 := V6$$

Velocities are sorted in ascending order:

$$V4 := \text{sort}(V4) \quad V5 := \text{sort}(V5) \quad V6 := \text{sort}(V6)$$

Sample mean of the adjusted impact velocities (in m/s) (feeds Table 2 of Section 6.4.3.1):

$$\text{mean}(V4) = 2.73 \quad \text{mean}(V5) = 3.07 \quad \text{mean}(V6) = 3.58$$

Sample standard deviation of the adjusted impact velocities (in m/s) (feeds Table 2 of Section 6.4.3.1):

$$\text{Stdev}(V4) = 1.53 \quad \text{Stdev}(V5) = 1.6 \quad \text{Stdev}(V6) = 1.82$$

Minimum observed adjusted impact velocity (in m/s) (feeds Table 2 of Section 6.4.3.1):

$$\min(V4) = 0.03 \quad \min(V5) = 0.04 \quad \min(V6) = 0.07$$

Maximum observed adjusted impact velocity (in m/s) (feeds Table 2 of Section 6.4.3.1):

$$\max(V4) = 7.204 \quad \max(V5) = 10.14 \quad \max(V6) = 12.59$$

Fitting of velocity data to exponential and Weibull distributions (see Section 6.4.3.5):

Based on Section 6.4.3.5, the lower threshold of the velocity data considered for the fitting to a Weibull distribution is qualitatively chosen at 4 m/s, 5 m/s and 5.5 m/s for the seismic events having an APE respectively equal to 10^{-4}, 10^{-5}, and 10^{-6}. The corresponding index in Vectors V4, V5, and V6 is now determined:

$$V4_{332} = 3.991 \quad V4_{333} = 4.03$$

$$V5_{1562} = 4.999 \quad V5_{1563} = 5.004$$

$$V6_{2424} = 5.492 \quad V6_{2425} = 5.5041$$

Therefore the minimum observed velocity data that are equal to or greater than the selected thresholds for the Weibull fitting have for index:

$$iwv4 := 333 \quad iwv5 := 1563 \quad iwv6 := 2425$$

Based on Section 6.4.3.5, the lower threshold of the velocity data considered for the fitting to an exponential distribution is qualitatively chosen at 5 m/s, 7 m/s and 9 m/s for the seismic events having an APE respectively equal to 10^{-4}, 10^{-5}, and 10^{-6}. The corresponding index in Vectors V4, V5, and V6 is now determined:

$V4_{397} = 4.985$ $V4_{398} = 5.004$

$V5_{1735} = 6.974$ $V5_{1736} = 7.009$

$V6_{2763} = 8.974$ $V6_{2764} = 9.009$

Therefore the minimum observed velocity data that are equal to or greater than the selected thresholds for the exponential fitting have for index:

iev4 := 398 iev5 := 1736 iev6 := 2764

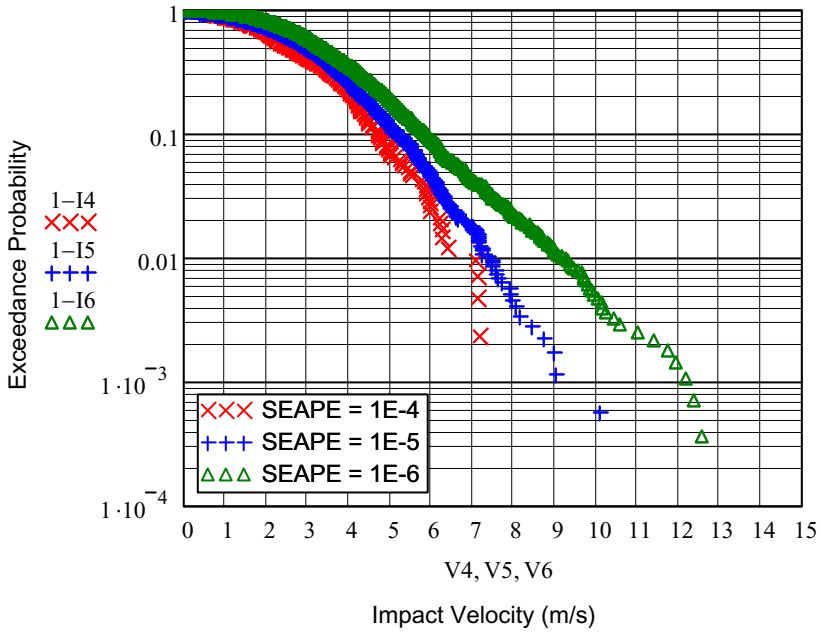

Figure A-3. Complementary Empirical Cumulative Distribution for Rockfall Impact Velocity

SEAPE = Seismic Event Annual Probability of Exceedance

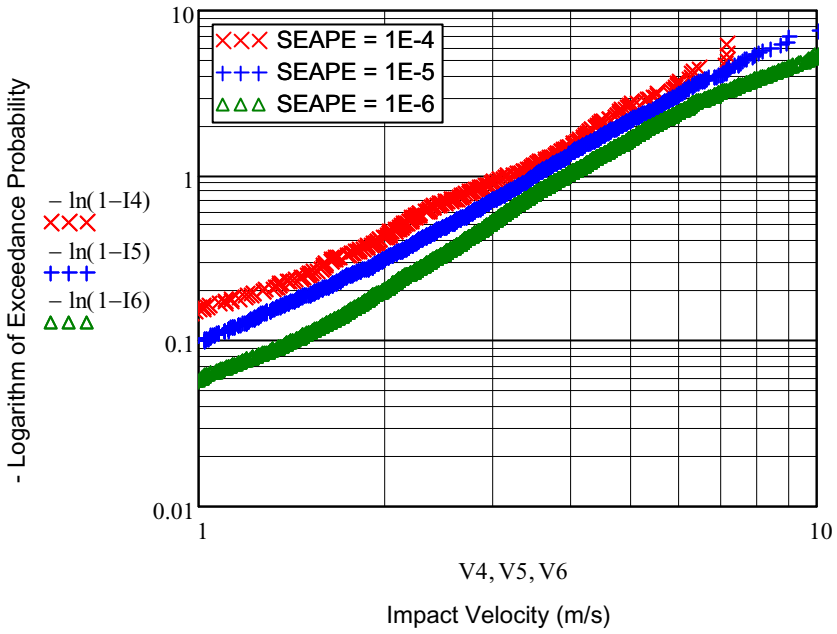

Figure A-4. Negative Logarithm of Complementary Empirical Cumulative Distribution for Rockfall Impact Velocity

SEAPE = Seismic Event Annual Probability of Exceedance

Intermediate variables for subsequent calculations:

$JW4 := \ln(-\ln(1 - I4))$ $JW5 := \ln(-\ln(1 - I5))$ $JW6 := \ln(-\ln(1 - I6))$

$JE4 := \ln(1 - I4)$ $JE5 := \ln(1 - I5)$ $JE6 := \ln(1 - I6)$

Input variables (abscissas) for linear regression - Weibull fitting (see Section 6.4.3.5):

$AWV4 := \text{submatrix}(JW4, iwv4, iev4 - 1, 0, 0)$

$AWV5 := \text{submatrix}(JW5, iwv5, iev5 - 1, 0, 0)$

$AWV6 := \text{submatrix}(JW6, iwv6, iev6 - 1, 0, 0)$

Observed data (ordinates) for linear regression - Weibull fitting (see Section 6.4.3.5):

$OWV4 := \text{submatrix}(\ln(V4), iwv4, iev4 - 1, 0, 0)$

$OWV5 := \text{submatrix}(\ln(V5), iwv5, iev5 - 1, 0, 0)$

$OWV6 := \text{submatrix}(\ln(V6), iwv6, iev6 - 1, 0, 0)$

Number of observations - Weibull fitting (feeds Table 3 of Section 6.4.3.5):

$nwv4 := length(AWV4)$ $nwv4 = 65$

$nwv5 := length(AWV5)$ $nwv5 = 173$

$nwv6 := length(AWV6)$ $nwv6 = 339$

Weibull fitting based on linear regression parameters, calculated using built-in Mathcad functions slope and intercept which use the least-squares estimation method:

shape parameter:

$$\beta V4 := \frac{1}{slope(AWV4, OWV4)} \qquad \beta V4 = 2.586$$

$$\beta V5 := \frac{1}{slope(AWV5, OWV5)} \qquad \beta V5 = 2.0647$$

$$\beta V6 := \frac{1}{slope(AWV6, OWV6)} \qquad \beta V6 = 1.641$$

scale parameter:

$\alpha V4 := \exp(intercept(AWV4, OWV4))$ $\alpha V4 = 3.41$ m/s

$\alpha V5 := \exp(intercept(AWV5, OWV5))$ $\alpha V5 = 3.475$ m/s

$\alpha V6 := \exp(intercept(AWV6, OWV6))$ $\alpha V6 = 3.526$ m/s

The values of the shape and scale parameter of the Weibull fitting found above feed Table 4 of Section 6.4.3.5.

Cumulative distribution function for fitted Weibull:

$$FWV4(x) := 1 - \exp\left[-\left(\frac{x}{\alpha V4}\right)^{\beta V4}\right]$$

$$FWV5(x) := 1 - \exp\left[-\left(\frac{x}{\alpha V5}\right)^{\beta V5}\right]$$

$$FWV6(x) := 1 - \exp\left[-\left(\frac{x}{\alpha V6}\right)^{\beta V6}\right]$$

Probability density function for fitted Weibull (based on Reference 2.2.3, p. A-18, for $\theta = 0$):

$$dFWV4(x) := \frac{\beta V4}{\alpha V4}\cdot\left(\frac{x}{\alpha V4}\right)^{\beta V4-1}\cdot\exp\left[-\left(\frac{x}{\alpha V4}\right)^{\beta V4}\right]$$

$$dFWV5(x) := \frac{\beta V5}{\alpha V5}\cdot\left(\frac{x}{\alpha V5}\right)^{\beta V5-1}\cdot\exp\left[-\left(\frac{x}{\alpha V5}\right)^{\beta V5}\right]$$

$$dFWV6(x) := \frac{\beta V6}{\alpha V6}\cdot\left(\frac{x}{\alpha V6}\right)^{\beta V6-1}\cdot\exp\left[-\left(\frac{x}{\alpha V6}\right)^{\beta V6}\right]$$

Cumulative probability value taken by fitted Weibull at lower velocity for exponential fitting:

$PV4u := FWV4\left(V4_{iev4}\right)$ $PV4u = 0.933$

$PV5u := FWV5\left(V5_{iev5}\right)$ $PV5u = 0.986$

$PV6u := FWV6\left(V6_{iev6}\right)$ $PV6u = 0.991$

Input variables (abscissas) for linear regression - exponential fitting (see Section 6.4.3.5):

$AEV4 := submatrix(JE4 - \ln(1 - PV4u), iev4, n4 - 1, 0, 0)$

$AEV5 := submatrix(JE5 - \ln(1 - PV5u), iev5, n5 - 1, 0, 0)$

$AEV6 := submatrix(JE6 - \ln(1 - PV6u), iev6, n6 - 1, 0, 0)$

Observed data (ordinates) for linear regression - exponential fitting (see Section 6.4.3.5):

$OEV4 := submatrix\left(V4 - V4_{iev4}, iev4, n4 - 1, 0, 0\right)$

$OEV5 := submatrix\left(V5 - V5_{iev5}, iev5, n5 - 1, 0, 0\right)$

$OEV6 := submatrix\left(V6 - V6_{iev6}, iev6, n6 - 1, 0, 0\right)$

Number of observations - exponential fitting (feeds Table 3 of Section 6.4.3.5):

$nev4 := length(AEV4)$ $nev5 := length(AEV5)$ $nev6 := length(AEV6)$

$nev4 = 30$ $nev5 = 31$ $nev6 = 33$

Exponential fitting based on linear regression parameter, calculated using built-in Mathcad function slope which uses the least-squares estimation method:

Inverse of parameter of exponential distribution (feeds Table 4 of Section 6.4.3.5):

$$\sigma V4 := -\text{slope}(AEV4, OEV4) \qquad \sigma V4 = 0.7343 \quad \text{m/s}$$

$$\sigma V5 := -\text{slope}(AEV5, OEV5) \qquad \sigma V5 = 0.8417 \quad \text{m/s}$$

$$\sigma V6 := -\text{slope}(AEV6, OEV6) \qquad \sigma V6 = 1.1938 \quad \text{m/s}$$

Cumulative distribution function for fitted exponential:

$$FEV4(x,\sigma) := PV4u + (1 - PV4u)\cdot\left[1 - \exp\left[\frac{-\left(x - V4_{iev4}\right)}{\sigma}\right]\right]$$

$$FEV5(x,\sigma) := PV5u + (1 - PV5u)\cdot\left[1 - \exp\left[\frac{-\left(x - V5_{iev5}\right)}{\sigma}\right]\right]$$

$$FEV6(x,\sigma) := PV6u + (1 - PV6u)\cdot\left[1 - \exp\left[\frac{-\left(x - V6_{iev6}\right)}{\sigma}\right]\right]$$

Probability density function for fitted exponential:

$$dFEV4(x,\sigma) := \frac{1 - PV4u}{\sigma}\cdot\exp\left[\frac{-\left(x - V4_{iev4}\right)}{\sigma}\right]$$

$$dFEV5(x,\sigma) := \frac{1 - PV5u}{\sigma}\cdot\exp\left[\frac{-\left(x - V5_{iev5}\right)}{\sigma}\right]$$

$$dFEV6(x,\sigma) := \frac{1 - PV6u}{\sigma}\cdot\exp\left[\frac{-\left(x - V6_{iev6}\right)}{\sigma}\right]$$

Cumulative distribution function for fitted overall impact velocity:

$$FV4(x,\sigma) := \text{if}\left(x < V4_{iev4}, FWV4(x), FEV4(x,\sigma)\right)$$

$$FV5(x,\sigma) := \text{if}\left(x < V5_{iev5}, FWV5(x), FEV5(x,\sigma)\right)$$

$$FV6(x,\sigma) := \text{if}\left(x < V6_{iev6}, FWV6(x), FEV6(x,\sigma)\right)$$

Probability density function for fitted overall impact velocity:

$$dFV4(x,\sigma) := if\left(x < V4_{iev4}, dFWV4(x), dFEV4(x,\sigma)\right)$$

$$dFV5(x,\sigma) := if\left(x < V5_{iev5}, dFWV5(x), dFEV5(x,\sigma)\right)$$

$$dFV6(x,\sigma) := if\left(x < V6_{iev6}, dFWV6(x), dFEV6(x,\sigma)\right)$$

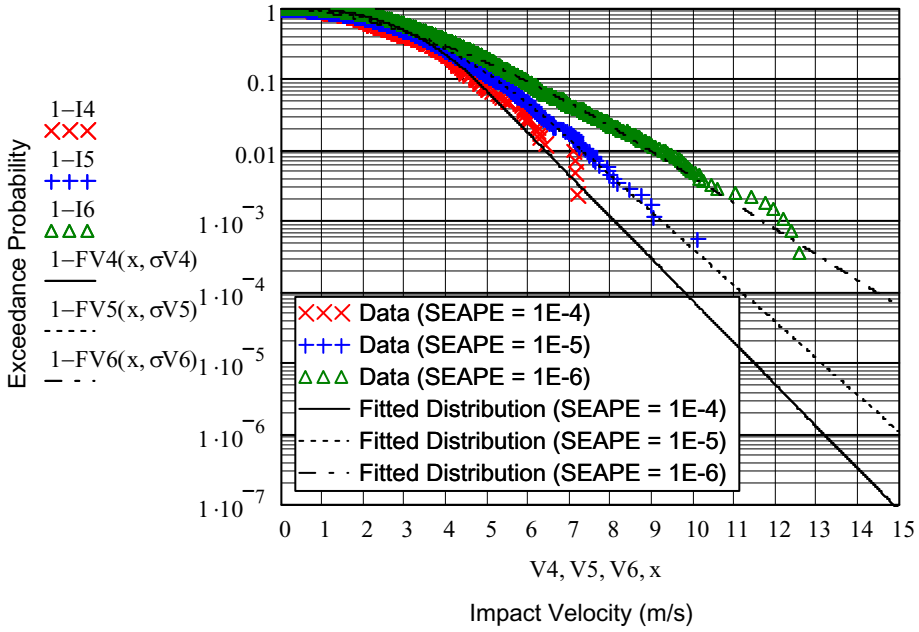

Figure A-5. Rockfall Impact Velocity Data with Fitted Distributions

SEAPE = Seismic Event Annual Probability of Exceedance

A quantitative verification that the Weibull fitting is adequate is demonstrated based on a Kolmogorov- Smirnov test on the normality of the residuals: see Section 6.4.3.5 and Reference 2.2.9 (Section 4.8.5):

Studentized residuals:

$$i := 0..nwv4 - 1$$

$$resWV4_i := \frac{OWV4_i - \left(slope(AWV4, OWV4)\cdot AWV4_i + intercept(AWV4, OWV4)\right)}{stderr(AWV4, OWV4)\cdot\left[1 - \frac{1}{nwv4} - \frac{\left(AWV4_i - mean(AWV4)\right)^2}{nwv4\cdot var(AWV4)}\right]^{0.5}}$$

$$i := 0 .. nwv5 - 1$$

$$resWV5_i := \frac{OWV5_i - \left(slope(AWV5, OWV5) \cdot AWV5_i + intercept(AWV5, OWV5)\right)}{stderr(AWV5, OWV5) \cdot \left[1 - \frac{1}{nwv5} - \frac{\left(AWV5_i - mean(AWV5)\right)^2}{nwv5 \cdot var(AWV5)}\right]^{0.5}}$$

$$i := 0 .. nwv6 - 1$$

$$resWV6_i := \frac{OWV6_i - \left(slope(AWV6, OWV6) \cdot AWV6_i + intercept(AWV6, OWV6)\right)}{stderr(AWV6, OWV6) \cdot \left[1 - \frac{1}{nwv6} - \frac{\left(AWV6_i - mean(AWV6)\right)^2}{nwv6 \cdot var(AWV6)}\right]^{0.5}}$$

Empirical distribution function estimates for residuals:

$i := 0 .. nwv4 - 1$ $\quad presWV4 := cnorm(sort(resWV4))$

$i := 0 .. nwv5 - 1$ $\quad presWV5 := cnorm(sort(resWV5))$

$i := 0 .. nwv6 - 1$ $\quad presWV6 := cnorm(sort(resWV6))$

Kolmogorov-Smirnov statistics: see formula in Reference 2.2.9 (p. 101, statistic D)

$i := 0 .. nwv4 - 1$ $\quad KPWV4_i := max\left(\frac{i+1}{nwv4} - presWV4_i\right)$ $\quad KMWV4_i := max\left(presWV4_i - \frac{i}{nwv4}\right)$

Kolmogorov Smirnov statistic: $KWV4 := max(KPWV4, KMWV4)$

$$KWV4 = 0.08$$

The threshold value for 5 percent significance level is 0.895 (Reference 2.2.9, Table 4.7, statistic D). Therefore, the Kolmogorov-Smirnov test is passed at that significance level.

$i := 0 .. nwv5 - 1$ $\quad KPWV5_i := max\left(\frac{i+1}{nwv5} - presWV5_i\right)$ $\quad KMWV5_i := max\left(presWV5_i - \frac{i}{nwv5}\right)$

Kolmogorov Smirnov statistic: $KWV5 := max(KPWV5, KMWV5)$

$$KWV5 = 0.042$$

The Kolmogorov-Smirnov test is passed at the 5 percent significance level.

$$i := 0..nwv6 - 1 \qquad KPWV6_i := \max\left(\frac{i+1}{nwv6} - presWV6_i\right) \qquad KMWV6_i := \max\left(presWV6_i - \frac{i}{nwv6}\right)$$

Kolmogorov Smirnov statistic: $KWV6 := \max(KPWV6, KMWV6)$

$$KWV6 = 0.053$$

The Kolmogorov-Smirnov test is passed at the 5 percent significance level.

A quantitative verification that the exponential fitting is adequate is performed with a Kolmogorov- Smirnov test on the normality of the residuals: see Section 6.4.3.5 and Reference 2.2.9 (Section 4.8.5):

Studentized residuals:

$i := 0..nev4 - 1$

$$resEV4_i := \frac{OEV4_i - \left(slope(AEV4, OEV4)\cdot AEV4_i + intercept(AEV4, OEV4)\right)}{stderr(AEV4, OEV4)\cdot\left[1 - \frac{1}{nev4} - \frac{\left(AEV4_i - mean(AEV4)\right)^2}{nev4\cdot var(AEV4)}\right]^{0.5}}$$

$i := 0..nev5 - 1$

$$resEV5_i := \frac{OEV5_i - \left(slope(AEV5, OEV5)\cdot AEV5_i + intercept(AEV5, OEV5)\right)}{stderr(AEV5, OEV5)\cdot\left[1 - \frac{1}{nev5} - \frac{\left(AEV5_i - mean(AEV5)\right)^2}{nev5\cdot var(AEV5)}\right]^{0.5}}$$

$i := 0..nev6 - 1$

$$resEV6_i := \frac{OEV6_i - \left(slope(AEV6, OEV6)\cdot AEV6_i + intercept(AEV6, OEV6)\right)}{stderr(AEV6, OEV6)\cdot\left[1 - \frac{1}{nev6} - \frac{\left(AEV6_i - mean(AEV6)\right)^2}{nev6\cdot var(AEV6)}\right]^{0.5}}$$

Empirical distribution function estimates for residuals:

$i := 0..nev4 - 1$ $\quad presEV4 := cnorm(sort(resEV4))$

$i := 0..nev5 - 1$ $\quad presEV5 := cnorm(sort(resEV5))$

$i := 0..nev6 - 1$ $\quad presEV6 := cnorm(sort(resEV6))$

Kolmogorov-Smirnov statistics: from Reference 2.2.9 (p. 101, statistic D):

$i := 0 .. nev4 - 1$ $\quad KPEV4_i := \max\left(\frac{i+1}{nev4} - presEV4_i\right)$ $\quad KMEV4_i := \max\left(presEV4_i - \frac{i}{nev4}\right)$

Kolmogorov Smirnov statistic: $KEV4 := \max(KPEV4, KMEV4)$

$KEV4 = 0.125$

The threshold value for the 5 percent significance level of the Kolmogorov-Smirnov statistic is 0.895 (Reference 2.2.9, Table 4.7, statistic D). Therefore, the Kolmogorov-Smirnov test is passed at that significance level.

$i := 0 .. nev5 - 1$ $\quad KPEV5_i := \max\left(\frac{i+1}{nev5} - presEV5_i\right)$ $\quad KMEV5_i := \max\left(presEV5_i - \frac{i}{nev5}\right)$

Kolmogorov Smirnov statistic: $KEV5 := \max(KPEV5, KMEV5)$

$KEV5 = 0.085$

The Kolmogorov-Smirnov test is passed at the 5 percent significance level.

$i := 0 .. nev6 - 1$ $\quad KPEV6_i := \max\left(\frac{i+1}{nev6} - presEV6_i\right)$ $\quad KMEV6_i := \max\left(presEV6_i - \frac{i}{nev6}\right)$

Kolmogorov Smirnov statistic: $KEV6 := \max(KPEV6, KMEV6)$

$KEV6 = 0.214$

The Kolmogorov-Smirnov test is passed at the 5 percent significance level.

The variability of the parameter of the fitted exponential distribution is now evaluated, using the information given in Section 6.4.3.6.

Express the linear model in a matrix form, in accordance with Reference 2.2.11 (p. 113):

$XEV4^{\langle 0 \rangle} := AEV4$

$XEV5^{\langle 0 \rangle} := AEV5$

$XEV6^{\langle 0 \rangle} := AEV6$

Intermediate variables for subsequent calculations, based on Reference 2.2.11 (p.116, Equation 2.7.15):

$$cV4 := \left[\left(XEV4^{T} \cdot XEV4 \right)^{-1} \right] \qquad cV4 = 0.023$$

$$cV5 := \left[\left(XEV5^{T} \cdot XEV5 \right)^{-1} \right] \qquad cV5 = 0.027$$

$$cV6 := \left[\left(XEV6^{T} \cdot XEV6 \right)^{-1} \right] \qquad cV6 = 0.025$$

Based on Reference 2.2.11 (p. 118, Equation 2.7.23), the regression coefficient r (slope) for the exponential fitting is related to a Student's t distribution with n-1 degrees of freedom, where n is the number of data points in the linear regression. This results in the inverse cumulative distribution associated with $\sigma = -r$ that can be expressed as:

$$\sigma sV4(x) := \sigma V4 + stderr(AEV4, OEV4) \cdot \sqrt{cV4} \cdot qt(x, nev4 - 1)$$

$$\sigma sV5(x) := \sigma V5 + stderr(AEV5, OEV5) \cdot \sqrt{cV5} \cdot qt(x, nev5 - 1)$$

$$\sigma sV6(x) := \sigma V6 + stderr(AEV6, OEV6) \cdot \sqrt{cV6} \cdot qt(x, nev6 - 1)$$

Values of σ associated with the 5th percentile and 95th percentile (feeds Table 5 of Section 6.4.3.6):

$\sigma sV4(0.05) = 0.688$	m/s	$\sigma sV4(0.95) = 0.781$	m/s
$\sigma sV5(0.05) = 0.814$	m/s	$\sigma sV5(0.95) = 0.869$	m/s
$\sigma sV6(0.05) = 1.1414$	m/s	$\sigma sV6(0.95) = 1.246$	m/s

A.4 Calculations Related to Rockfall Mass distribution (See Section 6.4.4):

In the matrices that gather the rockfall data (Inputs4, Inputs5, and Inputs6), the rockfall mass is in column 8, in metric tons. Row 0 contains a heading. Create a vector with the mass data for the different seismic events, sorted in ascending order:

$$i := 0 .. n4 - 1 \qquad M4_i := Inputs4_{i+1,8}$$

$$i := 0 .. n5 - 1 \qquad M5_i := Inputs5_{i+1,8}$$

$$i := 0 .. n6 - 1 \qquad M6_i := Inputs6_{i+1,8}$$

A copy of unsorted Vectors M4, M5, and M6 is made for later use in Section A.6:

MM4 := M4 MM5 := M5 MM6 := M6

M4 := sort(M4) M5 := sort(M5) M6 := sort(M6)

Sample mean of the rockfall mass (in metric tons) (feeds Table 6 of Section 6.4.4.1):

mean(M4) = 0.22 mean(M5) = 0.35 mean(M6) = 0.43

Sample standard deviation of the rockfall mass (in metric tons) (feeds Table 6 of Section 6.4.4.1):

Stdev(M4) = 0.33 Stdev(M5) = 0.93 Stdev(M6) = 1.3

Minimum observed rockfall mass (in metric tons) (feeds Table 6 of Section 6.4.4.1):

min(M4) = 0.02 min(M5) = 0.02 min(M6) = 0.02

Maximum observed rockfall mass (in metric tons) (feeds Table 6 of Section 6.4.4.1):

max(M4) = 2.716 max(M5) = 19.07 max(M6) = 28.22

Fitting of mass data to exponential and Weibull distributions (see Section 6.4.4.2):

Based on Section 6.4.4.2, the lower threshold of the mass data considered for the fitting to a Weibull distribution is qualitatively chosen at 0.2 metric ton, 1.5 metric tons, and 2 metric tons for the seismic events having an APE respectively equal to 10^{-4}, 10^{-5}, and 10^{-6}. The corresponding index in Vectors M4, M5, and M6 is now determined:

$M4_{305} = 0.199$ $M4_{306} = 0.201$

$M5_{1700} = 1.496$ $M5_{1701} = 1.538$

$M6_{2698} = 1.984$ $M6_{2699} = 2.003$

Therefore the minimum observed mass data that are equal to or greater than the selected thresholds for the Weibull fitting have for index:

iwm4:= 306 iwm5:= 1701 iwm6:= 2699

Based on Section 6.4.4.1, the exponential fitting of the mass data is performed on the 15 greatest observations yielded by the simulations.

$n4 - 15 = 413$ $n5 - 15 = 1.752 \times 10^{3}$ $n6 - 15 = 2.782 \times 10^{3}$

$iem4 := 413$ $iem5 := 1752$ $iem6 := 2782$

Lower mass data considered for fitting to exponential distribution, in metric tons (feeds Table 7 of Section 6.4.4.2):

$M4_{iem4} = 1.0166$ $M5_{iem5} = 4.957$ $M6_{iem6} = 7.923$

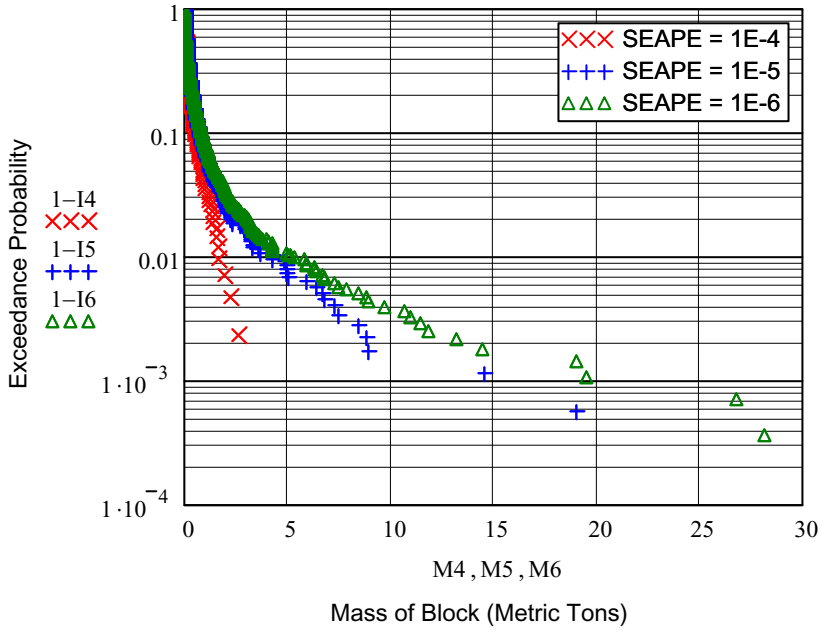

Figure A-6. Complementary Empirical Cumulative Distribution for Rockfall Mass

SEAPE = Seismic Event Annual Probability of Exceedance

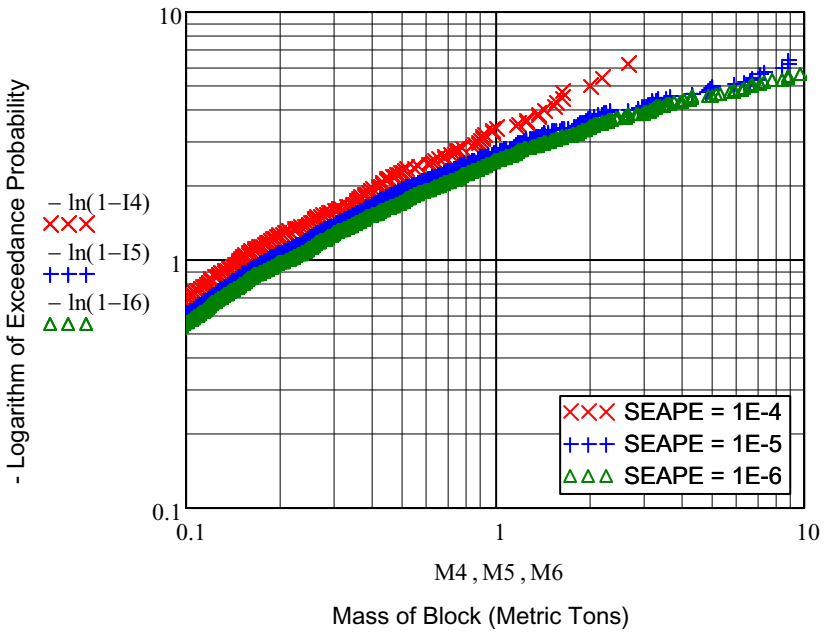

Figure A-7. Negative Logarithm of Complementary Empirical Cumulative Distribution for Rockfall Mass

SEAPE = Seismic Event Annual Probability of Exceedance

Input variables (abscissas) for linear regression - Weibull fitting:

$$AWM4 := submatrix(JW4, iwm4, iem4 - 1, 0, 0)$$

$$AWM5 := submatrix(JW5, iwm5, iem5 - 1, 0, 0)$$

$$AWM6 := submatrix(JW6, iwm6, iem6 - 1, 0, 0)$$

Observed data (ordinates) for linear regression - Weibull fitting:

$$OWM4 := submatrix(ln(M4), iwm4, iem4 - 1, 0, 0)$$

$$OWM5 := submatrix(ln(M5), iwm5, iem5 - 1, 0, 0)$$

$$OWM6 := submatrix(ln(M6), iwm6, iem6 - 1, 0, 0)$$

Number of observations - Weibull fitting (feeds Table 7 of Section 6.4.4.2):

$nwm4 := length(AWM4)$ $nwm5 := length(AWM5)$ $nwm6 := length(AWM6)$

$nwm4 = 107$ $nwm5 = 51$ $nwm6 = 83$

Weibull fitting based on linear regression parameters, calculated using built-in Mathcad functions slope and intercept which use the least-squares estimation method:

shape parameter:

$$\beta M4 := \frac{1}{\text{slope}(AWM4, OWM4)} \qquad \beta M4 = 0.613$$

$$\beta M5 := \frac{1}{\text{slope}(AWM5, OWM5)} \qquad \beta M5 = 0.351$$

$$\beta M6 := \frac{1}{\text{slope}(AWM6, OWM6)} \qquad \beta M6 = 0.318$$

scale parameter:

$\alpha M4 := \exp(\text{intercept}(AWM4, OWM4))$ $\alpha M4 = 0.143$ metric ton

$\alpha M5 := \exp(\text{intercept}(AWM5, OWM5))$ $\alpha M5 = 0.051$ metric ton

$\alpha M6 := \exp(\text{intercept}(AWM6, OWM6))$ $\alpha M6 = 0.042$ metric ton

The values of the shape and scale parameter of the Weibull fitting found above feed Table 8 of Section 6.4.4.2.

Cumulative distribution function for fitted Weibull:

$$FWM4(x) := 1 - \exp\left[-\left(\frac{x}{\alpha M4}\right)^{\beta M4}\right]$$

$$FWM5(x) := 1 - \exp\left[-\left(\frac{x}{\alpha M5}\right)^{\beta M5}\right]$$

$$FWM6(x) := 1 - \exp\left[-\left(\frac{x}{\alpha M6}\right)^{\beta M6}\right]$$

Cumulative probability value taken by fitted Weibull at lower velocity for exponential fitting:

$PM4u := FWM4\left(M4_{iem4}\right)$ $PM4u = 0.964$

$PM5u := FWM5\left(M5_{iem5}\right)$ $PM5u = 0.993$

$PM6u := FWM6\left(M6_{iem6}\right)$ $PM6u = 0.995$

Input variables (abscissas) for linear regression - exponential fitting:

$$AEM4 := submatrix(JE4 - \ln(1 - PM4u), iem4, n4 - 1, 0, 0)$$

$$AEM5 := submatrix(JE5 - \ln(1 - PM5u), iem5, n5 - 1, 0, 0)$$

$$AEM6 := submatrix(JE6 - \ln(1 - PM6u), iem6, n6 - 1, 0, 0)$$

Observed data (ordinates) for linear regression - exponential fitting:

$$OEM4 := submatrix\left(M4 - M4_{iem4}, iem4, n4 - 1, 0, 0\right)$$

$$OEM5 := submatrix\left(M5 - M5_{iem5}, iem5, n5 - 1, 0, 0\right)$$

$$OEM6 := submatrix\left(M6 - M6_{iem6}, iem6, n6 - 1, 0, 0\right)$$

Number of observations - exponential fitting:

$nem4 := length(AEM4)$ $nem5 := length(AEM5)$ $nem6 := length(AEM6)$

$nem4 = 15$ $nem5 = 15$ $nem6 = 15$

Exponential fitting based on linear regression parameter, calculated using built-in Mathcad function slope which uses the least-squares estimation method:

Inverse of parameter of exponential distribution (feeds Table 8 of Section 6.4.4.2):

$\sigma M4 := -slope(AEM4, OEM4)$	$\sigma M4 = 0.572$	metric ton
$\sigma M5 := -slope(AEM5, OEM5)$	$\sigma M5 = 4.778$	metric tons
$\sigma M6 := -slope(AEM6, OEM6)$	$\sigma M6 = 8.1542$	metric tons

Cumulative distribution function for fitted exponential:

$$FEM4(x, \sigma) := (1 - PM4u) \cdot \left[1 - \exp\left[\frac{-\left(x - M4_{iem4}\right)}{\sigma}\right]\right] + PM4u$$

$$FEM5(x, \sigma) := (1 - PM5u) \cdot \left[1 - \exp\left[\frac{-\left(x - M5_{iem5}\right)}{\sigma}\right]\right] + PM5u$$

$$FEM6(x, \sigma) := (1 - PM6u) \cdot \left[1 - \exp\left[\frac{-\left(x - M6_{iem6}\right)}{\sigma}\right]\right] + PM6u$$

Cumulative distribution function for fitted overall rockfall mass:

$$FM4(x, \sigma) := if\left(x < M4_{iem4}, FWM4(x), FEM4(x, \sigma)\right)$$

$$FM5(x, \sigma) := if\left(x < M5_{iem5}, FWM5(x), FEM5(x, \sigma)\right)$$

$$FM6(x, \sigma) := if\left(x < M6_{iem6}, FWM6(x), FEM6(x, \sigma)\right)$$

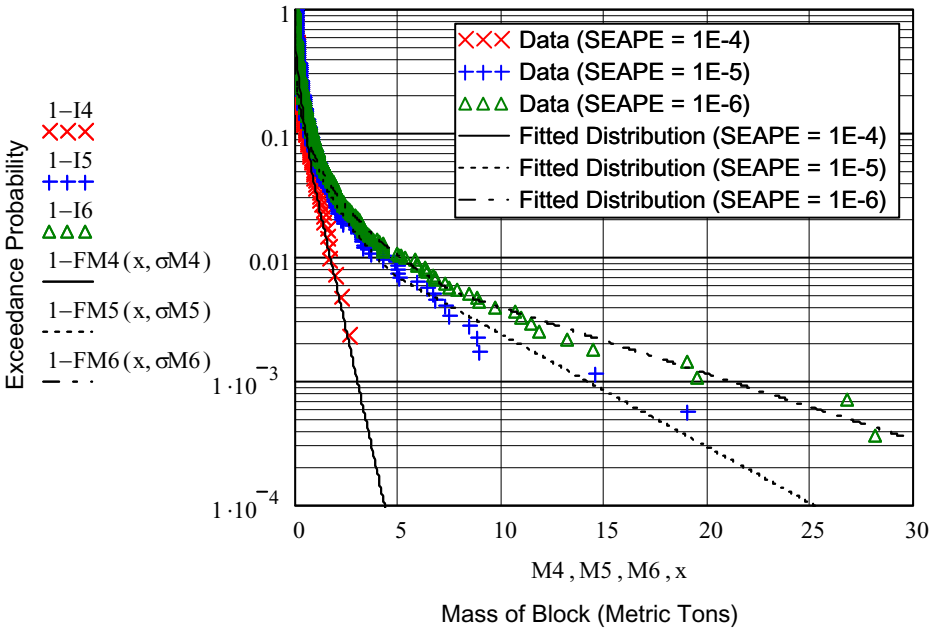

Figure A-8. Rockfall Mass Data with Fitted Distributions

SEAPE = Seismic Event Annual Probability of Exceedance

A quantitative verification that the Weibull fitting is adequate is performed with a Kolmogorov- Smirnov test on the normality of the residuals: see Section 6.4.4.2 and Reference 2.2.9 (Section 4.8.5):

Studentized residuals:

$$i := 0 .. nwm4 - 1$$

$$resWM4_i := \frac{OWM4_i - \left(slope(AWM4, OWM4)\cdot AWM4_i + intercept(AWM4, OWM4)\right)}{stderr(AWM4, OWM4)\cdot\left[1 - \frac{1}{nwm4} - \frac{\left(AWM4_i - mean(AWM4)\right)^2}{nwm4\cdot var(AWM4)}\right]^{0.5}}$$

$$i := 0 .. nwm5 - 1$$

$$resWM5_i := \frac{OWM5_i - \left(slope(AWM5, OWM5)\cdot AWM5_i + intercept(AWM5, OWM5)\right)}{stderr(AWM5, OWM5)\cdot\left[1 - \frac{1}{nwm5} - \frac{\left(AWM5_i - mean(AWM5)\right)^2}{nwm5\cdot var(AWM5)}\right]^{0.5}}$$

$$i := 0..\,nwm6 - 1$$

$$resWM6_i := \frac{OWM6_i - \left(slope(AWM6, OWM6)\cdot AWM6_i + intercept(AWM6, OWM6)\right)}{stderr(AWM6, OWM6)\cdot\left[1 - \frac{1}{nwm6} - \frac{\left(AWM6_i - mean(AWM6)\right)^2}{nwm6\cdot var(AWM6)}\right]^{0.5}}$$

Empirical distribution function estimates for residuals:

$$i := 0..\,nwm4 - 1 \qquad presWM4 := cnorm(sort(resWM4))$$

$$i := 0..\,nwm5 - 1 \qquad presWM5 := cnorm(sort(resWM5))$$

$$i := 0..\,nwm6 - 1 \qquad presWM6 := cnorm(sort(resWM6))$$

Kolmogorov-Smirnov statistics: see formula in Reference 2.2.9 (p. 101, statistic D):

$$i := 0..\,nwm4 - 1 \qquad KPWM4_i := max\left(\frac{i+1}{nwm4} - presWM4_i\right) \qquad KMWM4_i := max\left(presWM4_i - \frac{i}{nwm4}\right)$$

Kolmogorov Smirnov statistic: $KWM4 := max(KPWM4, KMWM4)$

$$KWM4 = 0.076$$

Threshold value for 5 percent significance level is 0.895 (Reference 2.2.9, Table 4.7, statistic D). Therefore, the Kolmogorov-Smirnov test is passed at that significance level.

$$i := 0..\,nwm5 - 1 \qquad KPWM5_i := max\left(\frac{i+1}{nwm5} - presWM5_i\right) \qquad KMWM5_i := max\left(presWM5_i - \frac{i}{nwm5}\right)$$

Kolmogorov Smirnov statistic: $KWM5 := max(KPWM5, KMWM5)$

$$KWM5 = 0.08$$

The Kolmogorov-Smirnov test is passed at the 5 percent significance level.

$$i := 0..\,nwm6 - 1 \qquad KPWM6_i := max\left(\frac{i+1}{nwm6} - presWM6_i\right) \qquad KMWM6_i := max\left(presWM6_i - \frac{i}{nwm6}\right)$$

Kolmogorov Smirnov statistic: $KWM6 := max(KPWM6, KMWM6)$

$$KWM6 = 0.06$$

The Kolmogorov-Smirnov test is passed at the 5 percent significance level.

A quantitative verification that the exponential fitting is adequate is demonstrated based on a Kolmogorov-Smirnov test: see Section 6.4.4.2 and Reference 2.2.9 (Section 4.8.5):

Studentized residuals:

$i := 0..\,nem4 - 1$

$$resEM4_i := \frac{OEM4_i - \left(slope(AEM4, OEM4)\cdot AEM4_i + intercept(AEM4, OEM4)\right)}{stderr(AEM4, OEM4)\cdot\left[1 - \frac{1}{nem4} - \frac{\left(AEM4_i - mean(AEM4)\right)^2}{nem4\cdot var(AEM4)}\right]^{-0.5}}$$

$i := 0..\,nem5 - 1$

$$resEM5_i := \frac{OEM5_i - \left(slope(AEM5, OEM5)\cdot AEM5_i + intercept(AEM5, OEM5)\right)}{stderr(AEM5, OEM5)\cdot\left[1 - \frac{1}{nem5} - \frac{\left(AEM5_i - mean(AEM5)\right)^2}{nem5\cdot var(AEM5)}\right]^{-0.5}}$$

$i := 0..\,nem6 - 1$

$$resEM6_i := \frac{OEM6_i - \left(slope(AEM6, OEM6)\cdot AEM6_i + intercept(AEM6, OEM6)\right)}{stderr(AEM6, OEM6)\cdot\left[1 - \frac{1}{nem6} - \frac{\left(AEM6_i - mean(AEM6)\right)^2}{nem6\cdot var(AEM6)}\right]^{-0.5}}$$

Empirical distribution function estimates for residuals:

$i := 0..\,nem4 - 1 \qquad presEM4 := cnorm(sort(resEM4))$

$i := 0..\,nem5 - 1 \qquad presEM5 := cnorm(sort(resEM5))$

$i := 0..\,nem6 - 1 \qquad presEM6 := cnorm(sort(resEM6))$

Kolmogorov-Smirnov estimates: see formula in Reference 2.2.9 (p. 101, statistic D)

$i := 0..\,nem4 - 1 \qquad KPEM4_i := max\left(\frac{i+1}{nem4} - presEM4_i\right) \qquad KMEM4_i := max\left(presEM4_i - \frac{i}{nem4}\right)$

Kolmogorov Smirnov statistic: $KEM4 := max(KPEM4, KMEM4)$

$KEM4 = 0.232$

Threshold value for 5 percent significance level is 0.895 (Reference 2.2.9, Table 4.7). Therefore, the Kolmogorov-Smirnov test is passed at that significance level.

$i := 0..nem5 - 1$ $KPEM5_i := \max\left(\frac{i+1}{nem5} - presEM5_i\right)$ $KMEM5_i := \max\left(presEM5_i - \frac{i}{nem5}\right)$

Kolmogorov Smirnov statistic: $KEM5 := \max(KPEM5, KMEM5)$

$KEM5 = 0.124$

The Kolmogorov-Smirnov test is passed at the 5 percent significance level.

$i := 0..nem6 - 1$ $KPEM6_i := \max\left(\frac{i+1}{nem6} - presEM6_i\right)$ $KMEM6_i := \max\left(presEM6_i - \frac{i}{nem6}\right)$

Kolmogorov Smirnov statistic: $KEM6 := \max(KPEM6, KMEM6)$

$KEM6 = 0.119$

The Kolmogorov-Smirnov test is passed at the 5 percent significance level.

Variability of the parameter of the fitted exponential distribution: see Section 6.4.4.3

Express the linear model in a matrix form, in accordance to Reference 2.2.11 (p. 113):

$XEM4^{\langle 0 \rangle} := AEM4$

$XEM5^{\langle 0 \rangle} := AEM5$

$XEM6^{\langle 0 \rangle} := AEM6$

Intermediate variables for subsequent calculations, based on Reference 2.2.11(p. 116, Equation 2.7.15):

$cM4 := \left[\left(XEM4^T \cdot XEM4\right)^{-1}\right]$ $cM4 = 0.05$

$cM5 := \left[\left(XEM5^T \cdot XEM5\right)^{-1}\right]$ $cM5 = 0.068$

$cM6 := \left[\left(XEM6^T \cdot XEM6\right)^{-1}\right]$ $cM6 = 0.056$

Based on Reference 2.2.11 (p. 118, Equation 2.7.23), the regression coefficient r (slope) for the exponential fitting is related to a Student's t distribution with n-1 degrees of freedom, where n is the number of data points in the linear regression.

This results in the inverse cumulative distribution associated with σ=–r that can be expressed as:

$$\sigma sM4(x) := \sigma M4 + \text{stderr}(AEM4, OEM4)\cdot\sqrt{cM4}\cdot qt(x, nem4 - 1)$$

$$\sigma sM5(x) := \sigma M5 + \text{stderr}(AEM5, OEM5)\cdot\sqrt{cM5}\cdot qt(x, nem5 - 1)$$

$$\sigma sM6(x) := \sigma M6 + \text{stderr}(AEM6, OEM6)\cdot\sqrt{cM6}\cdot qt(x, nem6 - 1)$$

Values of σ associated with the 5th percentile and 95th percentile (feeds Table 9 of Section 6.4.4.3):

$\sigma sM4(0.05) = 0.546$	metric ton	$\sigma sM4(0.95) = 0.599$	metric ton
$\sigma sM5(0.05) = 4.231$	metric tons	$\sigma sM5(0.95) = 5.326$	metric tons
$\sigma sM6(0.05) = 7.606$	metric tons	$\sigma sM6(0.95) = 8.703$	metric tons

A.5 Calculation of Bounding Credible Rockfall Kinetic Energy: see Section 6.4.5

Calculate the right-hand side of Equation 13 in Section 6.4.5.1, which represents the exceedance probability not to be exceeded by the complementary cumulative distribution function of the rockfall kinetic energy. As explained in Section 6.4.5.1, the probability of occurrence, over the preclosure period, of at least one earthquake with APE ranging respectively between 10^{-4} and 10^{-5}, 10^{-5} and 10^{-6}, and 10^{-6} or less is calculated using a binomial distribution. The right-hand side of Equation 13 is represented as a function of f, the rockfall rate, and n, the number of years in the preclosure period.

$$p4(f, n) := 1 - \left(1 - \frac{10^{-4}}{1 - \text{dbinom}\left(0, n, 10^{-4} - 10^{-5}\right)}\right)^{\frac{1}{L_{tot}\cdot f}}$$

$$p5(f, n) := 1 - \left(1 - \frac{10^{-4}}{1 - \text{dbinom}\left(0, n, 10^{-5} - 10^{-6}\right)}\right)^{\frac{1}{L_{tot}\cdot f}}$$

$$p6(f,n) := 1 - \left(1 - \frac{10^{-4}}{1 - \text{dbinom}\left(0, n, 10^{-6}\right)}\right)^{\frac{1}{L_{tot} \cdot f}}$$

Exceedance probabilities for average number of rockfalls per meter yielded by the simulations:

$p4\left(\text{mean}\left(LF4^{\langle 0 \rangle}\right), 100\right) = 1.678 \times 10^{-6}$

$p5\left(\text{mean}\left(LF5^{\langle 0 \rangle}\right), 100\right) = 6.665 \times 10^{-6}$

$p6\left(\text{mean}\left(LF6^{\langle 0 \rangle}\right), 105\right) = 1.089 \times 10^{-4}$ n here is assigned a value of 105 to ensure that the result remains a real number.

Explore the variability of parameter of fitted exponential distributions and variability of rockfall rate by Latin hypercube sampling (see Sections 6.4.5.1 and 6.4.5.2.1)

Create vectors of Latin hypercube samples between 0 and 1.

Size of the sampling: $nlhs := 10^3$

$Seed(100) = 1$ Ensures reproducibility of the results by fixing seed of random sampling

Intermediate variables for subsequent calculations:

$i := 0 .. nlhs - 1$ $RD_i := i$ Vector of ordered natural integers ranging between 0 and nlhs-1

$RD^{\langle 1 \rangle} := runif(nlhs, 0, 1)$

$RD^{\langle 2 \rangle} := runif(nlhs, 0, 1)$

$RD^{\langle 3 \rangle} := runif(nlhs, 0, 1)$

These are 3 vectors of random numbers uniformly distributed between 0 and 1.

Using Column 0 of these vectors, develop vectors of stratified random numbers comprised between 0 and 1:

$$RDf := \frac{csort(RD, 1)^{\langle 0 \rangle} + runif(nlhs, 0, 1)}{nlhs}$$

$$RDv := \frac{csort(RD, 2)^{\langle 0 \rangle} + runif(nlhs, 0, 1)}{nlhs}$$

$$RDm := \frac{csort(RD, 3)^{\langle 0 \rangle} + runif(nlhs, 0, 1)}{nlhs}$$

Each vector contains nlhs samples. Each sample is a number, randomly selected within an interval that is comprised between i/nlhs and (i+1)/nlhs, where i takes all integer values between 0 and nlhs-1.

Vector of sampled values for the rockfall rate (calculated by taking the inverse of the lognormal cumulative probability distribution associated with the rockfall rate):

$$fs4 := qlnorm(RDf, mc4, sc4)$$

$$fs5 := qlnorm(RDf, mc5, sc5)$$

$$fs6 := qlnorm(RDf, mc6, sc6)$$

Vector of sampled values for exceedance probabilities (right-hand side of Equation 13 in Section 6.4.5.1):

$$ps4 := p4(fs4, 100)$$

$$ps5 := p5(fs5, 100)$$

$$ps6 := p6(fs6, 105)$$

a value of 105 yrs is used to ensure that ps6 exists: see previous discussion and also Section 6.4.5.1.

Vector of sampled values for inverse of exponential parameter of rockfall impact velocity distribution and rockfall mass distribution:

$$\sigma Vs4 := \sigma sV4(RDv) \qquad \sigma Ms4 := \sigma sM4(RDm)$$

$$\sigma Vs5 := \sigma sV5(RDv) \qquad \sigma Ms5 := \sigma sM5(RDm)$$

$$\sigma Vs6 := \sigma sV6(RDv) \qquad \sigma Ms6 := \sigma sM6(RDm)$$

Exceedance probabilities as a function of kinetic energy (Equation 14 of Section 6.4.5.1):

$$PK4(K, \sigma Vs4, \sigma Ms4) := \int_0^{\infty} dFV4(x, \sigma Vs4) \cdot \left(1 - FM4\left(\frac{2 \cdot K}{1000 \cdot x^2}, \sigma Ms4\right)\right) dx$$

$$PK5(K, \sigma Vs5, \sigma Ms5) := \int_0^{\infty} dFV5(x, \sigma Vs5) \cdot \left(1 - FM5\left(\frac{2 \cdot K}{1000 \cdot x^2}, \sigma Ms5\right)\right) dx$$

$$PK6(K, \sigma Vs6, \sigma Ms6) := \int_0^{\infty} dFV6(x, \sigma Vs6) \cdot \left(1 - FM6\left(\frac{2 \cdot K}{1000 \cdot x^2}, \sigma Ms6\right)\right) dx$$

Vectors of sampled bounding credible kinetic energy are found by solving the following equations, in which initial guess values determined by trials and errors are used for the interval boundaries containing the solutions to the equations:

$i := 0 .. nlhs - 1$

$$K4_i := root\left(PK4(K, \sigma Vs4_i, \sigma Ms4_i) - ps4_i, K, 40000, 300000\right)$$

$$K5_i := root\left(PK5(K, \sigma Vs5_i, \sigma Ms5_i) - ps5_i, K, 50000, 2000000\right)$$

$$K6_i := root\left(PK6(K, \sigma Vs6_i, \sigma Ms6_i) - ps6_i, K, 40000, 2000000\right)$$

Sort the kinetic energies in ascending order:

$K4 := sort(K4)$ $K5 := sort(K5)$ $K6 := sort(K6)$

Create a vector for the empirical cumulative distribution associated with the sampling:

$$O_i := \frac{i + 1}{nlhs + 1}$$

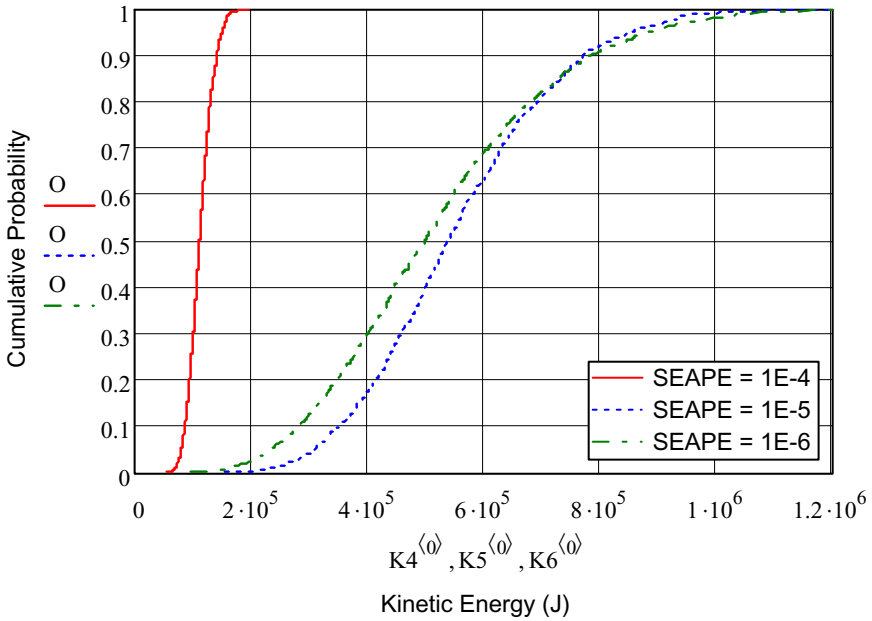

Figure A-9. Cumulative Distribution Function for Bounding Credible Rockfall Kinetic Energy

SEAPE = Seismic Event Annual Probability of Exceedance

Mean value of bounding credible kinetic energy (J):

$\text{mean}(K4) = 1.146 \times 10^5$

$\text{mean}(K5) = 5.571 \times 10^5$

$\text{mean}(K6) = 5.221 \times 10^5$

Corresponding closest percentile on the distribution:

$K4_{521} = 1.146 \times 10^5$	$O_{521} = 0.521$	52nd percentile
$K5_{535} = 5.571 \times 10^5$	$O_{535} = 0.535$	54th percentile
$K6_{539} = 5.219 \times 10^5$	$O_{539} = 0.539$	54th percentile

Calculated values near 1,000,000 J:

$K5_{992} = 1.012\times 10^{6}$ $O_{992} = 0.99$ 99th percentile

$K6_{980} = 1.003\times 10^{6}$ $O_{980} = 0.98$ 98th percentile

99th percentile of the bounding credible rockfall kinetic energy associated with the range of seismic events described by an APE equal to 10-4:

$K4_{990} = 1.661\times 10^{5}$ J

Multiple rockfall configurations: see Section 6.4.5.2.4

Fraction of rockfall rates greater than or equal to 2 rockfalls per meter:

$$1 - \text{plnorm}(2, mc4, sc4) = 0.066$$

$$1 - \text{plnorm}(2, mc5, sc5) = 0.284$$

$$1 - \text{plnorm}(2, mc6, sc6) = 0.48$$

Probability density function for fitted overall mass (based on Section 6.4.4.2):

A) for Weibull fittings (based on Reference 2.2.3, p. A-18):

$$dFWM4(x) := \frac{\beta M4}{\alpha M4}\cdot\left(\frac{x}{\alpha M4}\right)^{\beta M4-1}\cdot\exp\left[-\left(\frac{x}{\alpha M4}\right)^{\beta M4}\right]$$

$$dFWM5(x) := \frac{\beta M5}{\alpha M5}\cdot\left(\frac{x}{\alpha M5}\right)^{\beta M5-1}\cdot\exp\left[-\left(\frac{x}{\alpha M5}\right)^{\beta M5}\right]$$

$$dFWM6(x) := \frac{\beta M6}{\alpha M6}\cdot\left(\frac{x}{\alpha M6}\right)^{\beta M6-1}\cdot\exp\left[-\left(\frac{x}{\alpha M6}\right)^{\beta M6}\right]$$

B) for exponential fittings:

$$dFEM4(x,\sigma) := \frac{1 - PM4u}{\sigma}\cdot\exp\left[\frac{-\left(x - M4_{iem4}\right)}{\sigma}\right]$$

$$dFEM5(x,\sigma) := \frac{1 - PM5u}{\sigma} \cdot \exp\left[\frac{-(x - M5_{iem5})}{\sigma}\right]$$

$$dFEM6(x,\sigma) := \frac{1 - PM6u}{\sigma} \cdot \exp\left[\frac{-(x - M6_{iem6})}{\sigma}\right]$$

for overall distributions:

$$dFM4(x,\sigma) := if(x < M4_{iem4}, dFWM4(x), dFEM4(x,\sigma))$$

$$dFM5(x,\sigma) := if(x < M5_{iem5}, dFWM5(x), dFEM5(x,\sigma))$$

$$dFM6(x,\sigma) := if(x < M6_{iem6}, dFWM6(x), dFEM6(x,\sigma))$$

$$FMB4(x,\sigma) := if(x < 0, 0, FM4(x,\sigma))$$

$$FMB5(x,\sigma) := if(x < 0, 0, FM5(x,\sigma))$$

$$FMB6(x,\sigma) := if(x < 0, 0, FM6(x,\sigma))$$

Complementary cumulative distribution for total mass of multiple rockfall configuration involving two rock blocks: see Equation 15 of Section 6.4.5.2.4)

$$PM4(x) := \int_0^x dFM4(u,\sigma M4) \cdot (1 - FMB4(x - u,\sigma M4))\, du$$

$$PM5(x) := \int_0^x dFM5(u,\sigma M5) \cdot (1 - FMB5(x - u,\sigma M5))\, du$$

$$PM6(x) := \int_0^x dFM6(u,\sigma M6) \cdot (1 - FMB6(x - u,\sigma M6))\, du$$

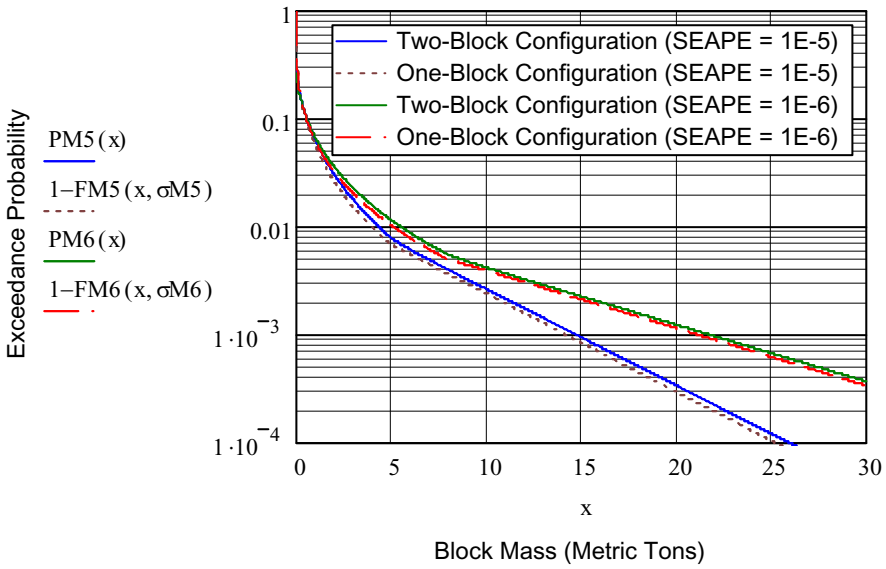

Figure A-10. Complementary Cumulative Distribution Functions for Rockfall Mass of One-Block and Two-Block Configurations

SEAPE = Seismic Event Annual Probability of Exceedance

Mass associated with an exceedance level of 0.001:

for two-block configuration and APE = 10^{-5}:

$$\text{root}(PM5(x) - 0.001, x, 10, 20) = 14.739 \quad \text{metric tons}$$

for one-block configuration and APE = 10^{-5}:

$$\text{root}(1 - FM5(x, \sigma M5) - 0.001, x, 10, 20) = 14.19 \quad \text{metric tons}$$

for two-block configuration and APE = 10^{-6}:

$$\text{root}(PM6(x) - 0.001, x, 15, 25) = 21.716 \quad \text{metric tons}$$

for one-block configuration and APE = 10^{-6}:

$$\text{root}(1 - FM6(x, \sigma M6) - 0.001, x, 15, 25) = 21.102 \quad \text{metric tons}$$

Characterization of bounding credible rockfall (see Section 6.4.5.2.5)

Find the velocity that maximizes the integrand in Equation 14 (Section 6.4.5.1):

$$pK5(K,x) := dFV5(x,\sigma V5)\cdot\left(1 - FM5\left(\frac{2\cdot K}{1000\cdot x^2},\sigma M5\right)\right)$$

$$pK6(K,x) := dFV6(x,\sigma V6)\cdot\left(1 - FM6\left(\frac{2\cdot K}{1000\cdot x^2},\sigma M6\right)\right)$$

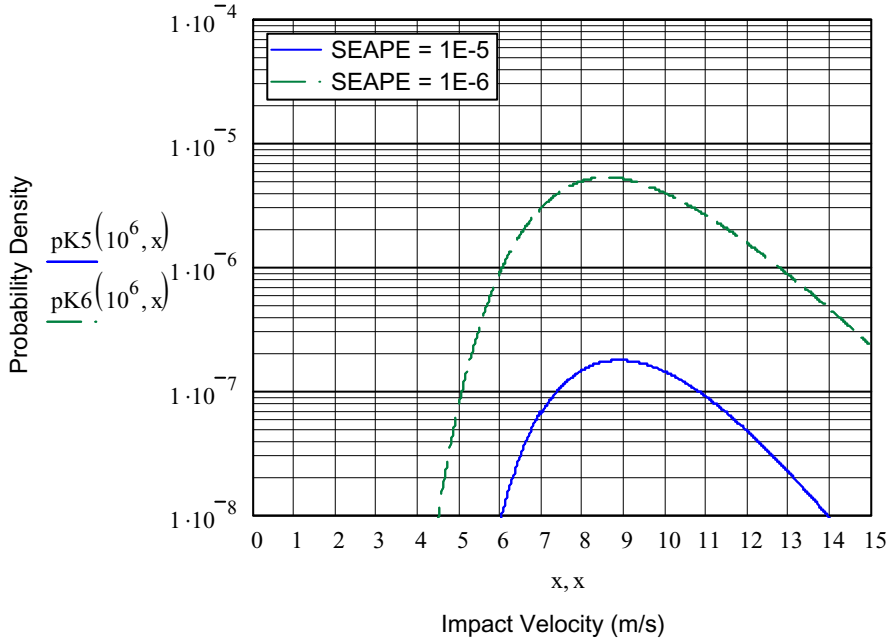

Figure A-11. Probability Density as a Function of Rockfall Impact Velocity

SEAPE = Seismic Event Annual Probability of Exceedance

A.6 Calculation of Rockfall Kinetic Energy: see Section 6.4.6

Calculate, in joules, the kinetic energy of each simulated rockfall, adjusted for impacts on waste packages. The adjusted velocity of each rockfall is given in Vectors VV4, VV5, and VV6 (created in Section A.3), while the mass of each rockfall is given in Vectors MM4, MM5, and MM6 (created in Section A.4).

$i := 0..n4 - 1 \qquad KK4_i := 0.5 \cdot MM4_i \cdot 1000 \cdot (VV4)^2$

$i := 0..n5 - 1 \qquad KK5_i := 0.5 \cdot MM5_i \cdot 1000 \cdot (VV5)^2$

$i := 0..n6 - 1 \qquad KK6_i := 0.5 \cdot MM6_i \cdot 1000 \cdot (VV6)^2$

KK4, KK5, and KK6 are the vectors of rockfall kinetic energy, expressed in joules.

Sort kinetic energy vectors in ascending order:

$KK4 := sort(KK4) \qquad KK5 := sort(KK5) \qquad KK6 := sort(KK6)$

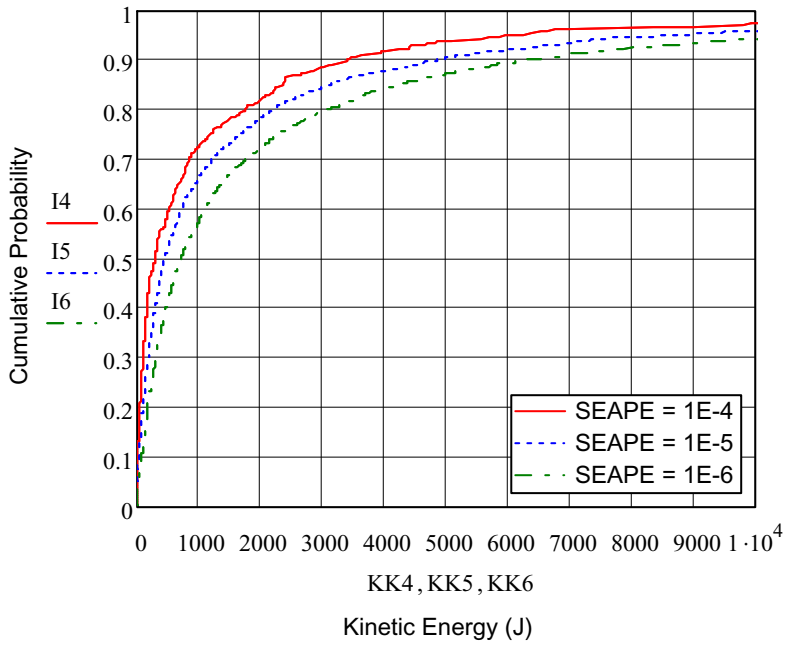

Figure A-12. Cumulative Distribution Function for Rockfall Kinetic Energy

SEAPE = Seismic Event Annual Probability of Exceedance

Kinetic energy (in J) associated with selected percentiles:

10th percentile:	$I4_{42} = 0.1$	$KK4_{42} = 18$	20th percentile:	$I4_{85} = 0.2$	$KK4_{85} = 61$
	$I5_{176} = 0.1$	$KK5_{176} = 36$		$I5_{353} = 0.2$	$KK5_{353} = 104$
	$I6_{279} = 0.1$	$KK6_{279} = 86$		$I6_{559} = 0.2$	$KK6_{559} = 188$

30th percentile: $I4_{128} = 0.3$ $KK4_{128} = 114$ 40th percentile: $I4_{171} = 0.4$ $KK4_{171} = 176$

$I5_{529} = 0.3$ $KK5_{529} = 199$ $I5_{706} = 0.4$ $KK5_{706} = 309$

$I6_{838} = 0.3$ $KK6_{838} = 324$ $I6_{1118} = 0.4$ $KK6_{1118} = 483$

50th percentile: $I4_{214} = 0.5$ $KK4_{214} = 303$ 60th percentile: $I4_{256} = 0.6$ $KK4_{256} = 537$

$I5_{883} = 0.5$ $KK5_{883} = 455$ $I5_{1060} = 0.6$ $KK5_{1060} = 738$

$I6_{1398} = 0.5$ $KK6_{1398} = 725$ $I6_{1678} = 0.6$ $KK6_{1678} = 1116$

70th percentile: $I4_{299} = 0.7$ $KK4_{299} = 861$ 80th percentile: $I4_{342} = 0.8$ $KK4_{342} = 1758$

$I5_{1237} = 0.7$ $KK5_{1237} = 1234$ $I5_{1413} = 0.8$ $KK5_{1413} = 2214$

$I6_{1958} = 0.7$ $KK6_{1958} = 1797$ $I6_{2237} = 0.8$ $KK6_{2237} = 3107$

90th percentile: $I4_{385} = 0.9$ $KK4_{385} = 3425$ 95th percentile: $I4_{407} = 0.95$ $KK4_{407} = 6252$

$I5_{1590} = 0.9$ $KK5_{1590} = 4901$ $I5_{1679} = 0.95$ $KK5_{1679} = 8873$

$I6_{2517} = 0.9$ $KK6_{2517} = 6259$ $I6_{2657} = 0.95$ $KK6_{2657} = 11062$

Mean rockfall kinetic energy (in J):

$$\text{mean(KK4)} = 1.357 \times 10^3$$

$$\text{mean(KK5)} = 2.42 \times 10^3$$

$$\text{mean(KK6)} = 3.004 \times 10^3$$

ATTACHMENT B

DRIP SHIELD AND WASTE PACKAGE GEOMETRY IN EMPLACEMENT DRIFT

The purpose of this attachment is to outline the drip shield and waste package geometry in order to support assumptions in Section 3.

B.1. Drip Shield Geometry in Emplacement Drift

This section outlines the drip shield geometry in emplacement drifts used in Reference 2.2.1 to evaluate the impact velocity of rockfalls. Based on this geometry, a representative distance traveled by a rock falling from the upper part of an emplacement drift and impacting the upper portion of a drip shield is calculated to support Assumption 3.2.5. Also, the angle α shown on Figure B-1 and representing the angle made by the drip shield shoulder above the drip shield horizontal centerline is calculated, in support of Assumption 3.2.4.

Reference 2.2.1 (Table 4-1) uses the same emplacement drift diameter as that considered for License Application and given in Reference 2.2.8 (Table 8) as 5.5 m, and bases the drip shield geometry on Reference 2.2.8 and Reference 2.2.18. Although these references are canceled or superseded, they are suitable for use in this section because what is analyzed here is the geometry of the drip shield in the emplacement drifts as it was modeled in Reference 2.2.1. This information is then adjusted (in Assumption 3.2.4 and Assumption 3.2.5) to the design considered for License Application and for rockfalls impact on waste packages. The information extracted from these references is as follows:

- Reference 2.2.8 gives the invert height, equal to 0.864 m (value rounded up to the nearest millimeter),

- Reference 2.2.18 (Directory Table) gives References 2.2.19 and 2.2.20 as the source documents for detailed information on the dimensions of the drip shield. Namely, Reference 2.2.19 indicates that the width of the drip shield is 2.533 m, its height 2.886 m, and the metal plate on the side of the drip shield has a height of 1.891 m (values rounded up to the nearest millimeter), and Reference 2.2.20 shows that the peripheral bulkhead adds approximately 0.238 m to this height, yielding a total height of the drip shield side equal to 0.238+1.891 = 2.129 m.

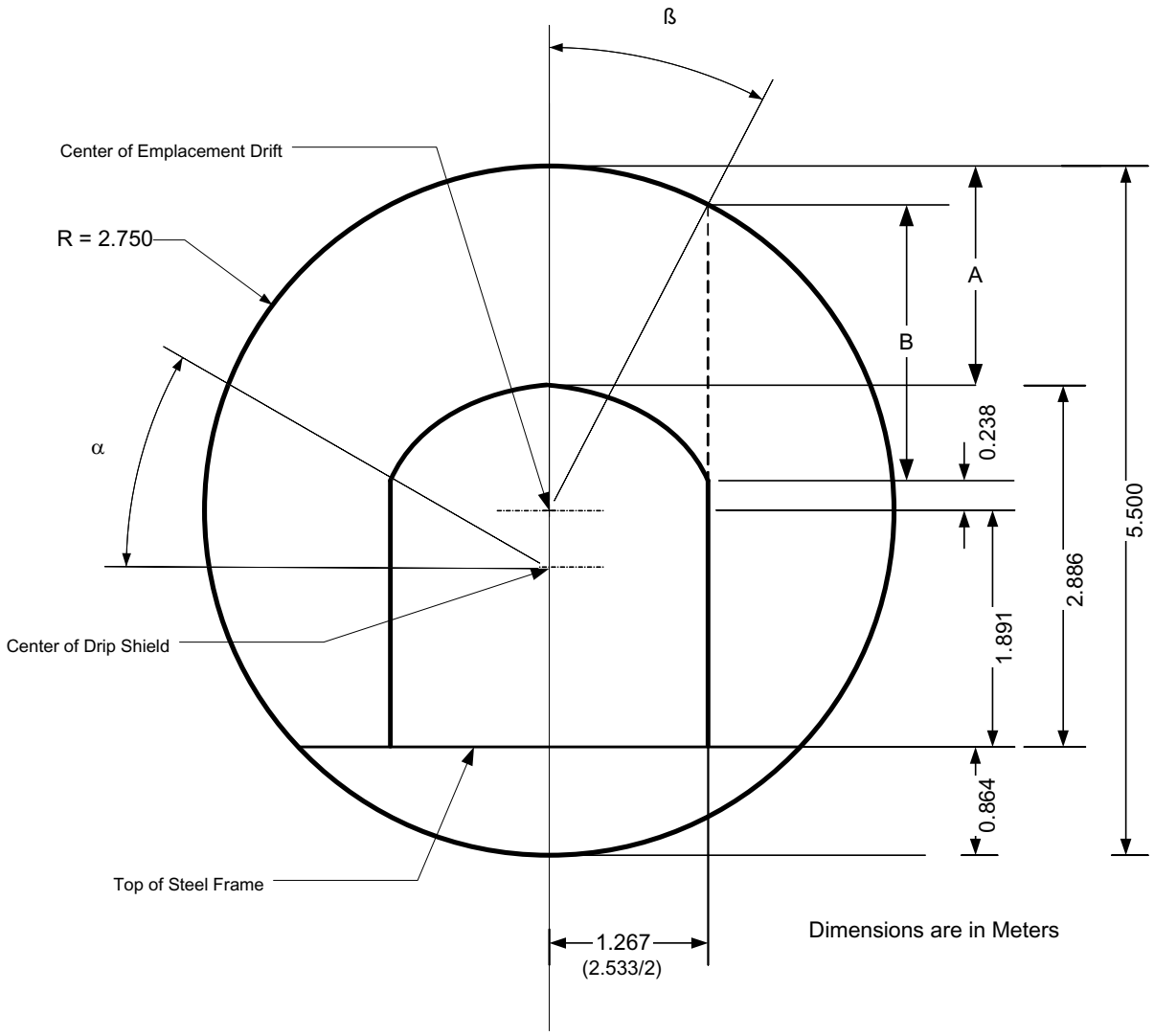

Figure B-1. Drip Shield Geometry in Emplacement Drift

Based on the geometry shown in Figure B-1, the parameters α, β, A, and B are calculated as follows:

- $\tan \alpha = (1.891 + 0.238 - 2.886/2)/1.267 = 0.5414$, hence $\alpha = 28.4°$
- $\sin \beta = 1.267/2.75 = 0.4607$, hence $\beta = 27.4°$
- $A = 5.5 - 0.864 - 2.886 = 1.750$ m
- $B = 2.75 + 2.75 \times (\cos \beta) - 0.864 - 1.891 - 0.238 = 2.198$ m

A representative distance traveled by a rock falling from the upper part of an emplacement drift and impacting the upper portion of a drip shield can be taken as the average of the distance between the crown (top) of the emplacement drift and the top of the drip shield (A on

Figure B-1), and the vertical distance between the rock surface and the shoulder of the drip shield (B on Figure B-1), which yields: (1.750 + 2.198)/2 = 1.974 m.

B.2. Waste Package Geometry in Emplacement Drift

This section outlines the waste package geometry in emplacement drifts, and support Assumption 3.2.5 by calculating a representative distance traveled by a rock falling from the upper part of an emplacement drift and impacting the upper portion of a waste package. This section also supports Assumption 3.2.2 by calculating the height reached by a waste package in an emplacement drift. Figure B-2 shows the geometry considered.

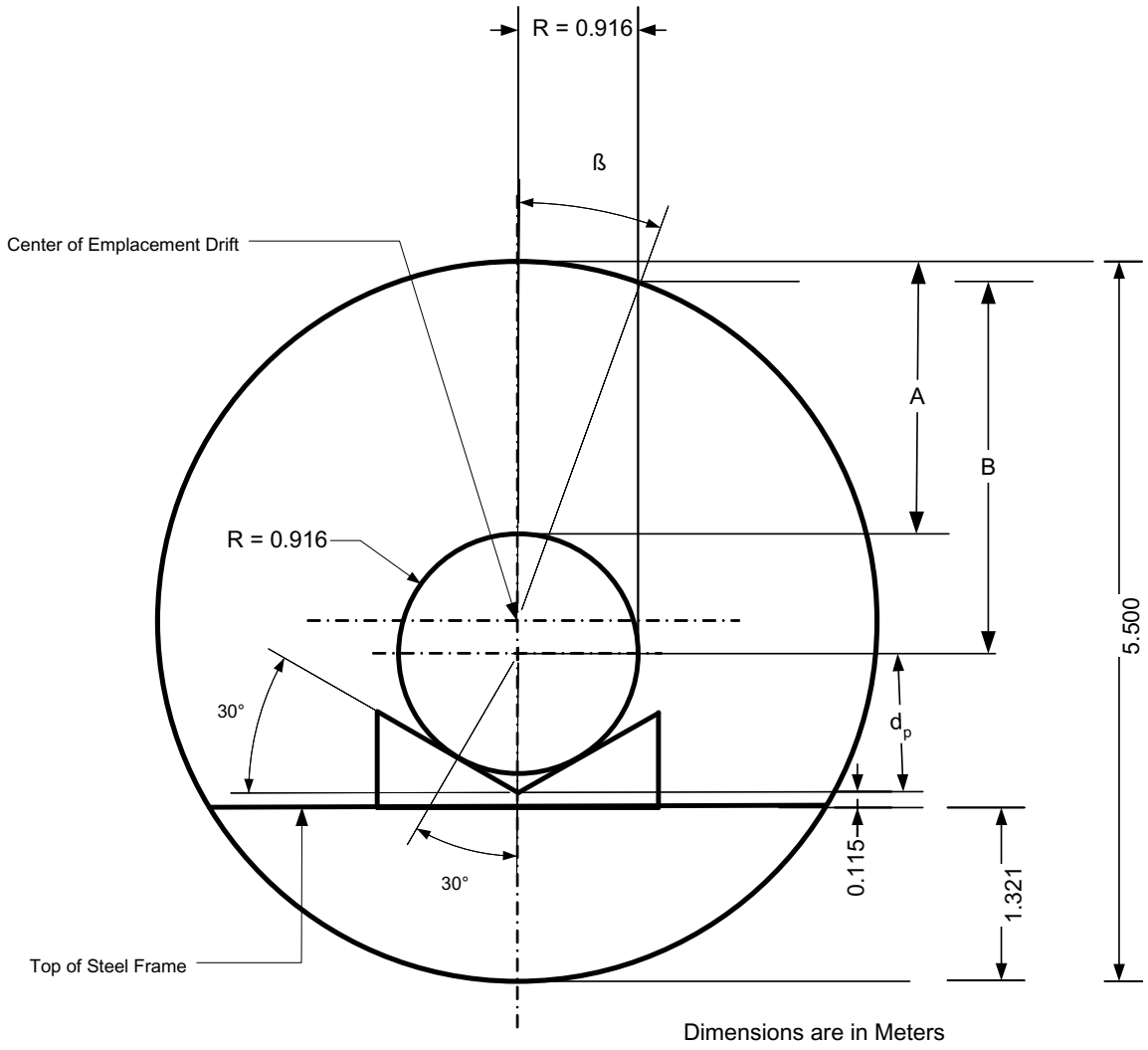

Figure B-2. Waste Package Geometry in Emplacement Drift

The dimensions shown on Figure B-2 reflect the design for License Application and are based on the following references:

- Reference 2.2.12 (Table 8), which indicates that the emplacement drift diameter is 5.5 m
- Reference 2.2.23, which indicates that the invert height is equal to 1.321 m (value rounded up to the nearest millimeter). This reference is suitable for use because it was issued to reflect the design for License Application.
- Reference 2.2.4, which indicates that the diameter of the 2-MCO/2DHLW waste package is 1.831 m, and therefore its radius is 0.916 m (values rounded up to the nearest millimeter). The 2-MCO/2DHLW waste package is chosen because it is the waste package with the smallest diameter, which yields conservative results, as indicated in Assumption 3.2.2 and Assumption 3.2.5.
- Reference 2.2.17, which indicates that the waste package supports of the emplacement pallet are at an angle of 30º from the horizontal, and are at their lowest part 0.115 m above the ground (value rounded to the closest millimeter).

Based on the geometry shown in Figure B-2, the parameters β, d_p, A and B are calculated as follows:

- $\sin \beta = 0.916/2.75 = 0.3331$, hence $\beta = 19.5^\circ$
- $d_p = 0.916/\cos 30^\circ = 1.058$ m
- $A = 5.5 - 1.321 - 0.115 - d_p - 0.916 = 2.090$ m
- $B = 2.75 + 2.75 \times (\cos \beta) - 1.321 - 0.115 - d_p = 2.848$ m

A representative distance traveled by a rock falling from the upper part of an emplacement drift and impacting the upper portion of the waste package shown in Figure B-2 can be taken as the average of the distance between the crown (top) of the emplacement drift and the top of the waste package (A on Figure B-2), and the vertical distance between the rock surface and the side of the waste package (B on Figure B-2), which yields: (2.090 + 2.848)/2 = 2.469 m.

In addition, the height reached by the waste package shown on Figure B-2 is equal to: 5.5 - A = 3.41 m.

ATTACHMENT C

COPY OF CORRESPONDENCE ON MODEL DRIFT LENGTH

BSC CORRESPONDENCE LOG #0306070493 **CCU.20070306.0002**

Sandia National Laboratories
Operated for the U.S. Department of Energy by
Sandia Corporation
P.O. Box 5800
Albuquerque, NM 87185-1389

M. Kathryn Knowles
Performance Assessment Manager

Phone: (702) 295-5550
Fax: (702) 295-3123
Internet: mkknowles@sandia.gov

March 5, 2007

Richard J. Tosetti
Manager, Repository Project Management
Bechtel SAIC Company, LLC
1180 Town Center Drive
Las Vegas, NV 89144

QA: NA

RECEIVED BY BSC CCU
DATE: 03/06/2007

SUBJECT: CONTRACT NO. DE-AC04-94AL-85000 – DRIFT LENGTH PER SIMULATION FOR THE NONLITHOPHYSAL ROCKFALL MODEL

Sandia National Laboratories (SNL) has initiated Condition Report 10115 regarding the drift length per simulation for the nonlithophysal rockfall model. Current rockfall information in nonlithophysal units is summarized in *Drift Degradation Analysis* (BSC 2004 [DIRS 166107], Tables 6-10, 6-13, 6-16, and 6-19) based on a drift length per simulation of 25 m. While 25 m is the length of the model space, it is not the length of the actual drift simulated as a result of imposed model boundaries and the drift azimuth (Figure 1).

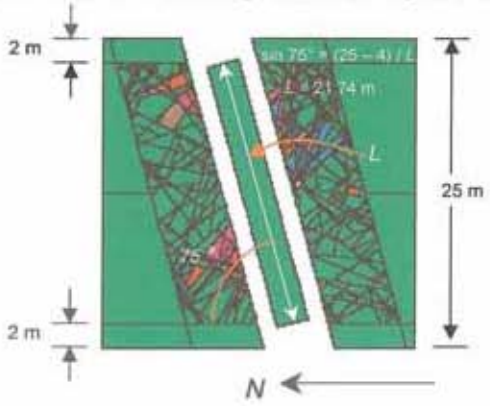

Figure 1. Drift Length Per Simulation. Clarified from Drift Degradation Analysis (BSC 2004 [DIRS 166107], Figure 6-34).

To support the development of calculation 800-00C-MGR0-00300-000-00A, SNL is clarifying that the actual drift length per simulation in the nonlithophysal rockfall model is 21.74 m.

The drift length per simulation impacts the reported total length of drift simulated, the number of blocks (i.e., rockfalls) per km of drift, and the volume of rockfall per km of drift (BSC 2004 [DIRS 166107], Tables 6-10, 6-13, 6-16, and 6-19). This information, which was initially provided based on a drift length per simulation of 25 m, has been corrected using a drift length per simulation of 21.74 m (Enclosure 1). The impacted information is also contained in *IED Geotechnical and Thermal Parameters III* (BSC 2007 [DIRS 178796], Sections XVI, XVII, and XVIII), and output DTN: MO0408MWDDDMIO.002 [DIRS 171483], files *nonlith rockfall characteristics in emplacement drifts with 1e-4 gm.xls, nonlith rockfall characteristics in emplacement drifts with 1e-5 gm.xls, nonlith rockfall*

Exceptional Service in the National Interest

07_376_YMP_LL_03-01-2007

characteristics in emplacement drifts with 1e-6 gm.xls, and *nonlith rockfall characteristics in emplacement drifts with 1e-7 gm.xls*.

The corrected information (Enclosure 1) is preliminary and should be treated as such. The final corrected drift length per simulation and corresponding rockfall information will be completed in February 2008. At that time, the final information will be provided through the interface control document process.

If you have any questions or concerns, please contact Paul Dixon at (702) 295-4250.

M. Kathryn Knowles

MKK:glm

Enclosure: Corrected Information from *Drift Degradation Analysis*

cc:
P.R. Dixon, LANL, Las Vegas, NV
T.W. Pfeifle, SNL, Las Vegas, NV
D.C. Kicker, Stoller, Las Vegas, NV
P.E. Macheret, BSC, Las Vegas, NV
R.L. Keller, BSC, Las Vegas, NV
J.T. Birkholzer, LBNL, Berkeley, CA
M. Gross, B&A, Las Vegas, NV

07_376_YMP-LL_03-01-2007

Enclosure 1
Corrected Information from *Drift Degradation Analysis*

The discrepancy in drift length per simulation for the nonlithophysal rockfall model is documented in Condition Report 10115. The actual drift length per simulation is 21.74 m. The corrected information from *Drift Degradation Analysis* (BSC 2004 [DIRS 166107], Tables 6-10, 6-13, 6-16, 6-19) is provided below, with the corrected preliminary information identified by red text.

Table 6-10. Summary of 3DEC Rockfall Prediction for 1×10^{-5} Annual Probability of Exceedance Hazard

Parameter	Value
Simulations Completed	50
Number of Simulations Predicting No Rockfall	1
Total Number of Rockfall	1767
Total Volume of Rockfall (m^3)	255.4
Total Length of Drift Simulated (m)	1087.0
Number of Blocks per km	1626
Volume of Rockfall per km (m^3)	234.9

Table 6-13. Summary of 3DEC Rockfall Prediction for 1×10^{-6} Annual Probability of Exceedance Hazard

Parameter	Value
Simulations Completed	50
Total Number of Rockfall	2797
Total Volume of Rockfall (m^3)	497.7
Total Length of Drift Simulated (m)	1087.0
Number of Blocks per km	2573
Volume of Rockfall per km (m^3)	457.8

Table 6-16. Summary of 3DEC Rockfall Prediction for 1×10^{-7} Annual Probability of Exceedance Hazard

Parameter	Value
Simulations Completed	44
Total Number of Rockfall	3387
Total Volume of Rockfall (m^3)	705.2
Total Length of Drift Simulated (m)	966.6
Number of Blocks per km	3541
Volume of Rockfall per km (m^3)	737.2

Table 6-19. Summary of 3DEC Rockfall Prediction for 1×10^{-4} Annual Probability of Exceedance Hazard

Parameter	Value
Simulations Completed	32
Total Number of Rockfall	428
Total Volume of Rockfall (m^3)	39.4
Total Length of Drift Simulated (m)	695.7
Number of Blocks per km	615
Volume of Rockfall per km (m^3)	56.7

INTENTIONALLY LEFT BLANK